Carlton Rhyolite Group in the Fort Sill area, Wichita Mountains

Shane A. Finegan[1] and Richard E. Hanson[2]
[1]XTO Energy, Inc., 810 Houston Street, Fort Worth, Texas 76102. Shane_Finegan@xtoenergy.com
[2]School of Geology, Energy, and the Environment, Texas Christian University, Fort Worth, Texas 76129. r.hanson@tcu.edu.
Corresponding author.

INTRODUCTION

The most extensive exposures of the Carlton Rhyolite Group in the Wichita Mountains occur in the Fort Sill area (Fig. 1), where two major, lithologically distinct rhyolite flows are present and are informally termed the Davidson metarhyolite and Fort Sill rhyolite (Fig. 2). The Fort Sill rhyolite is separated from the underlying Davidson metarhyolite by a discontinuous unit of clastic metasedimentary rock that includes the Pratt Hill quartzite of Sides and Miller (1982) and was deposited on an irregular erosional surface cut into the lower flow (Fig. 3). Both flows are intruded by Mount Scott Granite, which forms a large, sheet-like intrusion in this part of the Wichita Mountains. The Mount Scott Granite shown in Figure 2 also includes the smaller Rush Lake and Medicine Park Granites mapped in the study area by Price (paper, this guidebook), which he considers to be related to the Mount Scott Granite. All three of these units are shown as undivided Mount Scott Granite on Figure 2. The Quanah and Cache Granites intrude the Fort Sill rhyolite in the southwest part of the area (Fig. 2).

In this paper, we present detailed stratigraphic relations of the rhyolites in the Fort Sill area and document their internal structure, manner of emplacement, cooling history, and geochemical characteristics. This work builds on previous studies by Schoonover (1948), Gilbert (1982a, 1982b, 1986), Sides and Miller (1982), and Price (1998). In names for formal lithodemic units used herein all the words are capitalized. For informally named rock units the lithological term is lower case (e.g., "Pratt Hill quartzite").

GEOLOGIC SETTING OF THE STUDY AREA

In the general area of Fort Sill, at the far eastern edge of the Wichita Mountains, major geologic contacts have shallow dips of 10 to 15° to the south–southeast (Fig. 4), including the gabbro-granite contact on the north flank of Mount Scott (Gilbert and Hogan, 2010) and the contact between the base of the Fort Sill rhyolite and the Pratt Hill quartzite and laterally equivalent volcaniclastic rocks (Sides and Miller, 1982, and this paper). Just south of the study area, sandstones and carbonate rocks of the Upper Cambrian to Ordovician Timbered Hills and Arbuckle Groups are exposed in several small hills and typically dip 14° to 20° to the southeast or southwest (Chase et al., 1956), although these rocks are partly offset by faults (Chase et al., 1956; Ham et al., 1964). As shown in Figure 4, the Mount Scott Granite is inferred to form a sill beneath parts of the Carlton Rhyolite Group, similar to other granites in the Wichita Mountains and in parts of the subsurface in the Southern Oklahoma Aulacogen (Ham et al., 1964). This interpretation is consistent with regional field relations (Hogan and Gilbert, 1995; Hogan et al., 1998; Hogan et al., 2000; Price, paper, this guidebook), but differs from the interpretation of Gilbert (1982b) concerning relations in the area south of Mount Scott (discussed below).

Intrusive Igneous Contacts

Many currently recognized intrusive igneous contacts in the Wichita Mountains were originally depicted as faults on the first state geologic map of Oklahoma by Miser (1954), an interpretation later followed by Chase et al. (1956) and Havens (1977). Several factors played a role in the interpretation of faults on those maps, including prominent lineaments visible on aerial photographs and topographic maps and, in places, the exceptionally straight nature of the gabbro-granite contact that is commonly parallel to the lineaments. Gilbert (1984) argued that many of the faults drawn near geologic contacts on the earlier maps could instead be interpreted as intrusive igneous contacts. His work mainly focused on the gabbro-granite contact exposed in the central lowland of the eastern Wichita Mountains, west of the present study area.

In the present study area, intrusive igneous contacts between units of the Carlton Rhyolite Group and the Mount Scott and Quanah Granites are typically obscured or am-

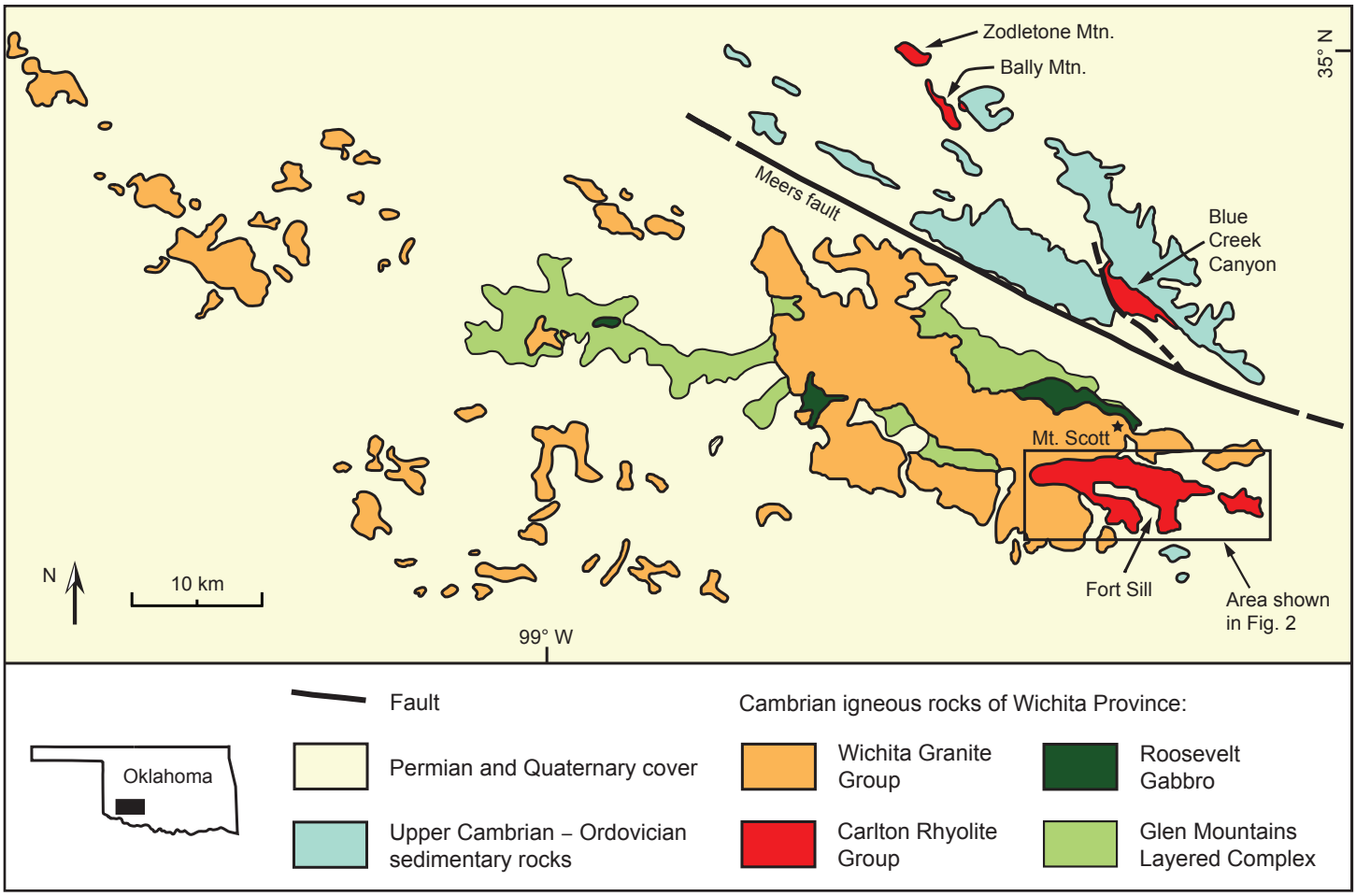

Figure 1. Geologic map of the Wichita Mountains. Location of the Fort Sill area shown in Figure 2 is indicated. Modified from Powell et al. (1980).

biguous in nature. They are commonly buried by Permian sediments of the Post Oak Formation and/or thin soil and alluvium or are covered by vegetation or water (e.g., Lake Elmer Thomas). Nevertheless, several key locations either exhibit well-defined contact relations or the relations between units can be reasonably inferred.

Along an unnamed ridge on the Fort Sill Military Reservation west of Lake Elmer Thomas, Mount Scott Granite can be observed intruding the base of the Fort Sill rhyolite along a relatively straight east-west-trending contact. At locality A (Fig. 5) complex, interfingering relations occur between Fort Sill rhyolite and the granite, and the contact is defined by a zone ~15 m wide with dike-like fingers of granite as much as 1 m wide injected into rhyolite. At the contact, thermal metamorphism has imparted a granoblastic texture to the groundmass of the Fort Sill rhyolite, and the granite develops a fine-grained chilled margin, particularly within fingers intruded into rhyolite. Away from the contact, the granite coarsens and contains distinct 2 to 3 mm ovoid alkali feldspar phenocrysts typical of the main part of the Mount Scott Granite (Price, paper, this guidebook).

Near a small drainage immediately to the east, Mount Scott Granite intrudes along the base of a rhyolitic volcaniclastic metasedimentary sequence that was deposited between the Davidson metarhyolite and overlying Fort Sill rhyolite (locality B, Figs. 5 and 6). There, the volcaniclastic rocks have also been thermally metamorphosed and the granite displays a chilled, fine-grained margin. The contact can be traced for several meters before becoming covered. The base of the Fort Sill rhyolite at this locality is obscured by grass and thin soil, although the outcrop configuration suggests an interfingering relationship similar to that described previously. Above the grass-covered base, the Fort Sill rhyolite shows a relatively coarse, sugary groundmass in hand sample that is suggestive of thermally induced granoblastic growth of the quartzo-feldspathic groundmass.

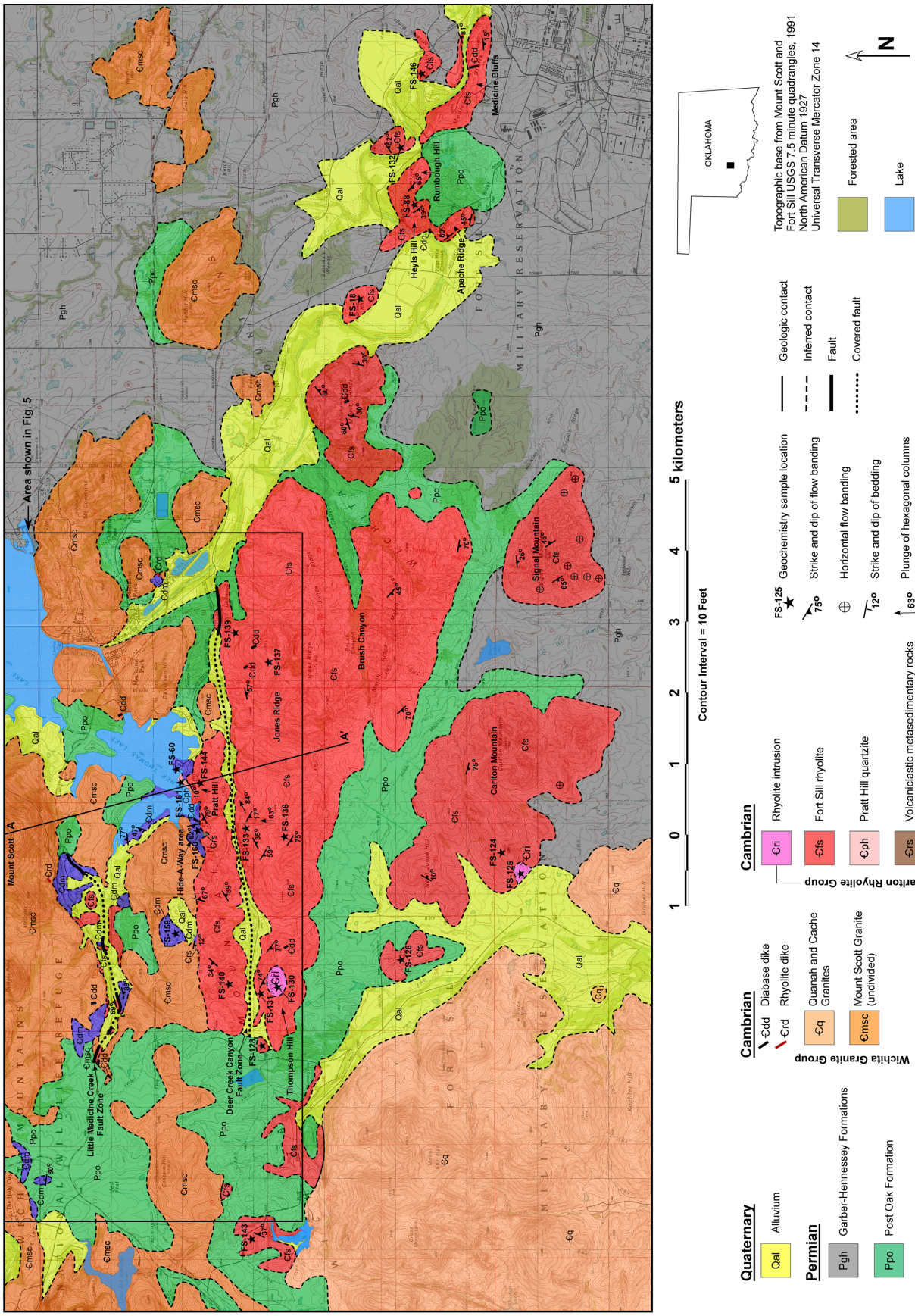

Figure 2. Geologic map of the Fort Sill area. Location shown in Figure 1. Rush Lake and Medicine Park Granites of Price (this guidebook) are included with Mount Scott Granite. Map includes data from Schoonover (1948), Gilbert (1982b, 1986), Miller et al. (1982), Gilbert and Powell (1988), and Price (1998).

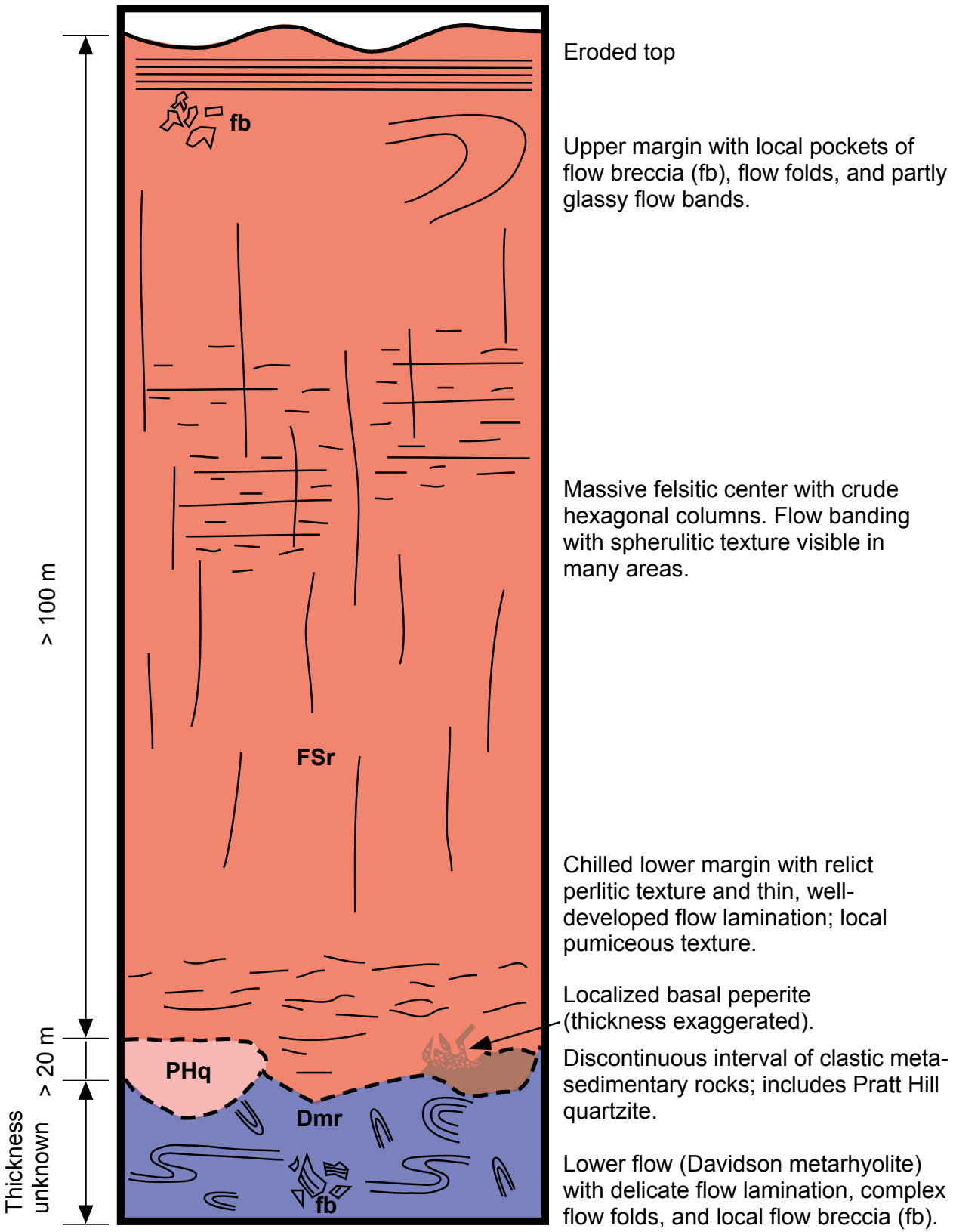

Figure 3. Schematic diagram of an idealized section through the Carlton Rhyolite Group in the Fort Sill area (not to scale). FSr = Fort Sill rhyolite; Dmr = Davidson metarhyolite; PHq = Pratt Hill quartzite.

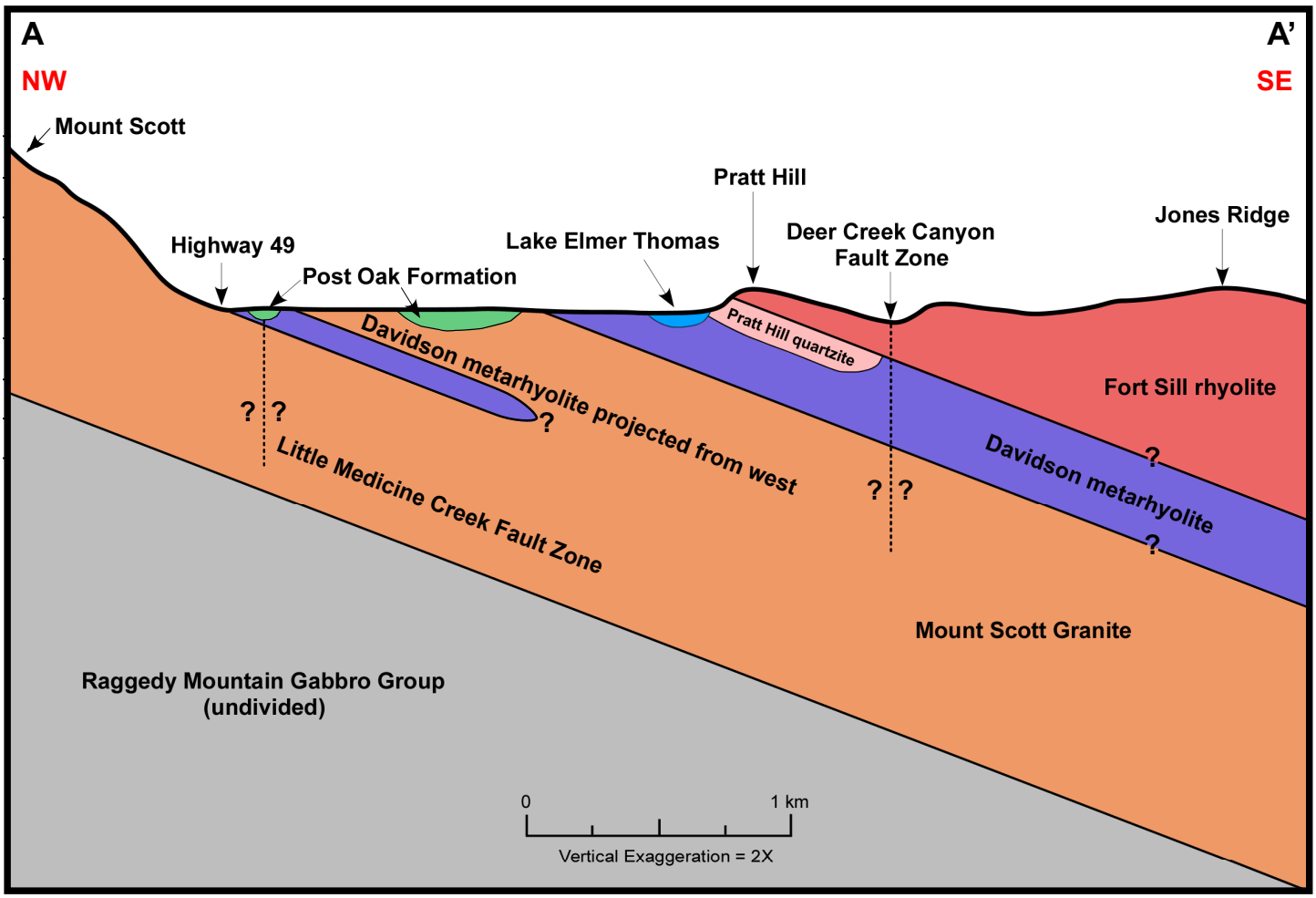

Figure 4. Cross-section A-A' across part of the Fort Sill area. Location is shown on Figure 2. Dip of units south of Pratt Hill is uncertain. Vertical exaggeration is 2:1.

Elsewhere in the mapped area (Fig. 2), except where covered by Permian and Quaternary sediments, the Davidson metarhyolite is truncated discordantly by Mount Scott Granite (Fig. 7). This relationship is best exposed in the Hide-A-Way area in Fort Sill (locality C, Fig. 5), where the contact is irregular. Blocks of Davidson metarhyolite as much as 50 m across are partly entrained within granite, suggesting an interfingering relationship, and some blocks as much as 5 m across are fully encased within the granite. The granite along the contact shows the same type of chilled margin as described above.

Gilbert (1982b) argued that in the area between Mount Scott and the southern end of Lake Elmer Thomas the Mount Scott Granite transgressed over the Fort Sill rhyolite. This interpretation conflicts with observations given above. Also, as discussed below, the contact metamorphic overprint in the Fort Sill rhyolite shows a marked decrease upward in the unit, which is inconsistent with the interpretation of Gilbert (1982b). We infer that outcrops of Davidson metarhyolite at the southern foot of Mount Scott represent a large xenolith or septum contained within the interior of the Mount Scott Granite sill (Fig. 4).

Faults

Two main faults occur in the study area (Fig. 2). In the Wichita Mountains Wildlife Refuge southwest of Mount Scott, the structurally complex Little Medicine Creek Fault Zone can be traced ~3 km from the headwater canyon of Little Medicine Creek eastward along the creek to the vicinity of the Mount Scott Picnic Area. Along the trace of the fault, cataclastically sheared and brecciated rhyolite (Fig. 8A) is, in places, juxtaposed against Mount Scott Granite showing similar shearing and brecciation. Gilbert and Powell (1988) previously noted this brittle deformation in the vicinity of Quetone Overlook (locality D, Fig. 5). Brittle deformation

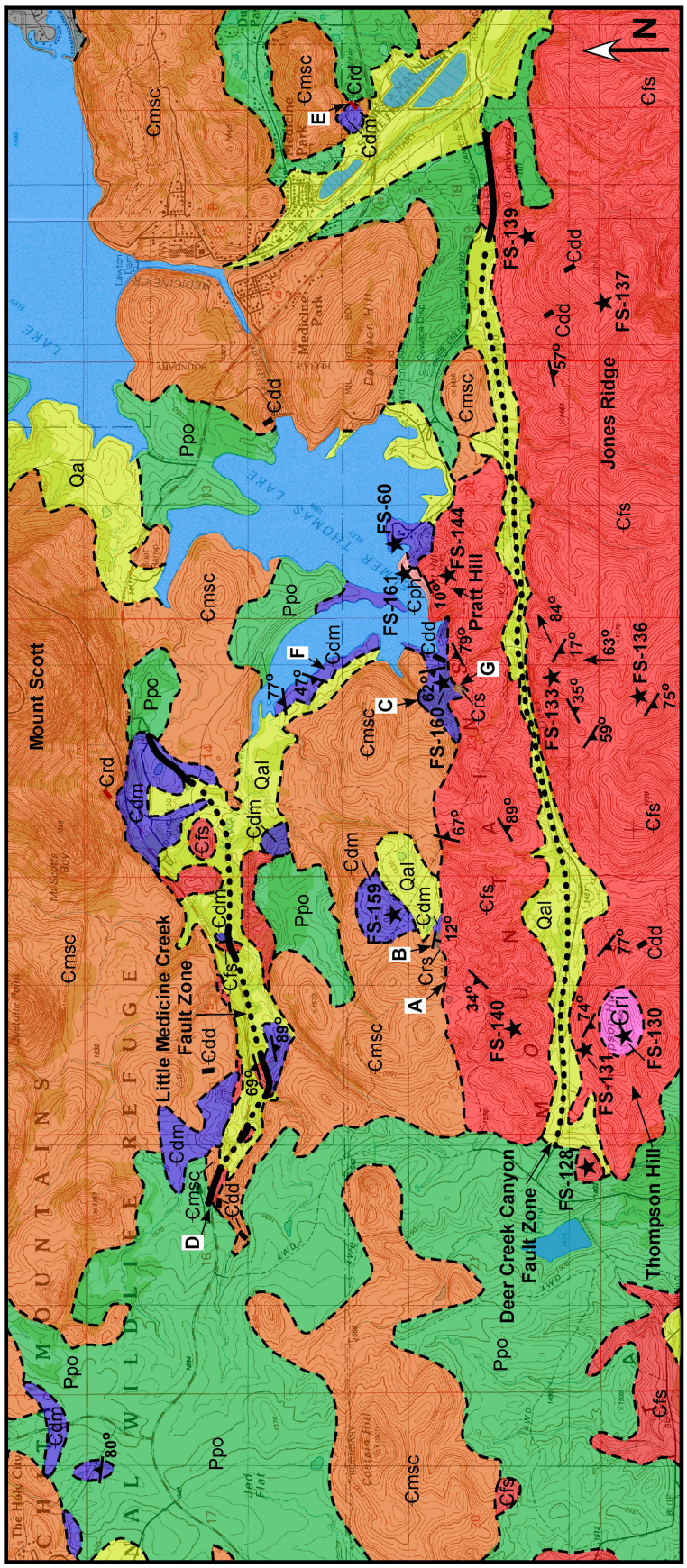

Figure 5. Geologic map of part of the Fort Sill area showing localities A-G discussed in text. See Figure 2 for location and legend.

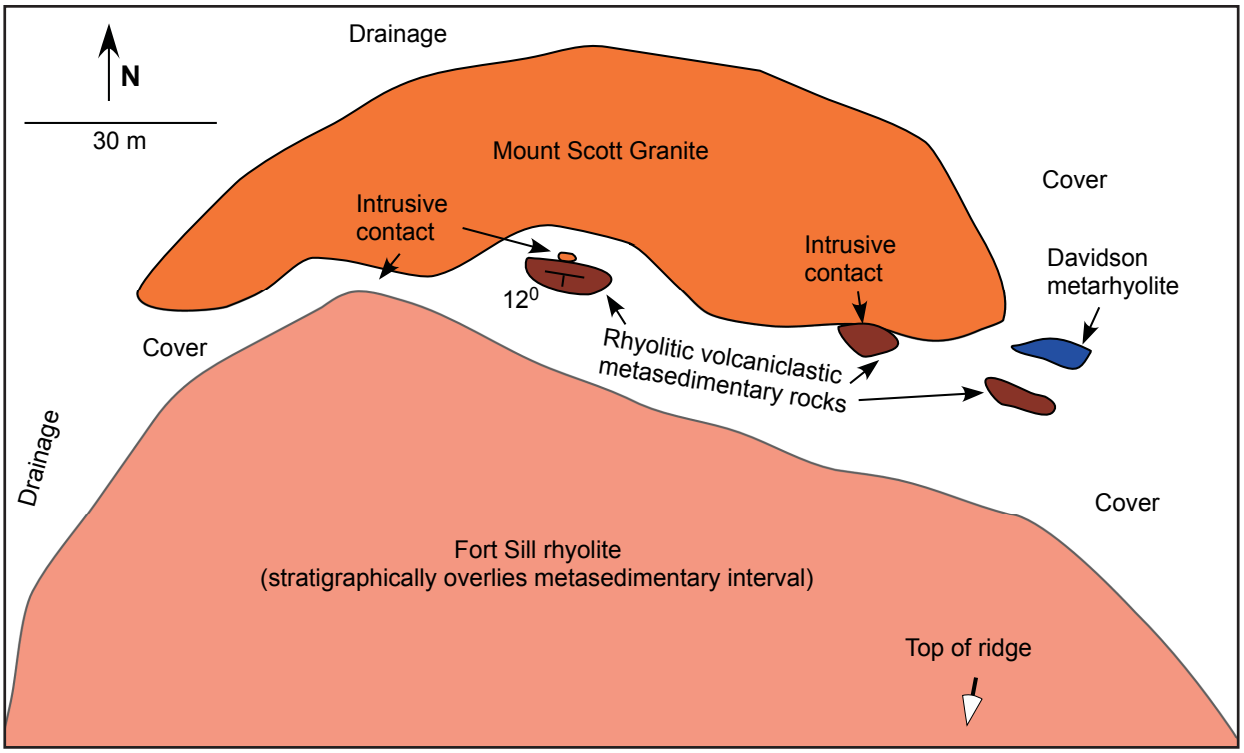

Figure 6. Outcrop map showing exposure of rhyolitic volcaniclastic metasedimentary interbed at the base of the Fort Sill rhyolite (locality B, Fig. 5). Mount Scott Granite has intruded along the base of the metasedimentary rocks.

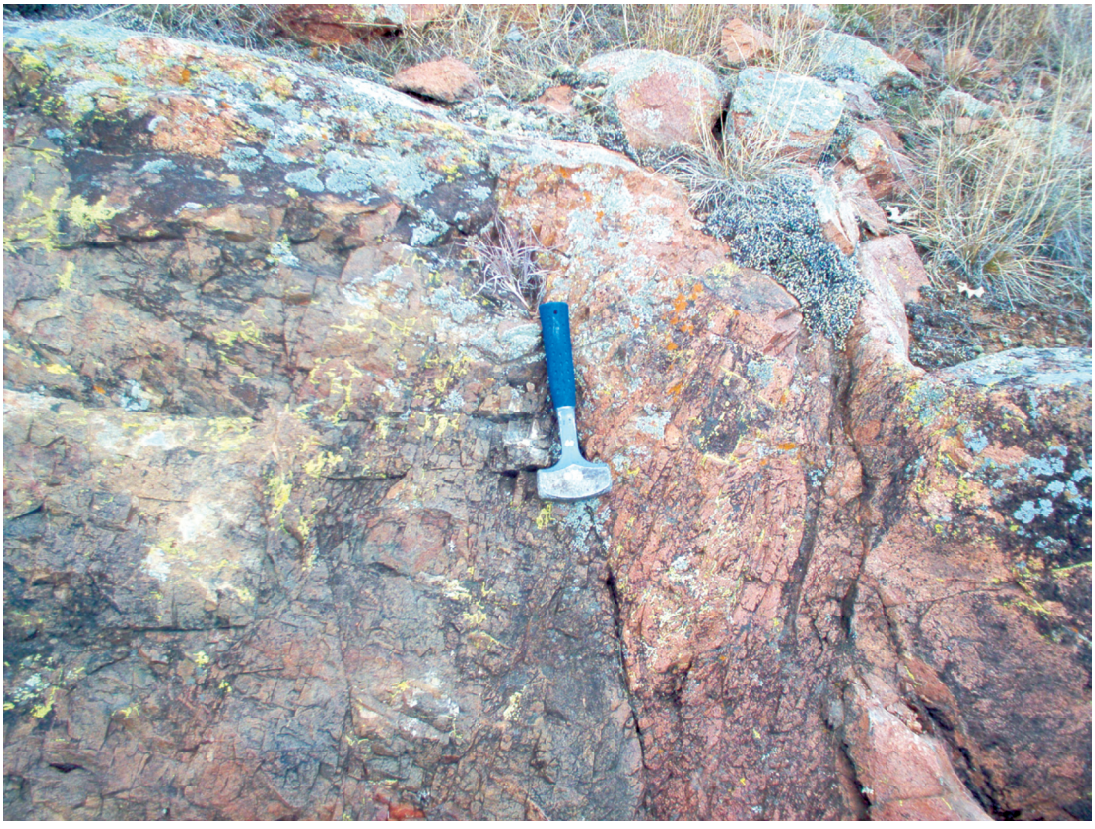

Figure 7. Sharp, intrusive contact between the Davidson metarhyolite (left of hammer) and Mount Scott Granite (right of hammer) at locality B (Fig. 5).

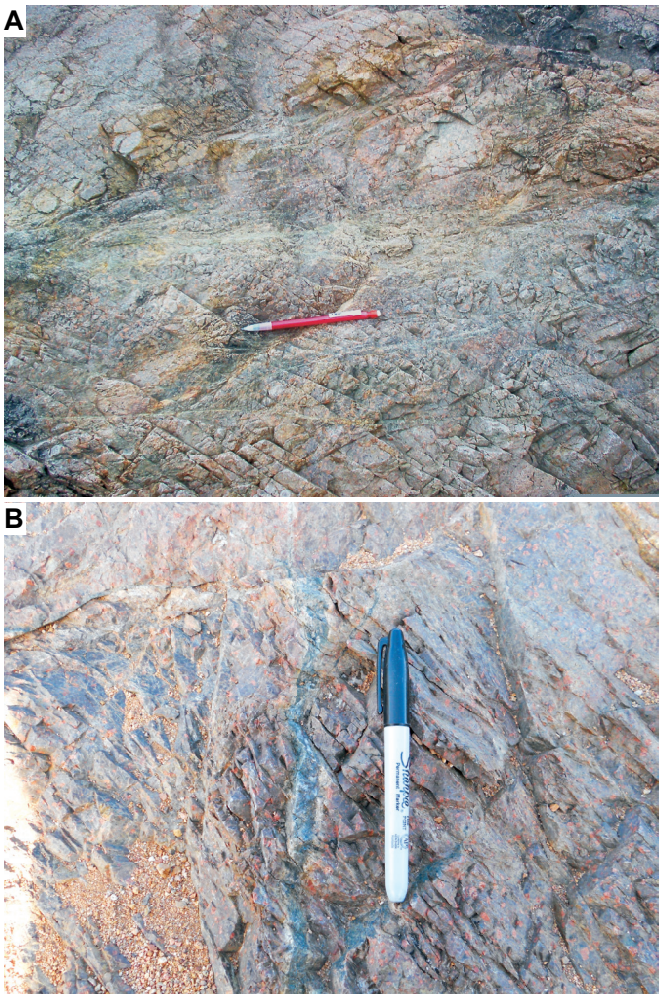

Figure 8. (A) Strongly fractured and cataclastically sheared Fort Sill rhyolite in Little Medicine Creek Fault Zone. (B) Pseudotachylite filling fractures in Fort Sill rhyolite in Little Medicine Creek Fault Zone.

TABLE 1. MODAL ANALYSES OF RHYOLITE SAMPLES FROM THE FORT SILL AREA

	Sample	Alkali feldspar (%)	Quartz (%)	Oxide (%)	Groundmass (%)	Alkali feldspar size (mm)	Quartz size (mm)
Fort Sill rhyolite	**FS-18**	11.4	4.8	1.0	82.8	5.0	3.0
	FS-88	13.8	3.8	1.2	81.2	5.0	3.0
	FS-124	12.0	5.4	1.8	80.8	5.0	3.0
	FS-126	12.8	2.6	1.2	83.4	5.0	2.0
	FS-128	15.0	7.0	0.6	77.4	6.0	3.0
	FS-131	12.8	7.0	1.4	78.8	4.0	2.0
	FS-132	14.6	5.4	2.8	77.2	5.0	3.0
	FS-133	7.2	3.4	1.0	88.4	7.0	2.0
	FS-136	10.0	7.6	1.6	80.8	7.0	2.0
	FS-137	16.6	7.0	1.6	74.8	6.0	2.0
	FS-139	15.8	4.8	2.8	76.6	7.0	3.0
	FS-140	19.6	5.6	2.4	72.4	6.0	2.0
	FS-143	18.2	9.4	1.4	71.0	7.0	3.0
	FS-144	15.6	7.8	1.2	75.4	6.0	2.5
	FS-146	17.6	5.0	2.6	74.8	5.0	2.5
Rhyolite intrusions	**FS-125**	15.0	4.2	3.0	76.2	4.0	3.0
	FS-130	18.2	2.6	1.0	78.2	7.0	2.0

related to the fault occurs in a zone ≥0.5 km wide, which disappears under cover to the east and west. Along the westernmost exposed part of the fault zone, south of Quetone Overlook (locality D, Fig. 5), a wedge-shaped outcrop of highly oxidized and fractured Fort Sill rhyolite extends up the north flank of the canyon cut by Little Medicine Creek and narrows westward. Pervasively fractured Mount Scott Granite surrounds this mass of Fort Sill rhyolite and is unconformably overlain by conglomerate of the Post Oak Formation. Along the creek bed towards the east, pseudotachylite occurs as veins ≤1 cm wide filling cracks between brecciated fragments of Fort Sill rhyolite (Fig. 8B).

To the south in Deer Creek Canyon, a second fault zone ~75 m wide cuts the Fort Sill rhyolite (Figs. 2 and 5). This fault zone, which we term the Deer Creek Canyon Fault Zone, is defined by an east-west-trending linear zone of cataclastically sheared and brecciated rhyolite that can be traced for ~6.3 km before disappearing under cover. The deformation style is entirely brittle and rapidly dissipates on either side of the fault zone. Exposures of Fort Sill rhyolite on opposite sides of the fault appear to represent the homogenous interior of the flow (see section on the Fort Sill rhyolite below), possibly suggesting minimal vertical offset along the fault.

The amount of offset and sense of motion are undetermined along both faults. Neither fault extends into the Permian Post Oak Formation to the west, suggesting deformation occurred during Pennsylvanian inversion of the Southern Oklahoma Aulacogen or during Cambrian rifting.

Rhyolite Intrusions

Two previously unrecognized small hypabyssal rhyolite intrusions with distinctly different groundmass textures from the Fort Sill rhyolite penetrate that unit in the Fort Sill area (Fig. 2). As shown later in this paper, the intrusions also have different geochemical compositions in some respects than either the Davidson metarhyolite or the Fort Sill rhyolite. At first glance outcrops of the rhyolite intrusions do not appear significantly different from typical Fort Sill rhyolite, and it is likely that such intrusions are more abundant in the Fort Sill area than currently recognized.

One intrusion is exposed on the lower southwest slope of Carlton Mountain (locality FS-125, Fig. 2), and the other crops out near the summit of Thompson Hill (locality FS-130, Figs. 2 and 5). They form isolated exposures with rounded outcrop morphology that protrude above the otherwise grass-covered hills. The intrusions are mineralogically similar to the Fort Sill rhyolite and contain 2.6 to 4.2% quartz and 15.0 to 18.2% alkali feldspar phenocrysts (Table 1). Accessory zircon ≤0.08 mm in length is also present. The intrusions have distinctly coarser groundmass textures than the Fort Sill rhyolite. Abundant, randomly oriented tridymite needles (now inverted to quartz) in the groundmass are ≤1 mm long (Fig. 9A) and occur with interstitial micrographyre (Fig. 9B). Also, unlike the Fort Sill rhyolite, the intrusions contain rare, rounded mafic inclusions with basaltic textures (Fig. 10A), which may record mingling of mafic and felsic magmas in the parent magma chamber. The inclusions are generally ≤3.5 cm across and typically weather out, leaving oval-shaped pits (Fig. 10B).

Rhyolite Dikes

Two rhyolite dikes cut Mount Scott Granite in the study area (Figs. 2 and 5). One of these dikes was mapped by Gilbert (1982b) at the southern base of Mount Scott. A more thoroughly documented rhyolite dike is exposed in a roadcut on Highway 49 directly north of the James A. Manning State Fish Hatchery (locality E, Fig. 5). Ham et al. (1964) first documented the dike and interpreted it as representing the contemporaneous nature of Wichita granites and Carlton Rhyolite. Later, Gilbert and Powell (1988) recognized the tectonic significance of the dike and concluded that a substantial amount of overburden was removed prior to emplacement of the dike, which must have been intruded late in the igneous history of the Southern Oklahoma Aulacogen. More recently, O'Donnell (2008) provided a textural analysis of the rhyolite dike, documenting the crystal-size distribution of quartz and alkali feldspar phenocrysts within it.

Diabase Dikes

Diabase intrusions in the Fort Sill area generally form small dikes. A number of dikes cutting felsic units in the area have been reported by earlier workers (Schoonover, 1948; Gilbert, 1982b, 1986; Gilbert and Powell, 1988; Miller et al., 1982; Price, 1998). In addition to those already reported, we have mapped three previously undocumented diabase dikes cutting the Fort Sill rhyolite in the study area (Figs. 2 and 5). The presence of one of these dikes, located on the east side of Jones Ridge (northeast of locality FS-137, Figs. 2 and 5), was only detected by the abrupt appearance of abundant, dark-colored diabase float standing out in stark contrast against the weathered, reddish Fort Sill rhyolite; in situ outcrops of the dike could not be located. A second diabase dike was mapped within a north-trending drainage northwest of the summit in the

Figure 10. (A) Rounded mafic inclusion within rhyolite intrusion exposed on Thompson Hill. (B) Outcrop of rhyolite intrusion exposed on Carlton Mountain showing oval-shaped pits caused by weathering of mafic inclusions.

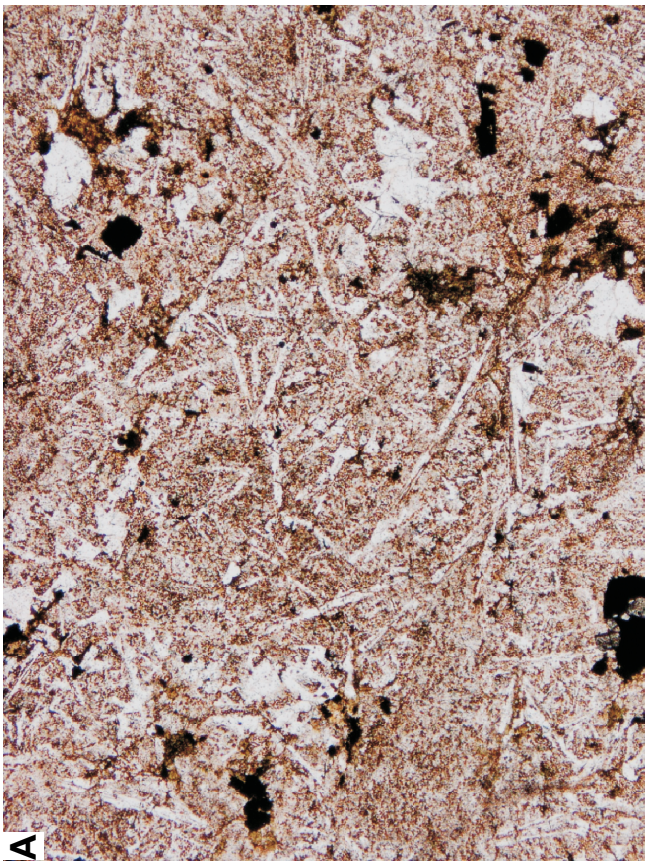

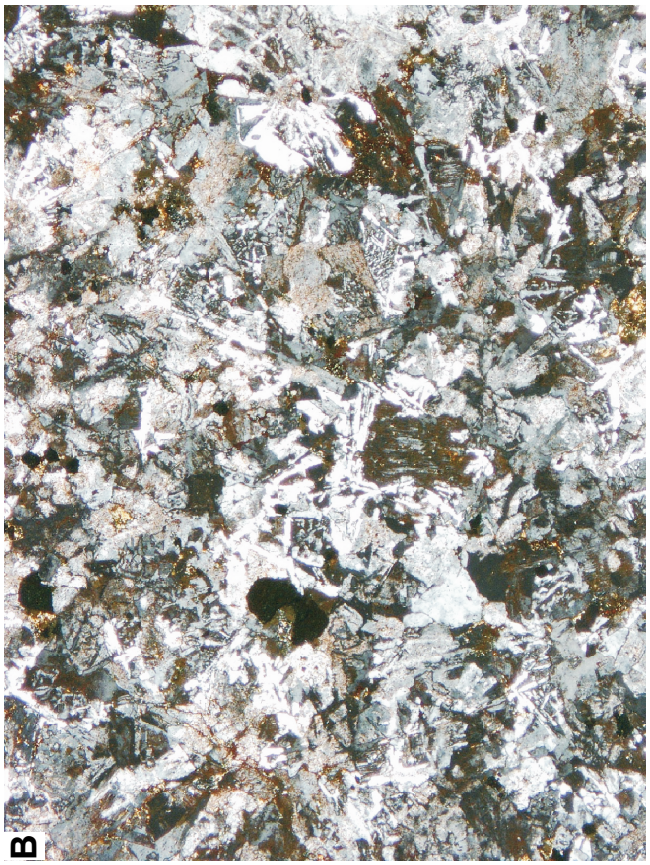

Figure 9. (A) Photomicrograph (plane light) of rhyolite intrusion on Carlton Mountain showing coarse, randomly oriented tridymite needles (inverted to quartz). Width of view is ~2.5 mm. (B) Photomicrograph (crossed polars) of same intrusion showing microgranophyric groundmass texture. Width of view is ~2.5 mm.

same general area (north of locality FS-137, Figs. 2 and 5). That dike trends N50°W and is ~4 m wide. It shows well-exposed contacts with the Fort Sill rhyolite, which has dark-gray baked zones adjacent to the dike. The length of the dike is unknown because it crops out for only a few meters across the width of the narrow drainage. A third diabase dike was mapped at the base of Heyls Hill along the east bank of Medicine Creek (near locality FS-88, Fig. 2). Due to poor exposure, the trend and dimensions of the dike could not be determined. In thin section, the dike exhibits subophitic texture defined by euhedral to subhedral plagioclase laths ≤0.7 mm long that are partially enclosed by clinopyroxene crystals (Fig. 11). Plagioclase is variably altered to sericite with minor calcite locally replacing parts of some laths. Clinopyroxene is generally less altered than plagioclase but shows some replacement by green clay, chlorite, and goethite/hematite. Fe-Ti oxides are present throughout the sample and include very fine grained, oriented inclusions in some clinopyroxene crystals that probably formed by exsolution.

Figure 11. Photomicrograph (crossed polars) showing subophitic texture in diabase dike exposed near Heyls Hill. Random plagioclase crystals are intergrown with clinopyroxene showing higher birefringence. Width of view is ~2.5 mm.

DAVIDSON METARHYOLITE

Overview

The Davidson metarhyolite and Pratt Hill quartzite have been the subject of controversy for nearly a century, due mainly to their fine-grained, recrystallized fabrics and close spatial association. The Pratt Hill quartzite is exposed only on the steep, north-facing slope of Pratt Hill (locality FS-161, Figs. 2 and 5) and overlies the Davidson metarhyolite. The Davidson metarhyolite is exposed immediately adjacent to Pratt Hill, on both the west and east, as well as elsewhere in the field area (Fig. 2), as described below. Many features typical of rhyolite lavas are well displayed throughout the Davidson, although they have been variably modified by metamorphic recrystallization, whereas the Pratt Hill quartzite lacks evidence for a volcanic origin.

Previous Work

In the past, most workers have assigned the Davidson metarhyolite and Pratt Hill quartzite to a single unit. Metamorphic rocks cropping out south of Mount Scott were interpreted by Taylor (1915) to be Precambrian quartzite xenoliths. Hoffman (1930) reinterpreted these rocks to belong to a shallow-level intrusion, which he named the Davidson granophyre. Schoonover (1948) followed this interpretation but renamed the unit the Davidson microgranite. In contrast, Ham et al. (1964) interpreted these rocks as hydrothermally altered lava and minor hornfelsic tuff of the Carlton Rhyolite Group. Sides and Miller (1982) first coined the informal term Pratt Hill quartzite and interpreted the protolith of the unit to be submature clastic sediments deposited along the unconformity between the Carlton Rhyolite and underlying gabbroic rocks. Moreover, Sides and Miller (1982) interpreted a portion of the Davidson metarhyolite located near the southwest shore of Lake Elmer Thomas, in the Hide-A-Way area, as part of the Pratt Hill quartzite.

Sides and Miller (1982) did not believe that the Pratt Hill quartzite was correlative with either the Meers Quartzite of Hoffman (1930) or the Tillman Metasedimentary Group of Ham et al. (1964), although they noted that all three of these units shared some compositional similarities. At the time Sides and Miller (1982) published their work, the Meers Quartzite was considered to represent metamorphosed sandstones occurring only as xenoliths in rocks of the Raggedy Mountain Gabbro and Wichita Granite Groups (Ham et al., 1964; Powell et al., 1980). Gilbert (1982a), in contrast, interpreted some examples of Meers Quartzite to represent sandstones deposited on the unconformable surface separating the Carlton Rhyolite from older, eroded gabbroic rocks, and he considered the rocks south of Mount Scott to be an argillaceous facies of Meers Quartzite occupying a similar stratigraphic position. Price (1998) and Price et al. (1998) interpreted some of the outcrops considered by Sides and Miller (1982) as Pratt Hill quartzite to represent contact-metamorphosed rhyolite, but retained the term Pratt Hill quartzite for metasedimentary rocks lying between the Davidson metarhyolite and the main flow of Carlton Rhyolite above.

Field Characteristics

The Davidson metarhyolite can be traced discontinuously along strike from west to east for ~9.25 km (Fig. 2). The unit typically crops out in areas of lower elevation where it is commonly exposed in intermittent creek drainages and other areas of recent erosion. The thickness and total extent of the Davidson are unknown. Large parts of it are presumably buried underneath deposits of Post Oak Formation and Quaternary alluvium. To the south the Davidson is stratigraphically overlain by Fort Sill rhyolite or, where present, by thin metasedimentary rocks (e.g., Pratt Hill quartzite). However, contacts with these overlying units are covered by water (e.g., Lake Elmer Thomas), vegetation, or thin soils. As previously discussed, margins of the Davidson are commonly discordantly truncated by granite.

Pervasive, delicate flow lamination with variable attitudes is present throughout the Davidson metarhyolite (Figs. 12A and 12B) and is commonly deformed by small-scale, complex flow folds, which is one of the defining characteristics of the unit. In hand sample, the flow lamination is generally defined by alternating pink and brown parallel laminae (Fig. 12A). The color differences are caused mostly by varying concentrations of feldspar and sericite in the pink laminae, versus abundant recrystallized quartz in the brown laminae, where hematite dust coating the mineral grains imparts a brown hue. Black laminae containing high concentrations of magnetite are also present (Fig. 13A). Steeply plunging, isoclinal to open flow folds have wavelengths ≤50 cm and amplitudes ≤10 cm (Fig. 13B). These features are common in most Davidson outcrops and are particularly well displayed in exposures along the northwest shore of Lake Elmer Thomas in the Wichita Mountains Wildlife Refuge (locality F, Fig. 5). There, progressive deformation during emplacement of the viscous lava has resulted in many refolded folds with highly complex fold geometries, similar to those documented in other parts of the Carlton Rhyolite Group (Eschberger et al., paper, this guidebook; Hanson et al., this guidebook).

Rare, subangular mafic inclusions ~2 cm long are present in places (Fig. 14A). Locally, flow-laminated and flow-folded metarhyolite grades into meter-scale areas of well-developed flow breccia. In the Hide-A-Way area (locality FS-160, Figs. 2 and 5), the flow breccia consists of angular, flow-laminated metarhyolite clasts ≥2 cm long (Fig. 14B). Similar flow breccia occurs in the upper parts of some of the other lava flows in the Carlton Rhyolite (Eschberger et al., paper, this guidebook; Hanson et al., this guidebook). Given the close proximity to overlying volcaniclastic metasedimentary rocks, the presence of flow breccia in this part of the Davidson is taken to indicate that the upper preserved part of the flow beneath the metasedimentary sequence is close to the original top of the flow.

Exposures of Davidson located west of the Hide-A-Way area (locality FS-159, Figs. 2 and 5) show crude, steeply plunging (near vertical) columnar jointing, which is approximately perpendicular to the base of the flow (Fig. 15). The columns are locally overprinted by sheeting joints with variable attitudes, which are inferred to have developed due to volume changes during devitrification (cf., Bonnichsen and Kauffman, 1987).

Thin magnetite- and quartz-rich veins cut parts of the Davidson metarhyolite and are inferred to have developed during contact metamorphism caused by intrusion of the Mount Scott Granite. Magnetite veins are as much as 10 cm wide, although they are typically much thinner (Figs. 13A and 16A). Quartz veins are less common and generally <2 cm wide. Pink alteration haloes along some quartz veins contain disseminated magnetite grains intergrown with the recrystallized rhyolite groundmass (Fig. 16B). The quartz veins are in some cases cut by magnetite veins, indicating two separate phases of fluid migration through the Davidson metarhyolite during contact metamorphism.

On fresh surfaces the Davidson metarhyolite ranges in color from light pink to brown or purple and typically weath-

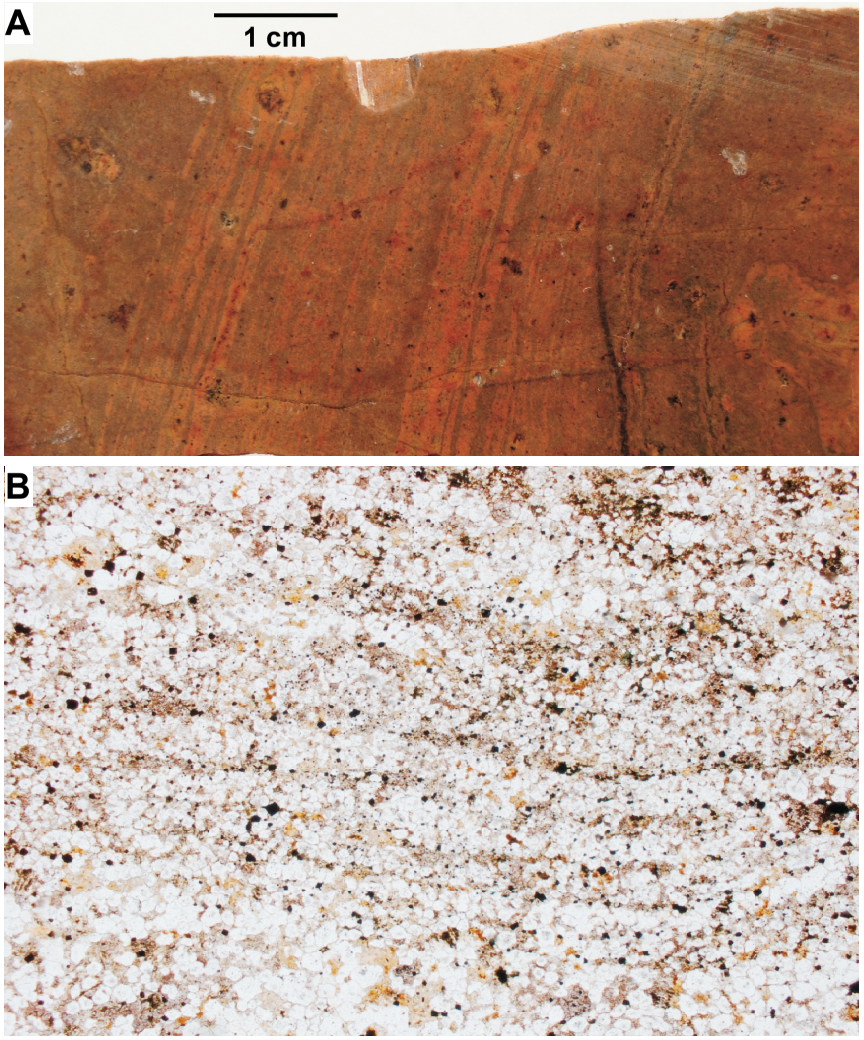

Figure 12. (A) Cut slab of Davidson metarhyolite showing flow lamination. (B) Photomicrograph (plane light) of Davidson metarhyolite showing relict flow lamination overprinted by granoblastic intergrowth of quartz and alkali feldspar. Width of view is ~5 mm.

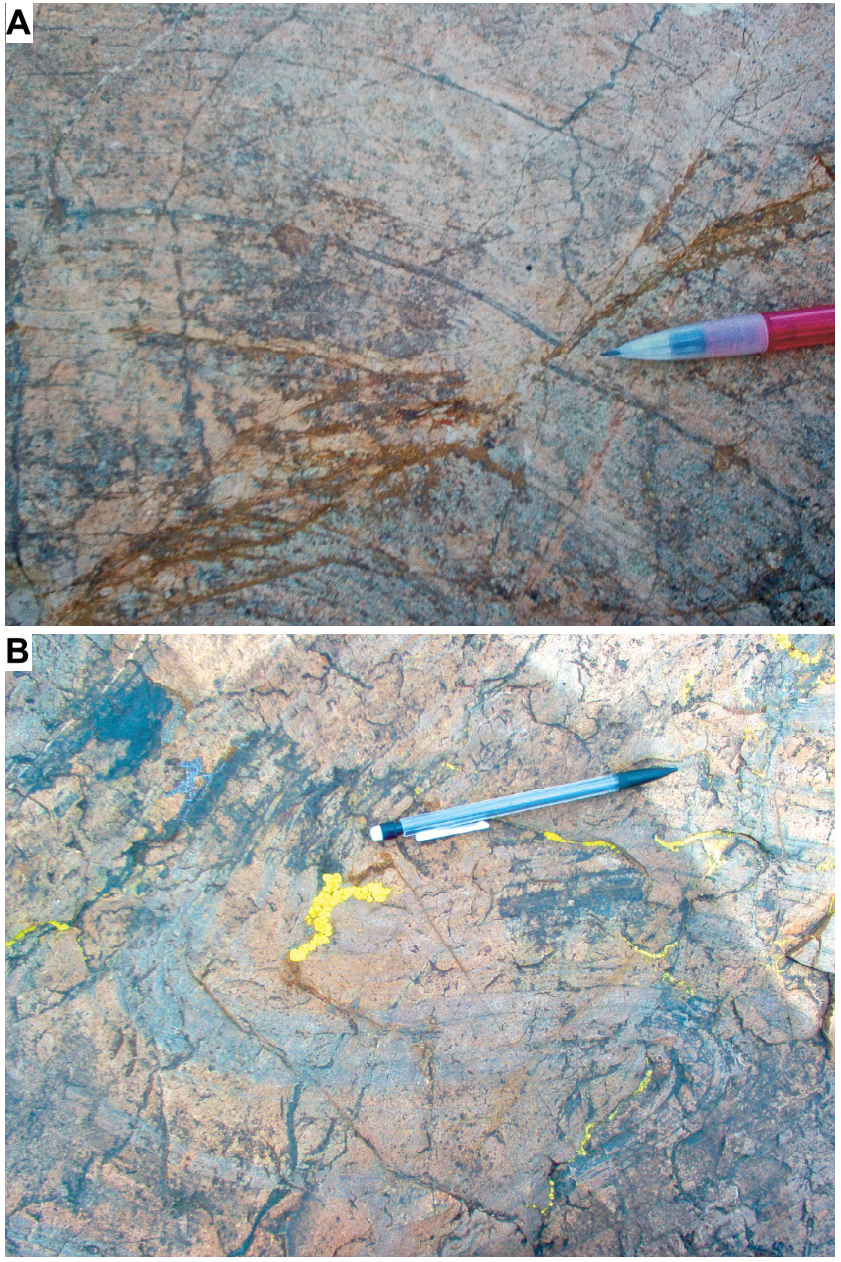

Figure 13. (A) Outcrop photo of Davidson metarhyolite showing black, magnetite-rich flow laminae. Note the small fault offsetting the laminae and the thin, irregular, cross-cutting magnetite veinlets. (B) Tight, steeply plunging flow folds deforming flow lamination in the Davidson metarhyolite.

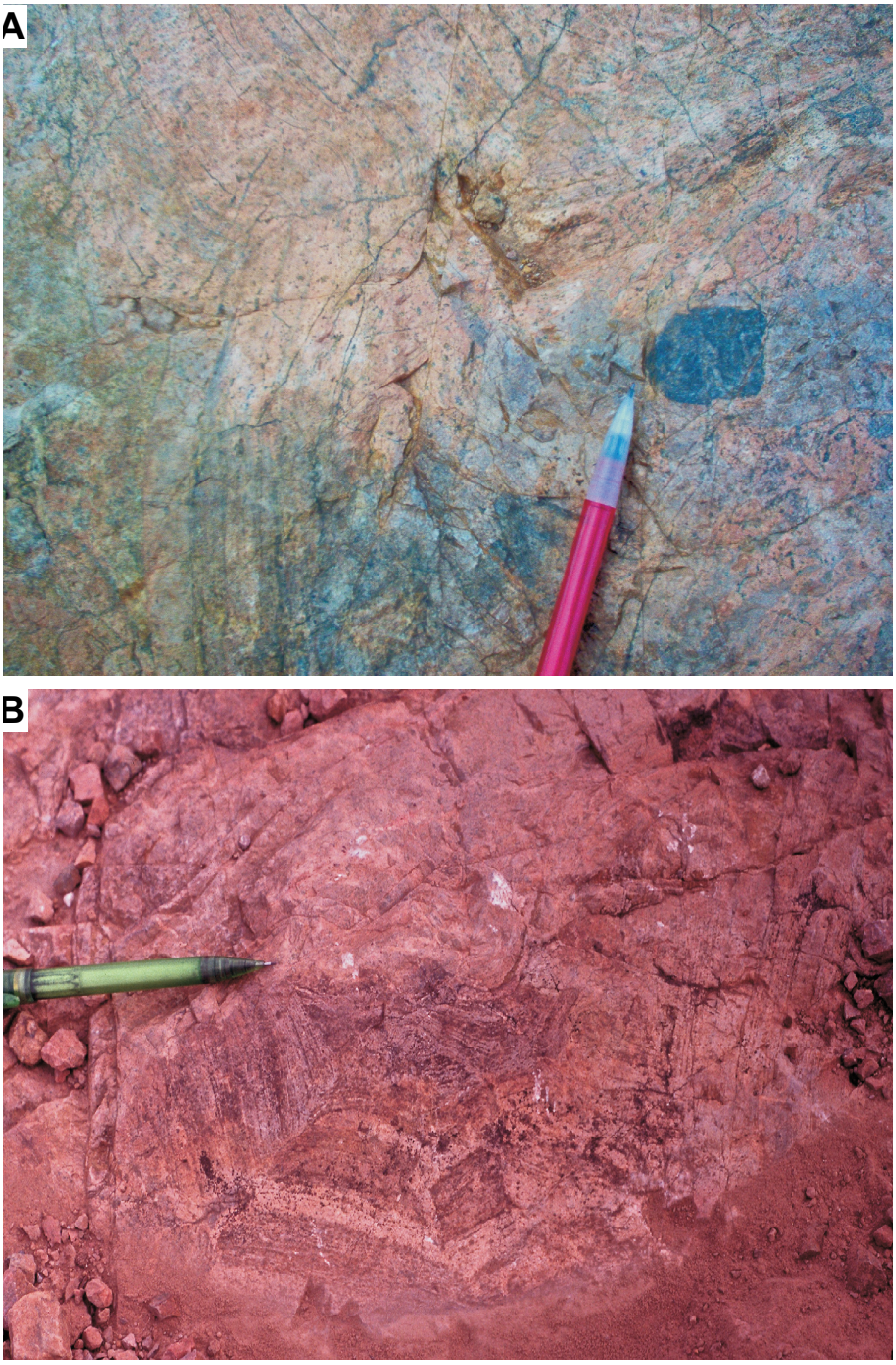

Figure 14. (A) Mafic inclusion within Davidson metarhyolite. Folded flow lamination is also visible. (B) Flow breccia in Davidson metarhyolite with angular, flow-laminated clasts.

ers to dark-brown or buff. Both in hand sample and thin section the unit is generally aphyric. However, some samples contain <1% altered alkali feldspar phenocrysts that are typically ≤1 mm long and subhedral (Fig. 17). In some cases, the feldspar phenocrysts are euhedral and as much as 2.25 mm in length. In thin section, these phenocrysts are commonly replaced by sericite and/or very fine grained quartz and are recognizable only by their rectangular outlines (Fig. 17). Rare examples show remnant chessboard albite twinning similar to that observed in alkali feldspar phenocrysts in the overlying Fort Sill rhyolite. Zircon is present as an accessory phase with individual crystals as much as 0.11 mm long and commonly occurs in glomerocrystic intergrowths with relict alkali feldspar phenocrysts.

In thin section, one of the most striking features of the Davidson is its fine-grained, recrystallized fabric of granoblastic quartz with interstitial feldspar that is mostly replaced by sericite. Individual quartz crystals average ~0.01 mm in size and make up ≥50% of the rock matrix. This texture is very similar to felsitic samples of Fort Sill rhyolite that have been mildly silicified and metamorphosed. The only difference is the slightly larger size of the granoblastic quartz crystals and altered feldspar in the groundmass of the Davidson, which reflects the higher degree of metamorphism experienced by that unit. Disseminated anhedral magnetite grains 0.02 to 0.25 mm in size are present in most samples and comprise as much as 10% of the rock.

Metamorphic minerals are ubiquitous in thin section, although they are too fine-grained to be seen in hand sample and occupy <1% of the rock volume. Chlorite, muscovite, and biotite are commonly present within the recrystallized groundmass and form microporphyroblasts as much as 0.2 mm long. Fibrolitic sillimanite ≤0.1 mm in length (Fig. 18A) was identified in the groundmass of a sample collected in the Lake Elmer Thomas Recreation Area (locality FS-60, Figs. 2 and 5) northeast of Pratt Hill. Samples collected in the Hide-A-Way area (locality FS-160, Figs. 2 and 5) contain rare subhedral to anhedral andalusite poikiloblasts ≤1.25 mm in size (Fig. 18B) that are intergrown with quartz and, less commonly, biotite ≤ 0.15 mm in length. Metamorphic subhedral plagioclase ≤ 0.25 mm in length is present in some cases. It occurs within a quartz veinlet in a sample from the Hide-A-Way area and

Figure 15. Outcrop of Davidson metarhyolite showing crude columnar jointing. Hammer for scale (circled) is approximately parallel to column long axes.

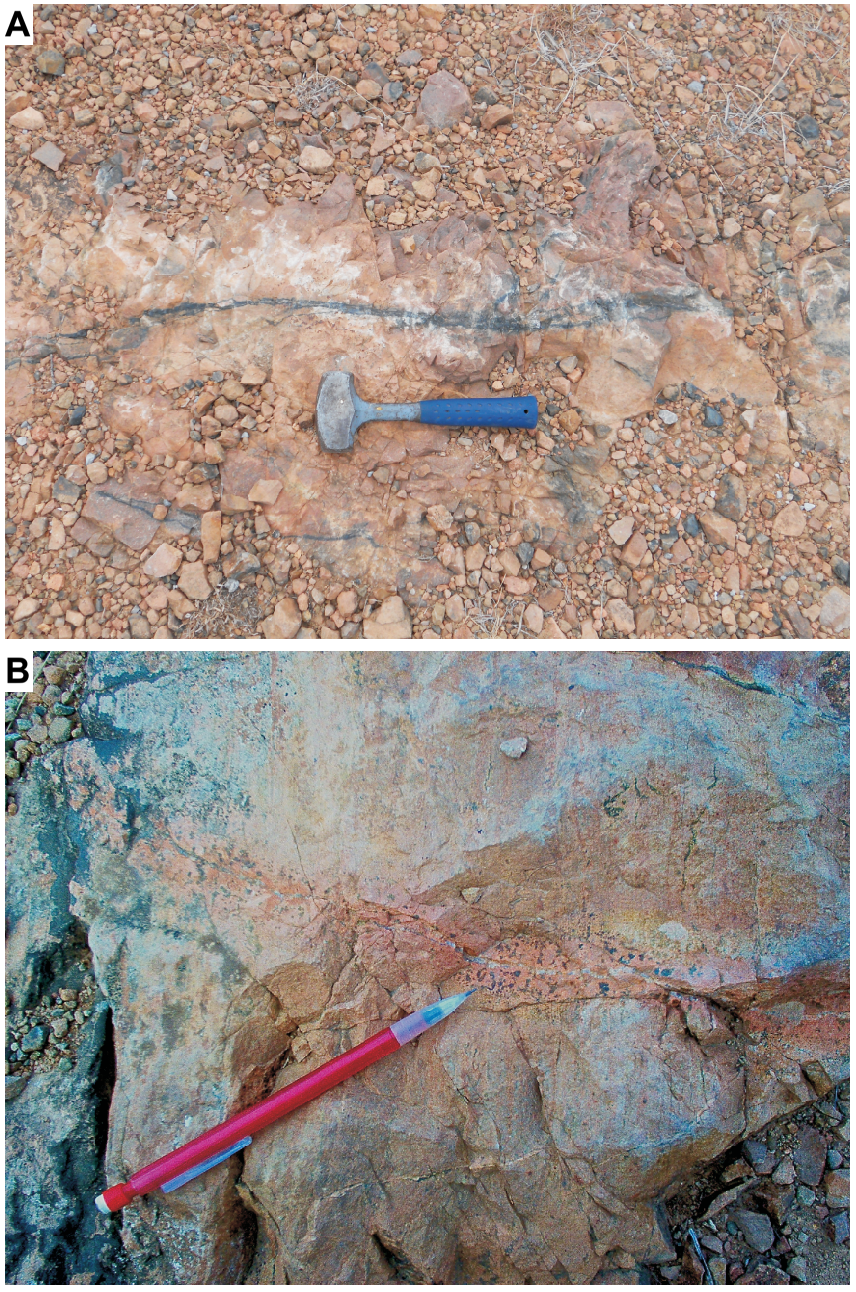

Figure 16. (A) Outcrop of Davidson metarhyolite with magnetite vein. (B) Outcrop of Davidson metarhyolite with quartz veinlet surrounded by pink alteration halo that contains disseminated magnetite grains.

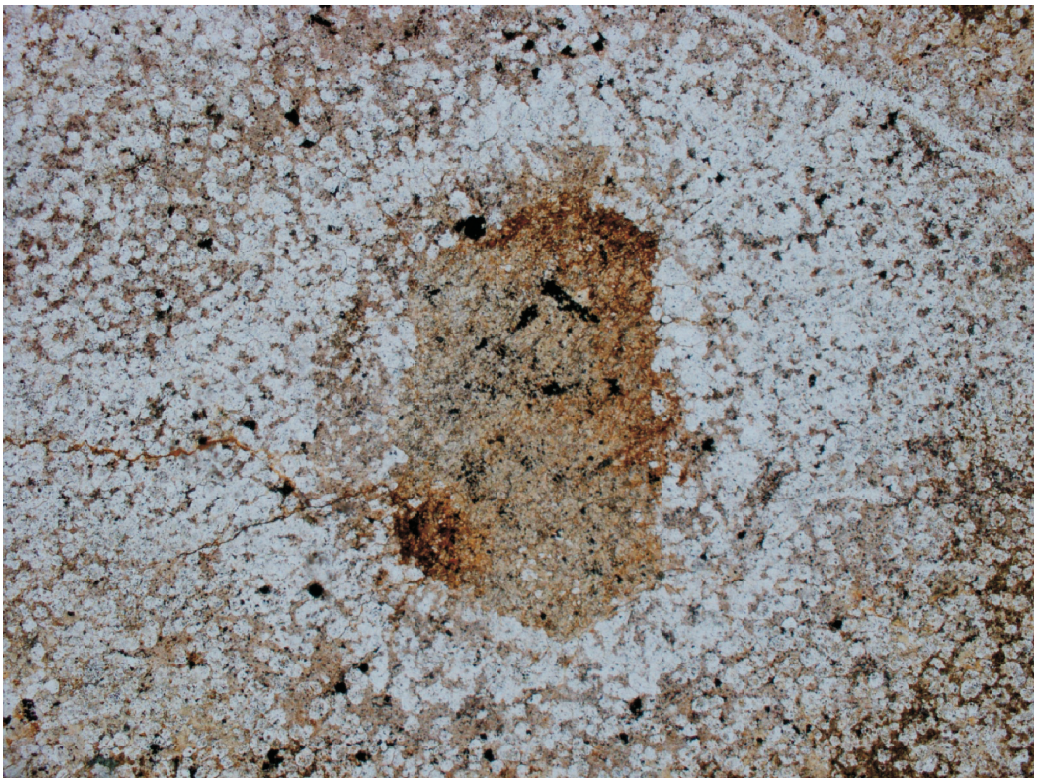

Figure 17. Photomicrograph (plane light) of Davidson metarhyolite showing subhedral alkali feldspar phenocryst completely replaced by sericite. Width of view is ~5 mm.

within the groundmass of a sample collected along the northwest shore of Lake Elmer Thomas (locality F, Fig. 5) in the Wichita Mountains Wildlife Refuge.

The presence of andalusite and sillimanite in the Davidson metarhyolite in the vicinity of Pratt Hill indicates that metamorphic conditions reached the hornblende hornfels and pyroxene hornfels facies. It should be noted that previous workers have also reported andalusite within the Pratt Hill quartzite (Miller et al., 1982; Price et al., 1998). Metamorphism may have occurred at lower grades where andalusite and sillimanite are absent in the Davidson, but the occurrence of these minerals may also be controlled by compositional variations. Formation of these aluminosilicate minerals in a metarhyolite requires development of alumina-oversaturated bulk compositions, which probably occurred by loss of alkalis during silicification and may have affected some samples more than others. A future systematic study might be able to map isograds across the Davidson but would require detailed attention to bulk compositional variations.

CLASTIC METASEDIMENTARY ROCKS

Overview

The Davidson metarhyolite is overlain by a discontinuous clastic metasedimentary unit dipping gently to the south (Figs. 2, 4, and 5). As discussed in the previous section, part of this unit has been termed the Pratt Hill quartzite where it is exposed at the base of Pratt Hill (locality FS-161, Figs. 2 and 5; Sides and Miller, 1982). Previously unrecognized clastic metasedimentary rocks stratigraphically equivalent to the Pratt Hill quartzite are exposed in the Hide-A-Way area (locality G, Fig. 5) and along an unnamed ridge farther west (locality B, Fig. 5). The clastic interval is ≥20 m thick at Pratt Hill (Sides and Miller, 1982) but the base is covered by Lake Elmer Thomas. The interval is only ~1 m thick west of the Hide-A-Way area. The clastic rocks are completely absent in places, suggesting they were deposited on an irregular surface developed on the Davidson metarhyolite. Some of these rocks consist of relatively pure quartzite similar to that at Pratt Hill, but coarse- to fine-grained rhyolitic volcaniclastic metasandstone and metasiltstone containing monocrystalline quartz, feldspar, and rhyolite lithic grains are also present. Coarse, monocrystalline quartz grains in these beds could not have been derived from the underlying Davidson metarhyolite and instead record influx of detritus from erosion of quartz-phyric rhyolite elsewhere in the developing volcanic pile. One or more volcaniclastic debris-flow deposits are intercalated with the fine-grained rocks and contain pebble-sized clasts of rhyolite and quartzite.

Pratt Hill Quartzite

The contact between the Pratt Hill quartzite and Davidson metarhyolite is covered by Lake Elmer Thomas. However, the contact with the overlying Fort Sill rhyolite is ex-

posed on the steep, north-facing slope of Pratt Hill (locality FS-161, Figs. 2 and 5), where it strikes N60°E and dips 10° southeast (Fig. 4; Sides and Miller, 1982). The contact is sharp and can be traced for several meters along the cliff face but varies in elevation due to its irregular nature. On part of the northern slope of Pratt Hill the contact is close to water level. Toward the east it climbs ~20 to 30 m above the lake level and can be followed eastward to near a small, intermittent stream, beyond which the contact is concealed by talus and thin soil. To the west, the quartzite thins dramatically, and the contact with the Fort Sill rhyolite disappears below water level (Sides and Miller, 1982). The nature of the irregular contact led Schoonover (1948) to interpret Pratt Hill as an uplifted horst block bounded on the east and west by faults. A more likely interpretation is that the contact represents an irregular erosional surface with moderate relief that developed on top of the Davidson metarhyolite prior to eruption of the overlying Fort Sill rhyolite (Price et al., 1998).

In hand sample, the Pratt Hill quartzite is generally gray to green and very fine grained (Fig. 19A), which gives the rock a sugary appearance. In thin section, the rock is composed of ~50 to 90% quartz grains that are very well sorted, with coarse silt to very fine sand-sized grains comprising most of the rock (Fig. 19B). Metamorphic recrystallization of quartz has imparted a well-developed granoblastic texture that overprints original grain shapes, although original, well-rounded grains can still be identified in some samples. Very fine grained interstitial sericite, coarser metamorphic muscovite flakes as much as 0.15 mm in length, and variable amounts of chlorite and green clay comprise most of the remaining rock volume.

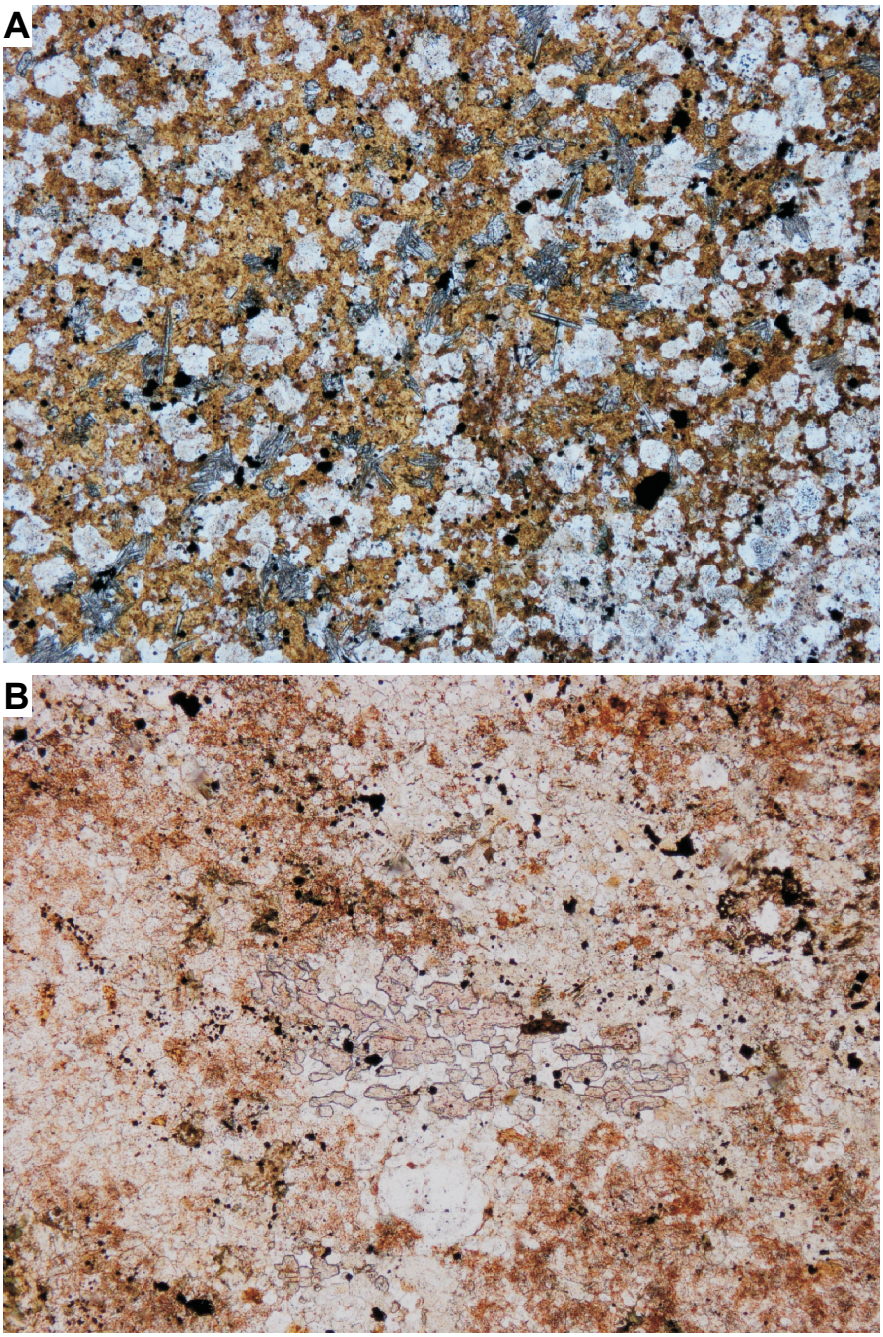

Figure 18. (A) Photomicrograph (plane light) of Davidson metarhyolite showing fibrolitic sillimanite. Width of view is ~2.5 mm. (B) Photomicrograph of Davidson metarhyolite showing andalusite poikiloblast intergrown with quartz in center of view. Width of view is ~2.5 mm

Other minor components of the Pratt Hill quartzite observed in this study include rare andalusite porphyroblasts ≤0.625 mm long and muscovite and biotite porphyroblasts of similar size. In some cases, the biotite shows poikiloblastic texture. Disseminated anhedral magnetite and pyrite (≤0.25 mm) that have been altered to yellow limonite or goethite and red hematite also occur, and zircon grains (≤0.08 mm) are distributed randomly throughout the rock.

Although bedding is not obvious in the field, some samples studied in thin section contain thin layers (mm- to cm-scale) composed of very well sorted, medium- to

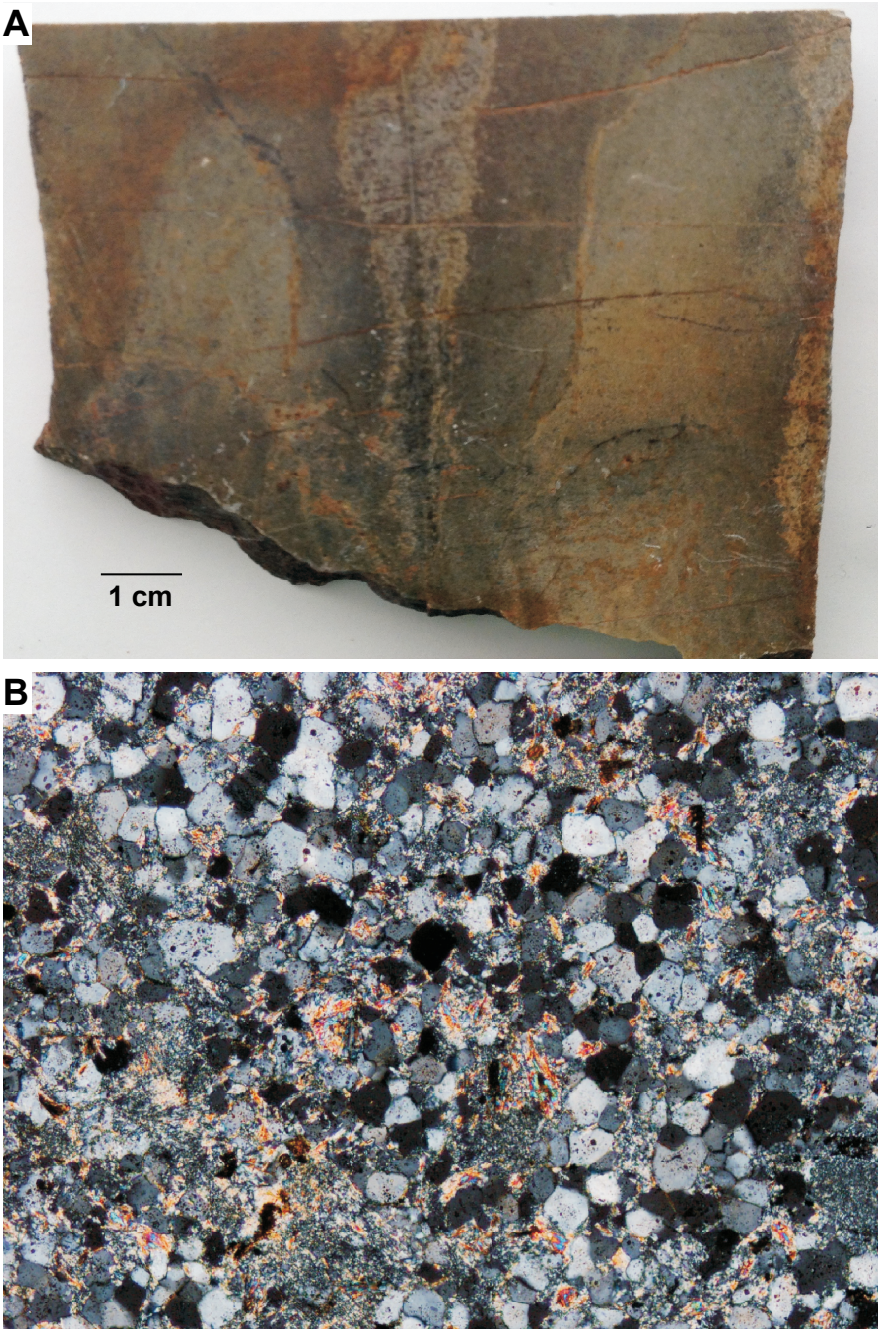

Figure 19. (A) Cut slab of Pratt Hill quartzite. Irregular color pattern is the result of variations in the degree of recrystallization. (B) Photomicrograph (crossed polars) of Pratt Hill quartzite showing recrystallized granoblastic quartz and interstitial sericite. Width of view is ~1.25 mm.

coarse-sand-sized quartz grains that grade into sericite-rich layers. Price et al. (1998) described similar layering, which they interpreted as relict graded bedding. They also identified abundant small andalusite scattered within the finer grained layers, whereas they observed rare, larger andalusite porphyroblasts that are rimmed by sericite in the coarser grained layers. Price et al. (1998) interpreted the more abundant andalusite in the finer grained layers to represent higher original clay content.

The Pratt Hill quartzite is capped by a ~1-m-thick, matrix-supported, polymict unit that lacks internal stratification and is directly overlain by the Fort Sill rhyolite. This unit is interpreted to be a debris-flow deposit. Pebble-sized, partly disaggregated clasts of Pratt Hill quartzite within the debris-flow deposit have released rounded silt grains into the adjacent matrix, which indicates that the protolith to the quartzite was at least partly unconsolidated during transport and deposition of the debris flow. The debris-flow deposit also contains angular, pebble-sized clasts of quartz-phyric rhyolite that lack alkali feldspar phenocrysts (Fig. 20). These rhyolite clasts are unlike the Davidson metarhyolite or the overlying Fort Sill rhyolite and must have come from a different source. The matrix of the deposit consists of poorly sorted, silt- to sand-sized quartz and alkali feldspar grains intermixed with abundant fine-grained, recrystallized vitroclastic material, including relict long-tube pumice clasts ranging from ash-sized to as much as 1.5 cm in length (Fig. 20). Some relict pumice clasts show flattening due to burial compaction (cf. Bull and McPhie, 2007). The vitroclastic material has been replaced by fine-grained, green phyllosilicates, giving the rock a green tint (Fig. 20). The coarser sand-sized quartz and alkali feldspar grains are inferred to represent reworked phenocrysts derived from erosion of rhyolite lava not exposed in the study area.

Hide-A-Way Area

A sequence of dominantly volcaniclastic metasedimentary rocks with some similarities to those described on Pratt Hill is exposed in a north-flowing intermittent stream in the Hide-A-Way area (locality G, Fig. 5; Fig. 21). The sequence dips 10 to 12° to the south, strikes roughly east-west, and is ~19 m thick. Extremely poor exposure impedes accurate bedding plane measurements, and the outcrops are limited to the actual

creek bed. In addition to poor exposure, the sequence has a relatively strong metamorphic overprint that has masked some primary features.

The Davidson metarhyolite is fairly well exposed in the Hide-A-Way area, and the southernmost outcrops of the unit where it is exposed in the intermittent stream are assumed to be very close to the erosional top of the flow. Above the stratigraphically highest Davidson outcrop, there is a mostly covered interval ~8.5 m thick (Fig. 21). In the middle of this interval, quartzite is very poorly exposed; it could possibly make up the entire interval, but this is speculative. The quartzite is gray-green in hand sample (Fig. 22A) and consists predominantly of recrystallized, coarse-silt-sized granoblastic quartz with fine-grained interstitial sericite and sparse, coarser crystals of muscovite (Fig. 22B). The quartz grains are well sorted and, despite the metamorphic overprint, relict rounded grains are still visible. Other constituents include zircon, disseminated magnetite, and minor biotite porphyroblasts ≤0.15 mm in length. Laminae composed of very well sorted, medium sand-sized quartz grains with very little interstitial sericite occur in places. This unit is lithologically identical to the Pratt Hill quartzite and is considered to be a westward extension of it (too small to show on the scale of Figure 5). The rapid westward thinning of the Pratt Hill quartzite is consistent with deposition in a small valley that deepens to the east and was eroded into underlying Davidson metarhyolite.

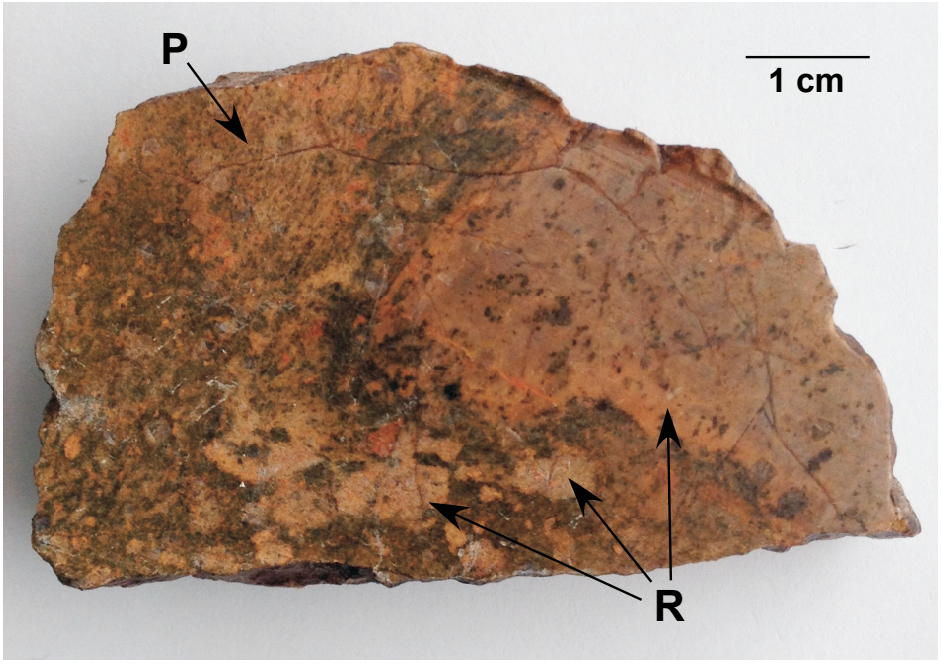

Figure 20. Cut slab of polymict debris-flow deposit overlying the Pratt Hill quartzite. Note the large quartz-phyric rhyolite lithic clasts (R), long-tube pumice clast (P), and green-colored, fine-grained vitroclastic matrix.

Above the covered interval is a poorly sorted, rhyolitic tuffaceous metasandstone ~3 m thick (Fig. 21). The unit is poorly exposed and no bedding or other sedimentary structures were observed in it. Approximately 15% of the rock is composed of angular to subrounded, medium- to coarse-sand-sized quartz and subordinate alkali feldspar grains (Figs. 23A and 23B). Some of the alkali feldspar grains have been partly altered to sericite, and others show relict chessboard albite twinning. The remainder of the rock is dominantly a very fine grained matrix of granoblastic quartz, alkali feldspar, rare plagioclase, and interstitial sericite with minor amounts of chlorite. The matrix material is inferred to mainly represent recrystallized vitroclastic debris and contains relict ash-sized, long-tube pumice clasts, sparse biotite and muscovite porphyroblasts ≤0.4 mm in size, and zircon and disseminated magnetite ≤0.25 mm in size.

The tuffaceous metasandstone is overlain by a matrix-supported, polymict debris-flow deposit ~6.5 m thick (Fig. 21) that contains subangular to angular, pebble-sized clasts of aphyric rhyolite similar to the Davidson metarhyolite (Fig. 24); porphyritic rhyolite clasts containing quartz and alkali feldspar phenocrysts (Fig. 25); and quartzite clasts composed of well-rounded, well-sorted, fine-sand-sized quartz grains (Figs. 24 and 26). The quartzite clasts are slightly coarser grained and have less interstitial sericite than is generally present in the Pratt Hill quartzite. Additionally, these subangular to angular clasts were well lithified during formation of the debris-flow deposit, which contrasts with evidence that the protolith to the upper Pratt Hill quartzite was poorly consolidated when clasts from that unit were incorporated into the overlying debris-flow deposit on Pratt Hill. It is possible that the protolith to the Pratt Hill quartzite showed different degrees of lithification during deposition of the overlying beds or that the well-lithified quartzite clasts in the debris-flow deposit in the Hide-A-Way area were derived from a different source. Furthermore, porphyritic rhyo-

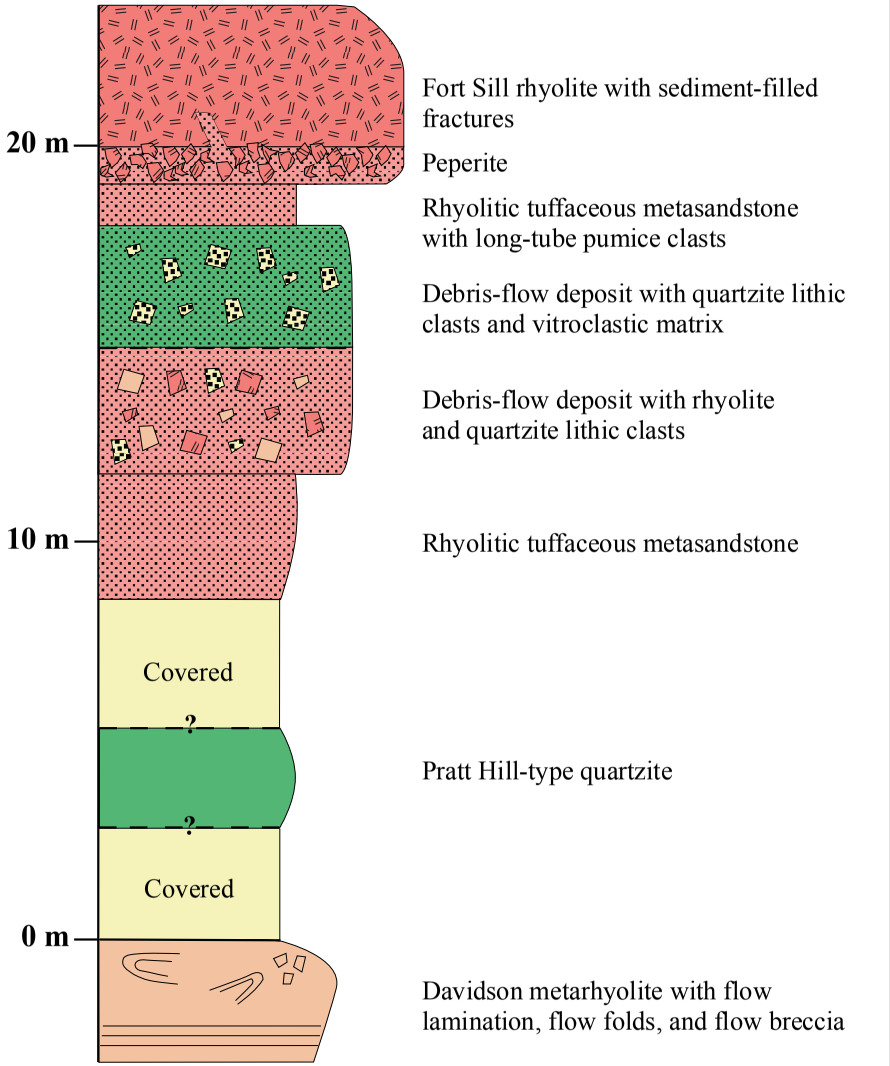

Figure 21. Measured section of volcaniclastic metasedimentary rocks exposed in the Hide-A-Way area at locality G on Figure 5.

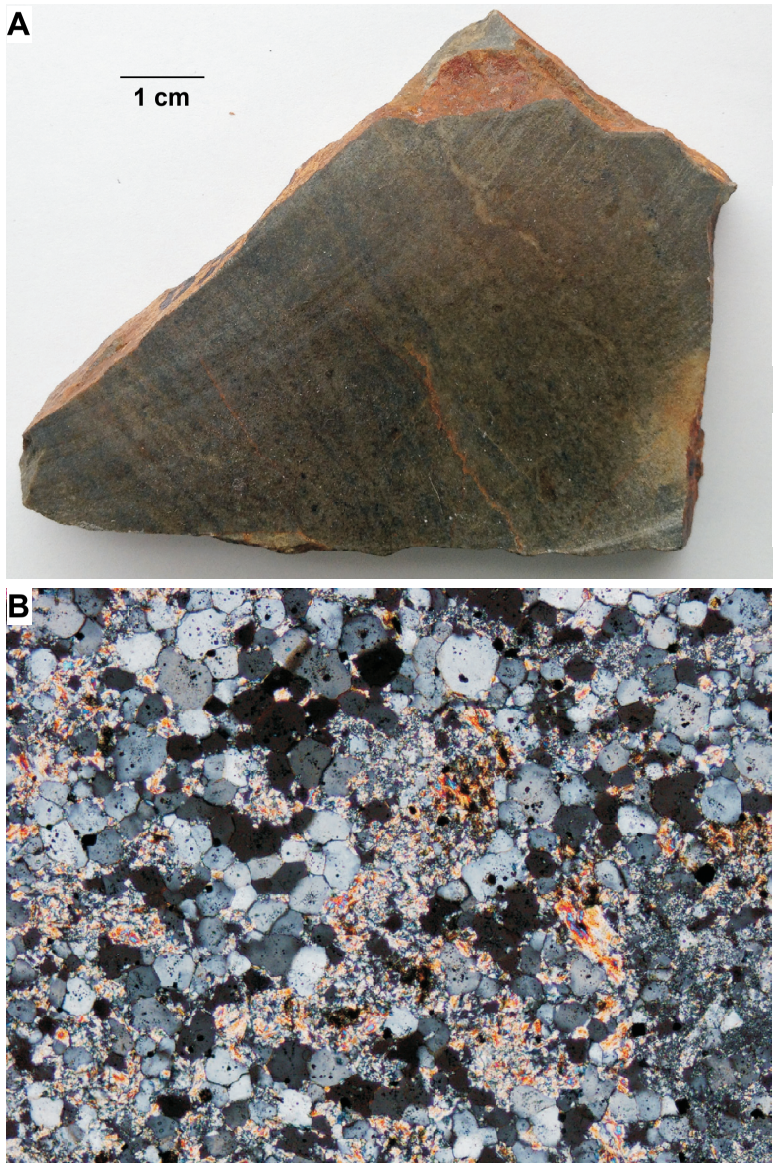

Figure 22. (A) Cut slab of Pratt Hill-type quartzite in the lower part of the volcaniclastic metasedimentary sequence exposed in the Hide-A-Way area. Planar lamination is visible running across the slab from upper left to lower right (saw marks run in the opposite direction). (B) Photomicrograph (crossed polars) of Pratt Hill type-quartzite exposed in the Hide-A-Way area showing recrystallized granoblastic quartz and interstitial sericite. Width of view is ~1.25 mm.

lite clasts record influx of volcanic debris that is unlike Davidson metarhyolite and predates emplacement of the Fort Sill rhyolite, suggesting a more complex evolution of the developing volcanic pile in the area than has previously been recognized.

The matrix of the debris-flow deposit is nearly identical to the underlying tuffaceous metasandstone except that it also contains coarse-silt-sized quartz grains. The lower half of the unit is pink in hand sample (Fig. 25) and contains moderate amounts of interstitial sericite. Fine-grained, interstitial vitroclastic material increases significantly in the upper part of the unit. The recrystallized vitroclastic material has been replaced by fine-grained green phyllosilicates, typically giving the rock a gray-green color in hand sample. The increase in interstitial vitroclastic material appears to be gradational, suggesting that both the pink and gray-green parts of this interval represent a single debris-flow deposit. Two separate debris-flow deposits could also be present, but extremely poor exposure precludes determination of contact relations. Nonetheless, this debris-flow interval occupies a similar stratigraphic position to the deposit that caps the Pratt Hill quartzite.

The debris-flow interval is overlain by a ~1-m-thick, rhyolitic tuffaceous metasandstone (Fig. 21) that contains relict long-tube pumice clasts as much as 4.75 mm long (Fig. 27). This unit is poorly sorted and contains 30 to 40% rounded, coarse-silt- to fine-sand-sized quartz grains. Medium to coarse, subangular to subrounded sand-sized quartz with subordinate alkali feldspar grains occur in amounts of 3 to 5%. Green metamorphic biotite ~0.3 mm in length and interstitial sericite, minor metamorphic plagioclase, and disseminated magnetite compose most of the remainder of the rock and are inferred to represent recrystallized vitroclastic material. Silt- and fine-sand-sized quartz grains from this unit have been intimately mixed with the base of the Fort Sill rhyolite, creating a peperite ~1 m thick (Fig. 21), which indicates that the sediment was wet and unconsolidated during emplacement of the overlying lava flow (see section on Fort Sill rhyolite below).

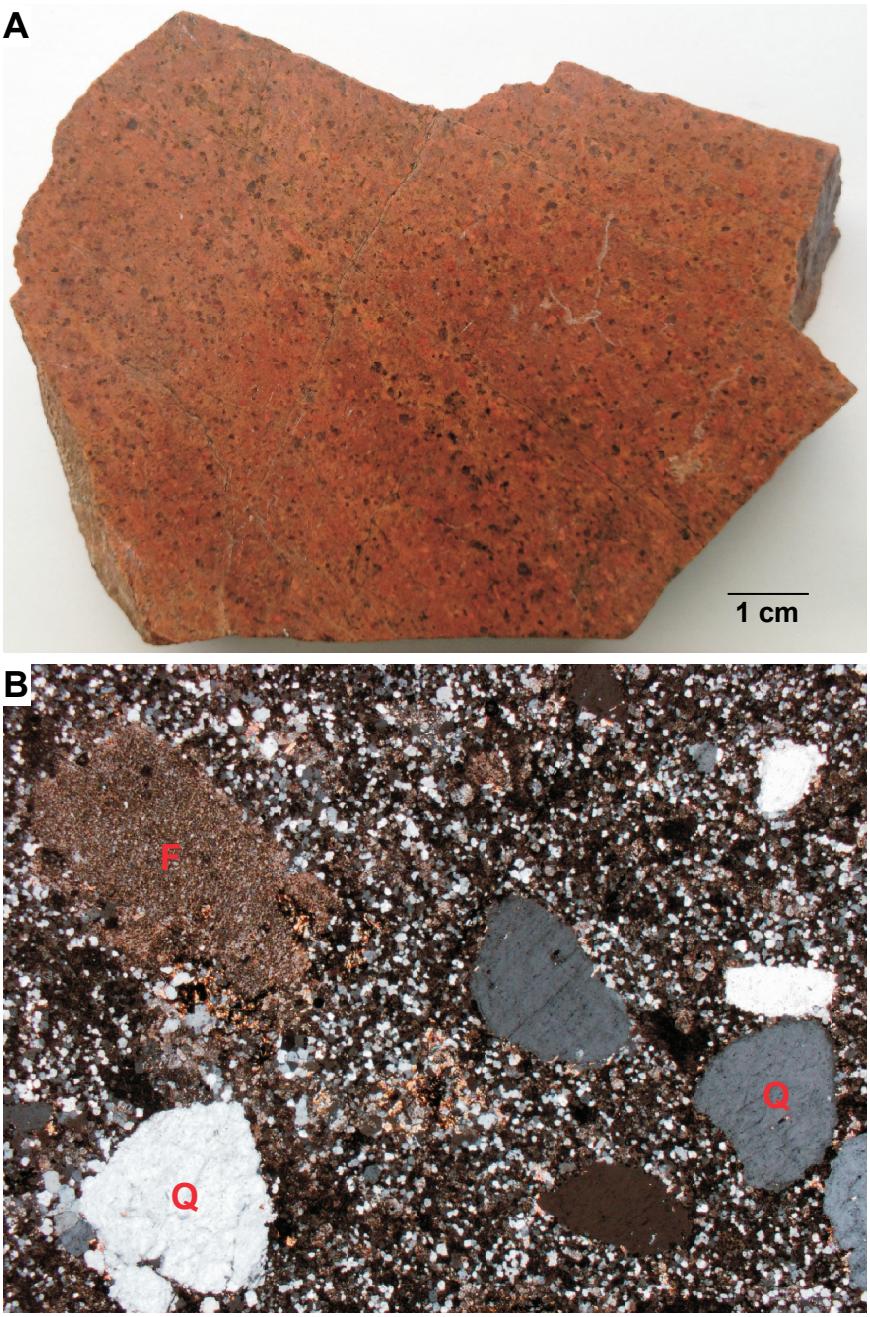

Figure 23. (A) Cut slab of lower unit of poorly sorted rhyolitic tuffaceous metasandstone exposed in the Hide-A-Way area. (B) Photomicrograph (crossed polars) of the same rock. Note the sand-sized quartz (Q) and alkali feldspar (F) grains in a very fine grained matrix. Width of view is ~5 mm.

West of the Hide-A-Way Area

Along an unnamed ridge ~2.3 km west of Pratt Hill is another exposure of rhyolitic volcaniclastic metasedimenta-

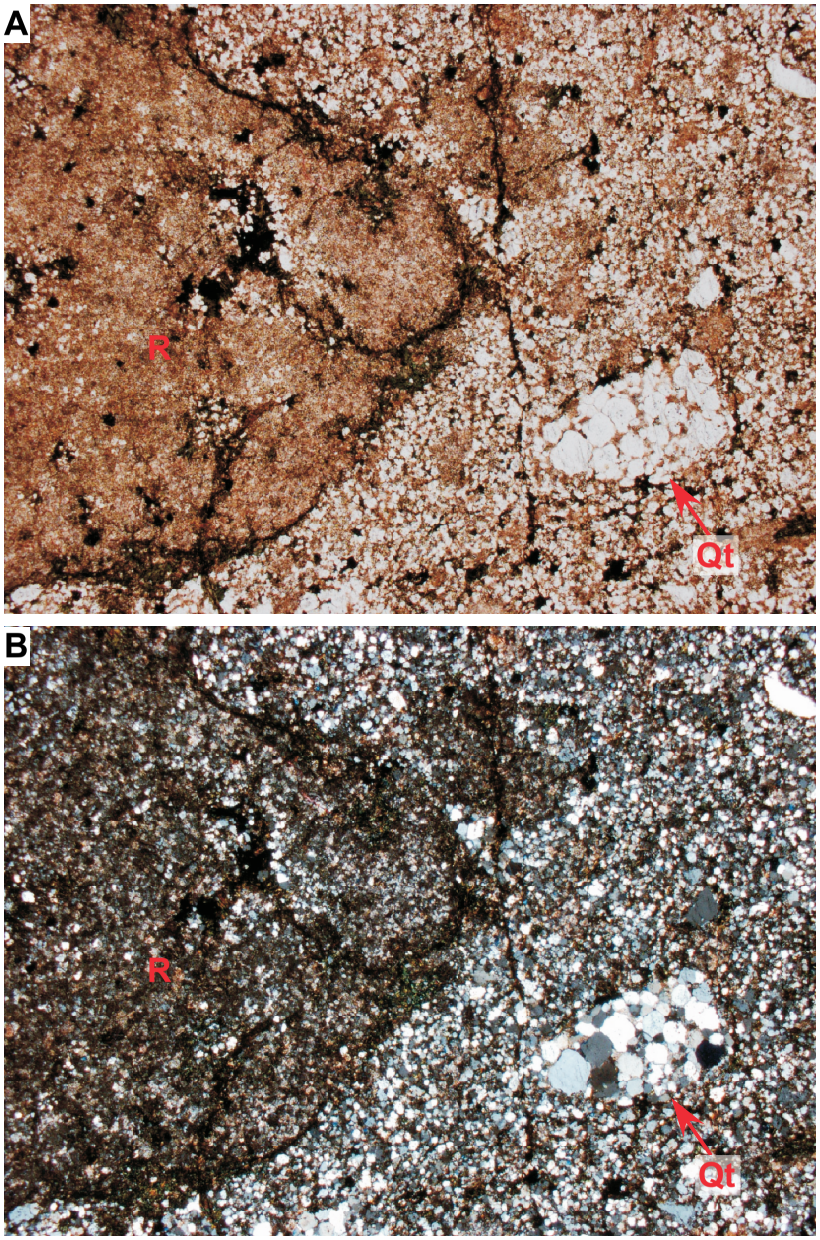

Figure 24. (A) Photomicrograph (plane light) of polymict debris-flow deposit showing clasts of aphyric, Davidson-type metarhyolite (R) and quartzite (Qt) enclosed in a poorly sorted, silt-sized, quartz-rich matrix. Width of view is ~5 mm. (B) Same view as in A with crossed polars.

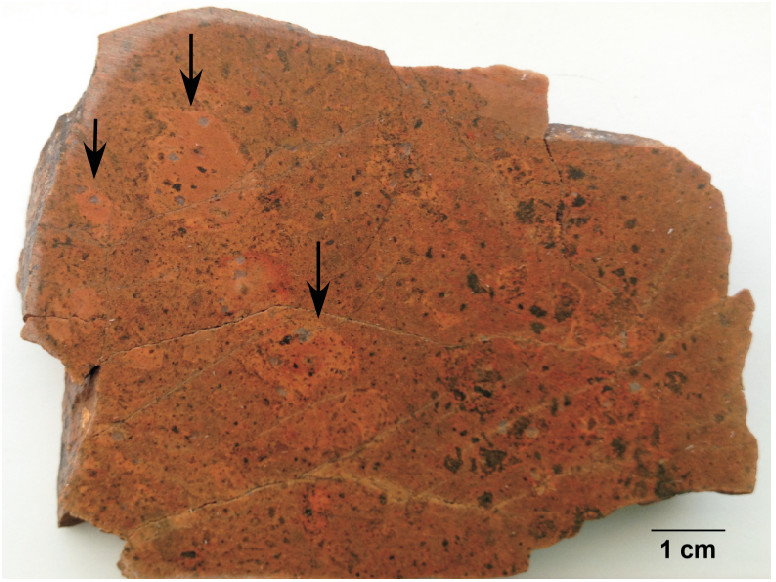

Figure 25. Cut slab showing porphyritic rhyolite lithic clasts (arrowed) in the lower part of the polymict debris-flow deposit exposed in the Hide-A-Way area.

Figure 26. Cut slab showing quartzite clast (lower right) and altered vitroclastic matrix in the upper part of the debris-flow deposit exposed in the Hide-A-Way area.

ry rocks that dip 12° to the south-southwest (locality B, Figs. 5 and 6). The outcrop consists mostly of a ~1-m-thick, rhyolitic volcaniclastic metasandstone with thin relict planar bedding and lamination (Fig. 28). This unit can be traced discontinuously along strike for ~94 m (Fig. 6). The metasandstone is poorly sorted and composed dominantly of subrounded to rounded, coarse-sand-sized alkali feldspar and quartz grains in roughly equal proportions (Fig. 29A and 29B), with interstitial recrystallized, coarse silt-sized quartz and alkali feldspar grains. The interstitial alkali feldspar grains have largely been replaced by sericite. Minor biotite ≤0.25 mm in length is present along with detrital zircon and disseminated magnetite. In places, the unit is capped by a metasiltstone 5 to 10 cm thick that is composed of ≥50% medium- to coarse-silt-sized quartz grains and interstitial sericite (Fig. 29A and 29B). The upper contact of the unit with the Fort Sill rhyolite is covered by thin soil and grass. As previously discussed, the base of the unit has been intruded by Mount Scott Granite (Fig. 6).

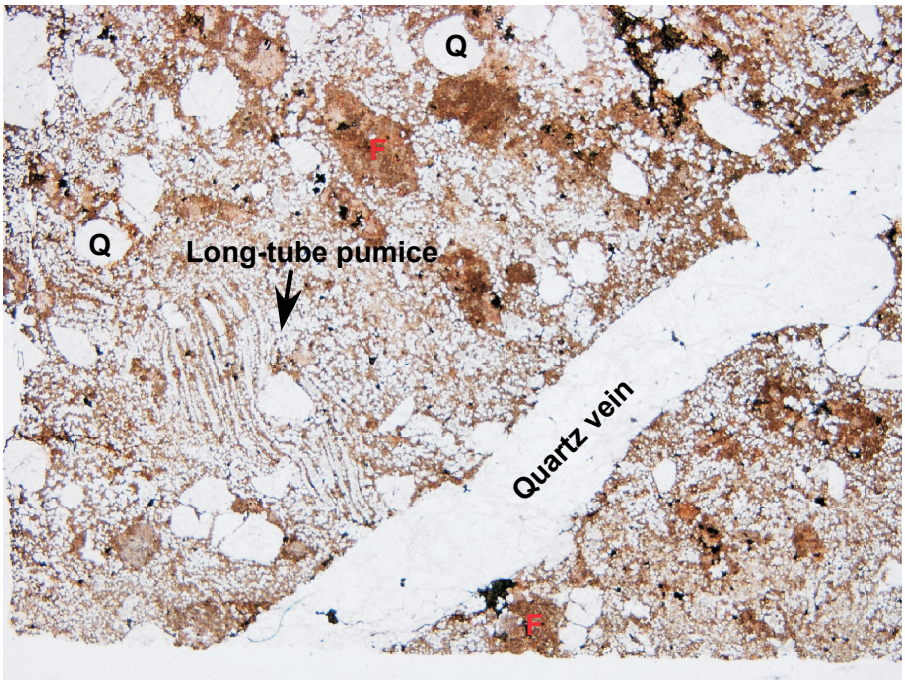

Figure 27. Photomicrograph (plane light) of poorly sorted, tuffaceous metasandstone in the upper part of the volcaniclastic metasedimentary sequence exposed in the Hide-A-Way area. A relict long-tube pumice clast is indicated. Quartz sand grains (Q) are visible, along with smaller amounts of alkali feldspar grains (F). Width of view is ~1.3 cm.

FORT SILL RHYOLITE

Introduction

The Davidson metarhyolite and the discontinuous interval of volcaniclastic metasedimentary rocks above it are overlain by the distinctive Fort Sill rhyolite. In contrast to the Davidson, the Fort Sill rhyolite contains abundant quartz and alkali feldspar phenocrysts and displays a vertical zonation defined by changes in groundmass texture and outcrop characteristics. This unit forms the majority of rhyolite exposed in the Fort Sill area (Fig. 2) and is the longest documented flow in the Carlton Rhyolite Group.

Previous Work

Beginning with Taff (1904), most of the fieldwork done on the Fort Sill rhyolite has been reconnaissance in nature. Taff

Figure 28. Outcrop of rhyolitic volcaniclastic metasedimentary rocks exposed west of the Hide-A-Way area showing thin planar bedding and lamination.

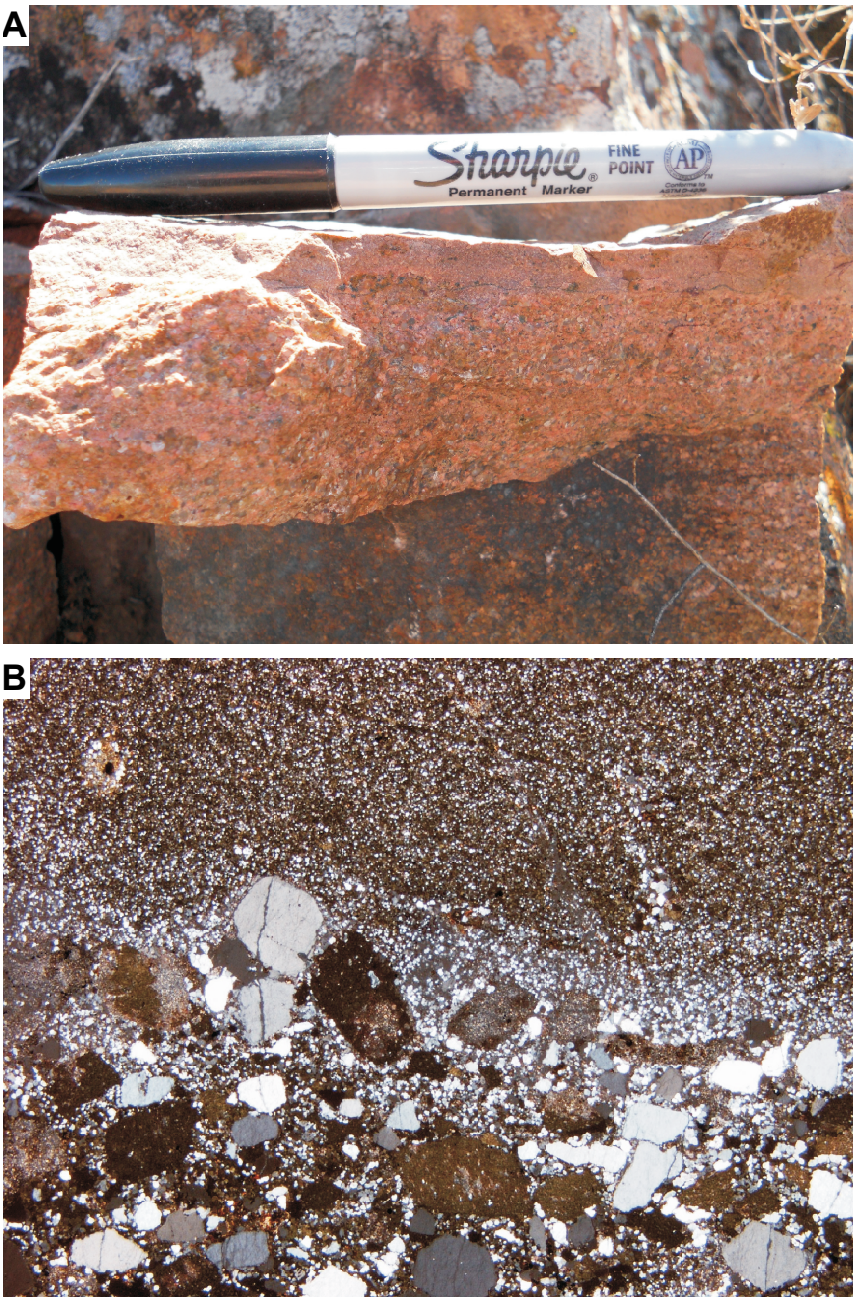

Figure 29. (A) Planar-bedded rhyolitic volcaniclastic metasandstone capped by a thin veneer of metasiltstone. (B) Photomicrograph (crossed polars) of metasandstone containing quartz and alkali feldspar grains, overlain by thin metasiltstone. Width of view is ~1.6 cm.

(1904) referred to the distinctive topography of rounded, grass-covered hills underlain by the rhyolite (Fig. 30) as the Carlton Mountain Group physiographic region and considered the rocks exposed there to be granite porphyry and associated aporhyolite (an old term for devitrified, originally glassy rhyolite). The name Carlton Mountain now refers only to a single peak among a series of hills in the area; this peak is largely within an artillery impact zone in Fort Sill and strictly off limits to the public. Hoffman (1930) interpreted the rocks underlying the hills in the Fort Sill area to be of shallow intrusive origin and named them the Carlton granophyre. Schoonover (1948) renamed the unit Carlton Rhyolite. Ham et al. (1964) included parts of the Fort Sill rhyolite in their study on the basement rocks of southern Oklahoma and introduced the term Carlton Rhyolite Group to include all related surface and subsurface rhyolite in the Wichita Igneous Province. However, they chose Bally Mountain, in the Slick Hills to the north (Fig. 1), as the type section of the group because a thick, well-exposed rhyolite sequence occurs in that area (see Hanson et al., this guidebook). In the first geochemical study of the Carlton Rhyolite, Hanson (1977) included samples from the Fort Sill rhyolite. In their study of the Pratt Hill quartzite, Sides and Miller (1982) included a portion of Fort Sill rhyolite that caps that hill. Gilbert (1982b), Miller et al. (1982), and Gilbert (1986) included some of the Fort Sill rhyolite in small limited studies in the Mount Scott Campground, Hide-A-Way, and Medicine Bluff areas, respectively. Additionally, Price (1998) included areas of Fort Sill rhyolite in his study on the Mount Scott Granite.

Field Characteristics and Devitrification Textures

The Fort Sill rhyolite can be traced along strike in a roughly east-west direction for ~18.5 km before becoming covered or being truncated by intrusive granite; thus its original extent is unknown (Fig. 2). Its base is poorly exposed along strike in limited areas where it overlies the Pratt Hill quartzite at Pratt Hill and associated volcaniclastic metasedimentary rocks at points to the west (Fig. 5). In those areas, the rhyolite dips ~10 to 12° to the south (Fig. 4), as defined by contacts with the underlying bedded metasedimentary rocks. The top is erosional, and the unit has a minimum exposed thickness of ~100 m at Medicine Bluffs. The total thickness of the Fort Sill rhyolite cannot be determined based on available data. One problem is that a cross-section from the exposed base

at Pratt Hill southward across the field area to Signal Mountain yields an unreasonable thickness of over 1 km (only part of this cross-section is shown in Figure 4). This assumes a constant dip of 10° to the south, as measured at the contact with the Pratt Hill quartzite. If the dip shallows to the south the rhyolite could be considerably less than 1 km thick. Furthermore, the amount of vertical displacement along the Deer Creek Canyon Fault Zone is unknown, and there is also a second prominent lineament to the south along Brush Canyon (Fig. 2) that parallels the Deer Creek Canyon Fault Zone. That lineament could not be investigated because it lies within the artillery impact zone. It is possible that the lineament along Brush Canyon represents another fault zone with unknown vertical displacement that offsets the Fort Sill rhyolite.

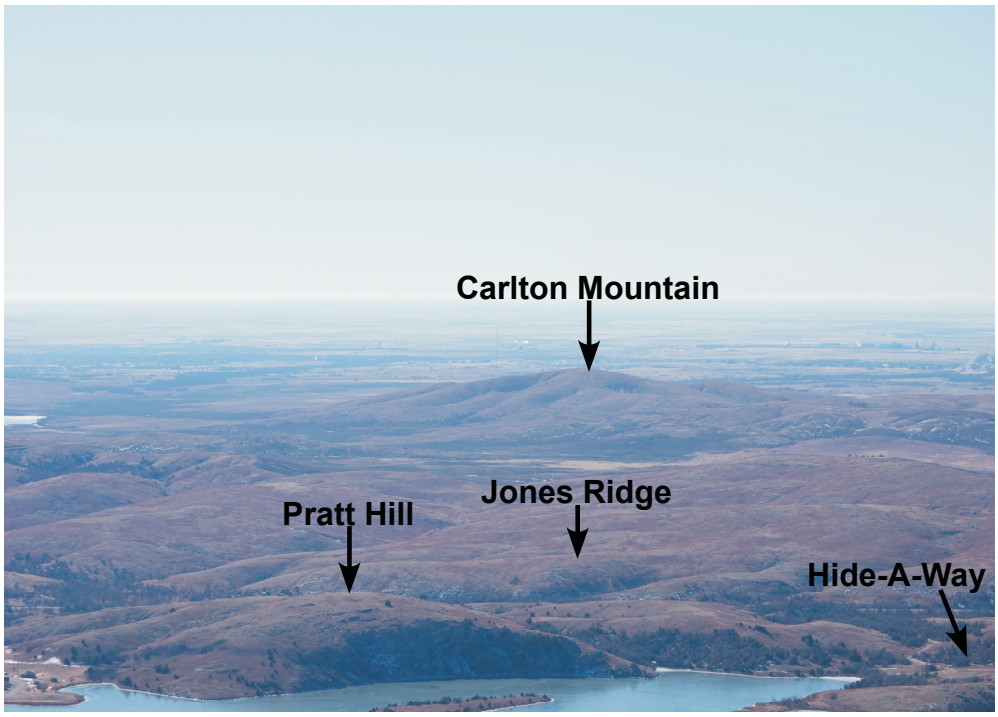

Figure 30. Photograph from the top of Mount Scott looking south toward Fort Sill Military Reservation. The characteristic topography of rounded, grass-covered hills underlain by Fort Sill rhyolite is well displayed by Pratt Hill, Jones Ridge, and Carlton Mountain. The base of the Fort Sill rhyolite is exposed on the steep, north-facing cliff of Pratt Hill. Location of the Hide-A-Way area is also indicated.

At its northern outcrop margin the Fort Sill rhyolite is truncated by the Little Medicine Creek Fault Zone, as previously discussed, or is intruded by Mount Scott Granite. To the south and east, the unit is either intruded by granite or covered by Permian sedimentary rocks and Quaternary alluvium (Fig. 2).

Vertical Zonation

In the Slick Hills to the north, individual flows within the Carlton Rhyolite typically display a readily identifiable vertical zonation defined by changes in groundmass textures and outcrop features (Hanson et al., this guidebook). Likewise, the Fort Sill rhyolite demonstrates a vertical zonation (Fig. 3), although some features contrast markedly with those described in units exposed in the Slick Hills. Three main zones characterize the Fort Sill rhyolite and are described below. Groundmass textures in the lowest part of the rhyolite show a clear metamorphic overprint, with development of granoblastic quartz and feldspar. The textures are similar to those developed in the Davidson metarhyolite, but the overprint progressively decreases upward. Higher in the Fort Sill rhyolite, there is little or no evidence for contact metamorphism.

Lower Part of Flow

In places, a very subtle vertical zonation in the Fort Sill rhyolite is present in the lower part of the flow and is defined by changes in groundmass textures visible at thin-section scale. This vertical zonation is best expressed where the base of the Fort Sill rhyolite is exposed at Pratt Hill (locality FS-144, Figs. 2 and 5). There, the groundmass in the basal ~0.5 m of the flow shows relict perlitic texture (Fig. 31A), indicating the original presence of glass. Although the perlitic texture has a strong metamorphic overprint, the diagnostic curved, onion-skin-like cracks are still readily apparent.

Immediately above the basal glassy zone, the groundmass in a transitional zone making up the next few meters of the flow is characterized by fine-scale snowflake texture (Fig. 31B), which is a devitrification texture defined by optically continuous patches of micropoikilitic quartz surrounding numerous feldspar microlites (Anderson, 1969). Anderson (1969, 1970) considered snowflake texture to be a diagnostic feature of welded ignimbrites. However, Green (1970) pointed out that the texture is common in lava flows,

and experiments by Lofgren (1971) showed the texture to result from the devitrification of silicic glass. Snowflake texture has been reported to occur within many other lava flows within the Carlton Rhyolite Group (e.g., Bigger and Hanson, 1992; Philips, 2002; Burkholder, 2005; Eschberger et al., paper, this guidebook).

Within this transitional zone rare, ovoid amygdules as much as 0.7 mm across are present and are lined with drusy quartz and filled with anhedral Fe-Ti oxides ~0.05 mm across, in addition to very fine grained green to yellow clay (Fig. 31B). Another feature of the transitional zone is a very delicate flow lamination that wraps around quartz and alkali feldspar phenocrysts and is parallel to the base of flow (Fig. 32A). This transitional zone grades rapidly into the homogenous interior of the flow that is mostly characterized by felsitic groundmass texture (Fig. 32B).

In addition to the originally glassy, perlitic base exposed on Pratt Hill, the base of the Fort Sill rhyolite is also exposed in a small drainage in the Hide-A-Way area west of Pratt Hill, where the rhyolite overlies the clastic metasedimentary interval (locality G, Fig. 5). Despite poor exposure, the basal ~1 m can be seen to consist of a discontinuous zone of peperite. The peperite contains angular to subangular fragments of rhyolite as much as ~5.5 cm across intimately mixed with rounded to subrounded silt- and fine-sand-sized quartz grains (Figs. 33A and 33B). The rhyolite clasts have a recrystallized groundmass, and some are also flow laminated. Immediately above the basal peperite, thin fractures extending at least 1.5 m up into coherent rhyolite are filled with similar sedimentary quartz grains (Fig. 34). Together, these features indicate that the rhyolite lava flowed over wet, unconsolidated sediment, causing quench fragmentation at the base and upward injection of fluidized sediment into fractures in the lava (e.g., Kokelaar, 1982). The base of the rhyolite in this area, as at Pratt Hill, contains a relatively strong metamorphic overprint with granoblastic quartz developed in the groundmass of some samples. The metamorphic overprint appears to be more intense in the Hide-A-Way area and tends to mask the vertical zonation in groundmass textures documented at Pratt Hill.

Flow Interior

Most of the outcrops of the Fort Sill rhyolite represent the interior of a large, tabular flow, and columnar jointing is visible in several places above the basal, originally glassy zone, including exposures at Pratt Hill above the lower glassy and transitional zones. Columns are as much as 1.5 m wide and plunge steeply, approximately perpendicular to the base of the flow. The best examples occur at Medicine Bluffs (Figs. 2 and 35) where a section of the flow ~100 m thick above the basal zone is well exposed in steep cliffs carved by Medicine Creek (Gilbert, 1986). Well-developed columns also occur on parts of Jones Ridge and Thompson Hill (Fig. 36). Development of these regular columns points to uniform cooling of a single, thick flow.

Parts of the flow interior are characterized by a uniform, unbanded felsitic appearance in both hand sample and thin section (Fig. 32B). The transition from the lower glassy chilled margin into homogeneous felsitic rhyolite is well displayed on Pratt Hill, as noted above. However, the interior of the rhyolite in many other places exhibits well-developed but discontinuous flow banding, in which individual bands in many cases are only traceable for ≤1 m (Fig. 37). This texture is particularly obvious along Jones Ridge and on Thompson Hill (localities FS-131, FS-136, and FS-137, Figs. 2 and 5). The banding is characterized by pink, planar domains that range from 0.5 mm to 4 cm wide and are contained within gray to dark-brown rhyolite showing relatively fine grained felsitic and/or snowflake texture in thin section. Many of the pink bands show flame-like terminations and hence could be termed fiamme (Figs. 38A and 38B), using this term in the nongenetic sense of Bull and McPhie (2007).

The banding generally shows highly variable attitudes and in places is clearly deformed by meter-scale flow folds, although poor exposure due to thick lichen cover and manganese staining precludes determination of fold geometries. In thin section, the internal texture of the pink bands consists partly of a distinctive intergrowth of quartz and alkali feldspar that is significantly coarser than the adjacent groundmass in the gray to dark brown bands (Figs. 38B and 39A). The texture is also partly spherulitic, with randomly oriented to radiating tridymite crystals (now inverted to quartz) as much as 0.38 mm in length (Fig. 39B). Radial, coalescing spherulites ≤0.75 mm in diameter dominate the texture in some cases. Axiolitic spherulites ≤0.3 mm long have developed along the inner boundaries of many of the pink bands (Fig. 39B). Along the outer margins of the bands, laminae defined by opaque microlites have, in places, been deformed into microscopic tight to isoclinal flow folds and partly incorporated into the bands (Fig. 39B). Discordant domains with identical coarse devitrification textures extend from some bands at high angles and cross-cut or connect with adjacent bands (Fig. 38). Such features are inconsistent with the interpretation that the discontinuous pink bands are highly flattened pumice formed within a strongly welded ignimbrite. Discontinuous lenticular domains somewhat similar to the discontinuous bands in the Fort Sill rhyolite have been described within extensive Devonian silicic lava flows

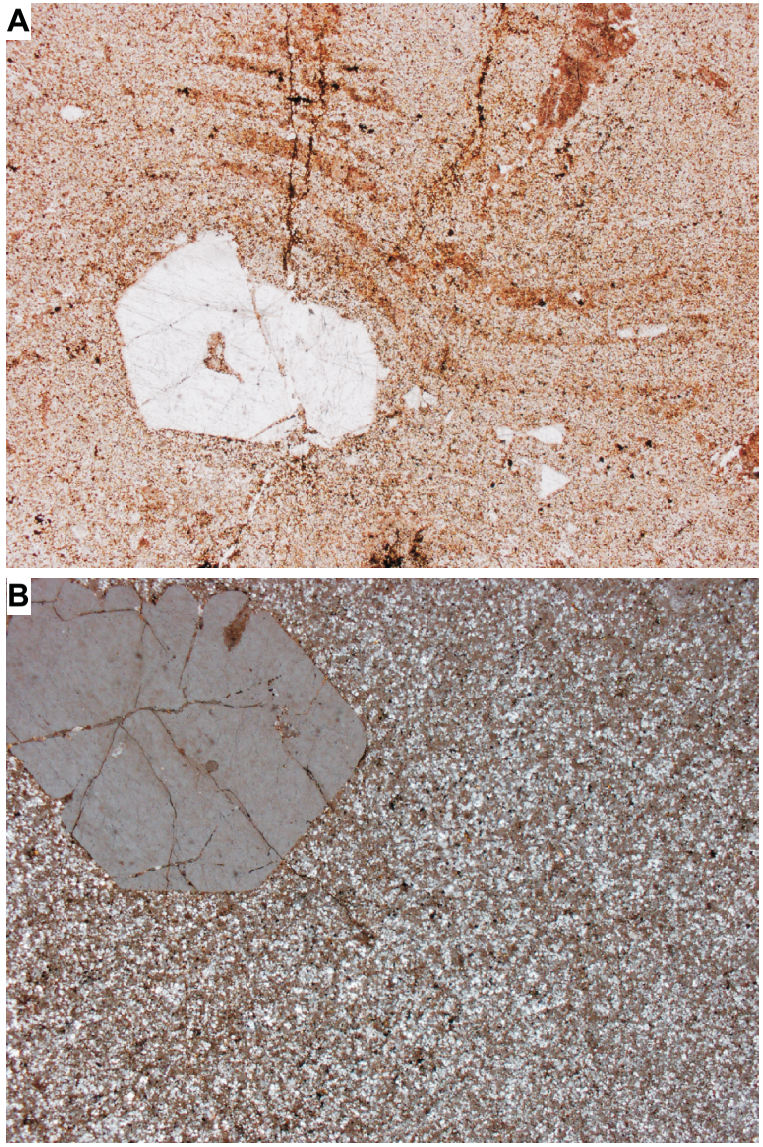

Figure 32. (A) Photomicrograph (plane light) of flow lamination wrapping around a quartz phenocryst in the basal transition zone of the Fort Sill rhyolite exposed on Pratt Hill. The quartz phenocryst has been tectonically fractured. Width of view is ~5 mm. (B) Photomicrograph (crossed polars) showing characteristic felsitic groundmass texture in the interior of the Fort Sill rhyolite exposed on Pratt Hill. A quartz phenocryst is visible in top left corner. Width of view is ~5 mm.

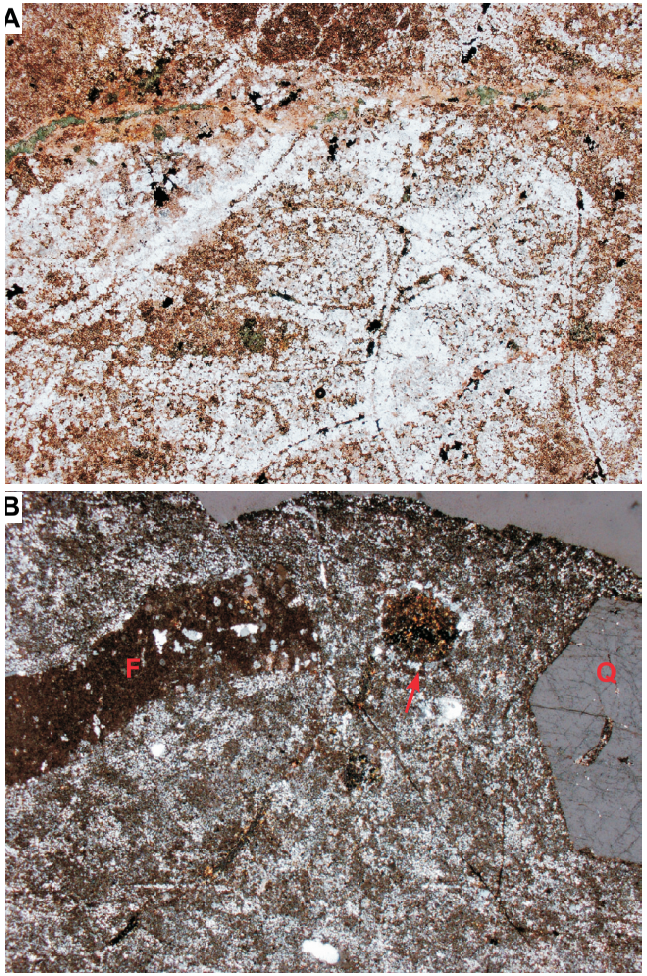

Figure 31. (A) Photomicrograph (plane light) of relict perlitic texture from the base of the Fort Sill rhyolite exposed on Pratt Hill. Very fine grained quartz and alkali feldspar mosaic formed during devitrification has been recrystallized during metamorphism, with some secondary silicification. Secondary silica and very fine grained opaque granules outline relict perlitic cracks. Width of view is ~5 mm. (B) Photomicrograph (crossed polars) of a sample from the transition zone between the originally glassy base and felsitic interior of the Fort Sill rhyolite exposed on Pratt Hill. Note the fine-scale snowflake groundmass texture and ovoid amygdule (arrow) filled with green-yellow clay and lined with drusy quartz. Quartz (Q) and partly silicified alkali feldspar (F) phenocrysts are also visible. Width of view is ~5 mm.

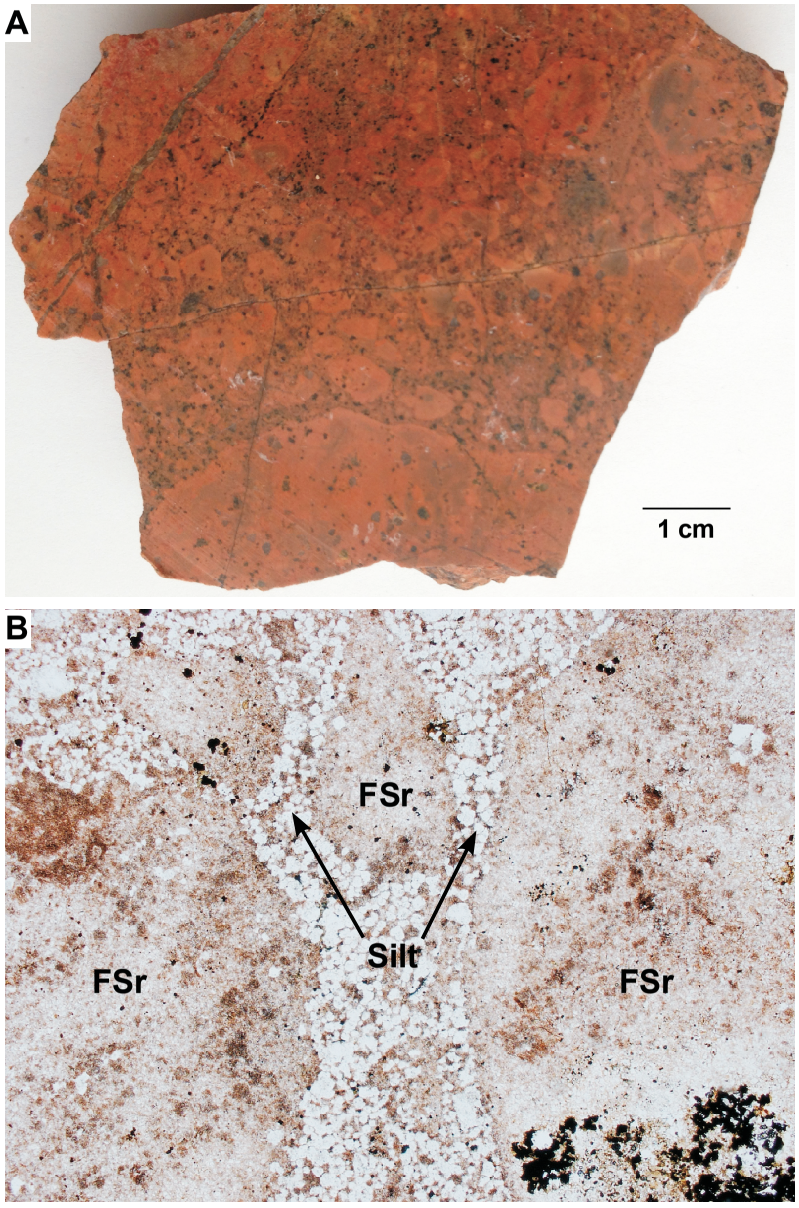

Figure 33. (A) Cut slab of peperite at the base of the Fort Sill rhyolite exposed in the Hide-A-Way area showing angular to subangular rhyolite clasts in a recrystallized matrix of sedimentary quartz grains. Dark-gray quartz phenocrysts are visible in the rhyolite. (B) Photomicrograph (plane light) of peperite. Note the silt grains injected into fractured rhyolite. FSr = Fort Sill rhyolite. Width of view is ~5 mm.

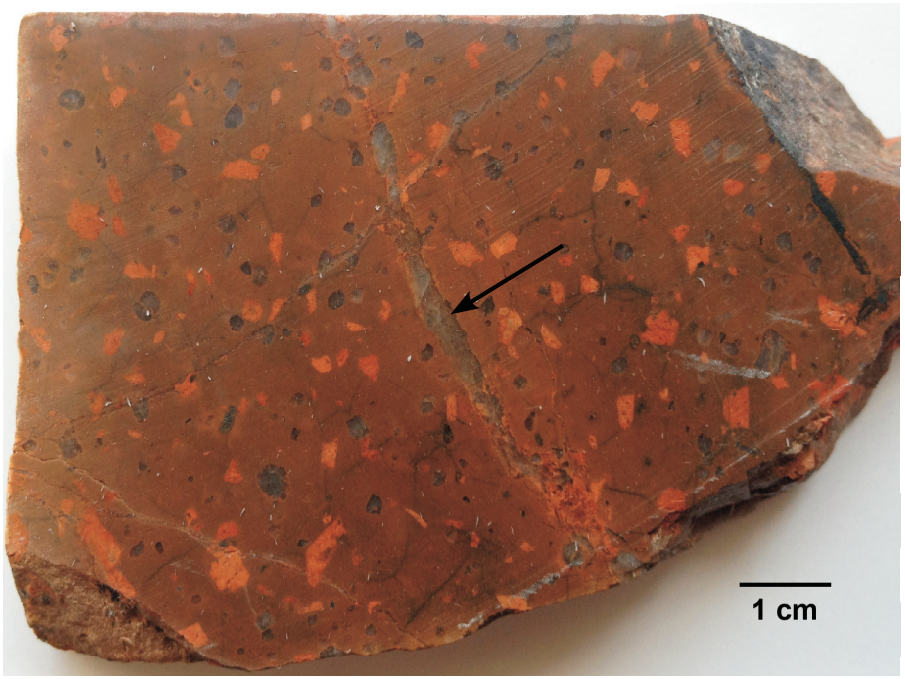

Figure 34. Cut slab of Fort Sill rhyolite overlying the basal peperite and showing a fracture filled with sedimentary quartz grains (arrow). Dark-gray quartz and pink alkali feldspar phenocrysts are visible in the rhyolite.

Figure 35. (A) Columnar jointing in the interior of the Fort Sill rhyolite exposed at Medicine Bluffs. Height of the bluff is ~100 m. (B) Closer view of columnar jointing in the interior of the Fort Sill rhyolite exposed at Medicine Bluffs. Width of columns is ~1 to 2 m.

Figure 36. Columnar jointing in the interior of the Fort Sill rhyolite exposed at Thompson Hill (Fig. 2), ~15 km west of Medicine Bluffs. Width of columns is ~1.5 m. Hammer (circled) for scale.

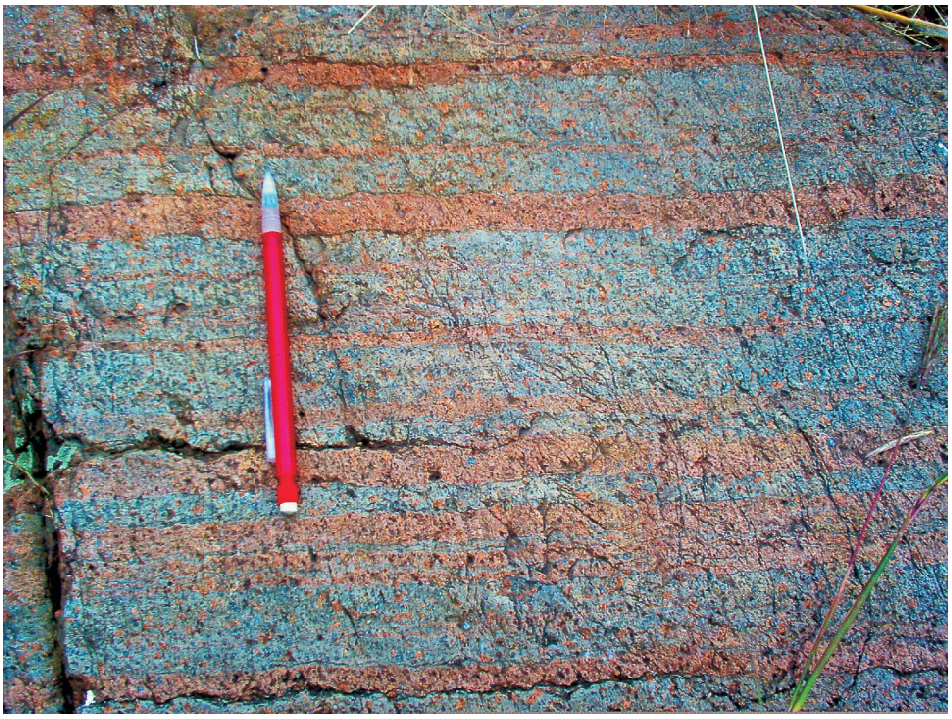

Figure 37. Outcrop of discontinuous flow banding developed in the interior of the Fort Sill rhyolite on Jones Ridge. Pencil points to a thin, discontinuous pink flow band that tapers to each side.

in southeastern Australia by Dadd (1992). As in the Fort Sill rhyolite, the features documented by Dadd (1992) show flame-like terminations and have coarser grained devitrification textures than adjacent parts of the lava. Dadd (1992) attributed these discontinuous domains to the concentration of volatiles along shear planes developed during laminar viscous flow, with subsequent selective devitrification affecting the volatile-rich domains (see also Bull and McPhie, 2007). We interpret the discontinuous bands with flame-like terminations in the interior of the Fort Sill rhyolite to have formed in a similar manner. Sides and Miller (1982) previously recognized fiamme-like features in the lower part of the Fort Sill rhyolite in the Pratt Hill area and used these features to support emplacement of the unit as an ignimbrite. We disagree with this interpretation for the reasons given above.

Upper Part of Flow

To the northwest of Medicine Bluffs, the rhyolite is also well exposed in the Heyls Hill-Rumbough Hill-Apache Ridge area (locality FS-88, Fig. 2). In that area, flow banding is unusually well developed and differs significantly from that described above from the interior of the rhyolite. Near the top of Heyls Hill, individual flow bands lack flame-like terminations and can be traced continuously for several meters in zones as much as 10 m thick. They are deformed in places by steeply plunging, open flow folds with wavelengths of as much as 2 to 3 m (Fig. 40A). Small-scale upright, open flow folds with wavelengths ≤10 cm are present along Apache Ridge (Fig. 40B).

Flow bands in this part of the flow are defined by alternations of orange-gray, felsitic rhyolite and dark green, originally glassy rhyolite; the thicker bands internally show a delicate, fine-scale flow lamination (Fig. 41A). In thin section, the banding is overprinted by well-developed snowflake texture. Flow lineation is developed on flow-band surfaces (Fig. 41B), and local areas of flow breccia ~1 m across are also present. This combination of features, including the relative abundance of original glass and the presence of flow breccia, suggests that the outcrops in the Heyls Hill-Rumbough Hill-Apache Ridge area are near the original top of the rhyolite flow.

Mineralogy and Phenocryst Textures

Modal analyses for 15 representative samples from the Fort Sill rhyolite and the two hypabyssal rhyolite bodies that intrude it are given in Table 1; sample locations are shown in Figures 2 and 5. For each sample, a total of 500 points was counted on cut slabs, on which major phenocryst phases are readily visible. Total phenocryst abundances for the Fort Sill rhyolite range from 11.6 to 29.0 %.

Alkali feldspar phenocrysts are the dominant phase in most samples, with abundances ranging from 7.2 to 19.6 %. These crystals are as much as 7 mm in length and range from euhedral to anhedral but are most commonly subhedral. Carlsbad twinning is not uncommon, particularly on euhedral to subhedral crystals. Some of the larger feldspar phenocrysts have been resorbed to some degree, which imparts a spongy texture and indicates reaction with the melt in the magma chamber prior to eruption or during magma ascent. Variable alteration to sericite is very common and chlorite has partially replaced some phenocrysts, indicating some element mobility during alteration. Hematite dust permeates the groundmass and also occurs within alkali feldspar

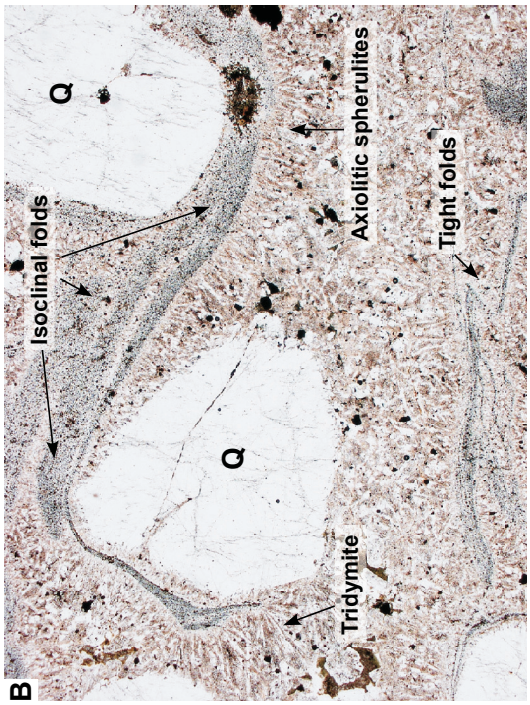

Figure 39. (A) Photomicrograph (crossed polars) of pink band from the interior of the Fort Sill rhyolite on Jones Ridge showing coarse devitrification texture that consists of a distinctive quartz and alkali feldspar intergrowth. Q = quartz phenocrysts. Width of view ~5 mm. (B) Photomicrograph (plane light) of same view as in A. Note randomly oriented tridymite needles (inverted to quartz), axiolitic spherulites growing inward from the margins of the band, and tight to isoclinal flow folds defined by laminae of opaque microlites along margins of the band. Width of view is ~5 mm.

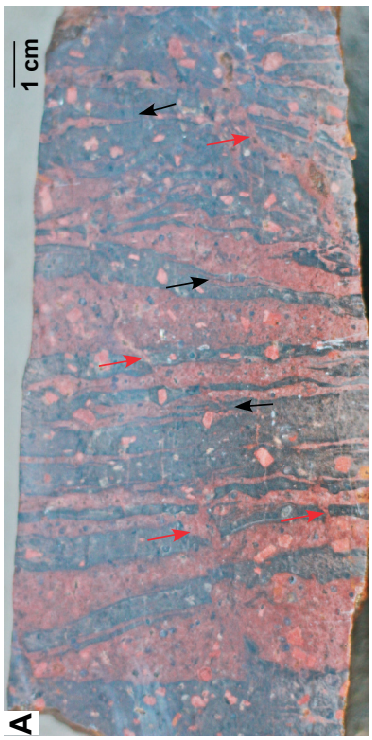

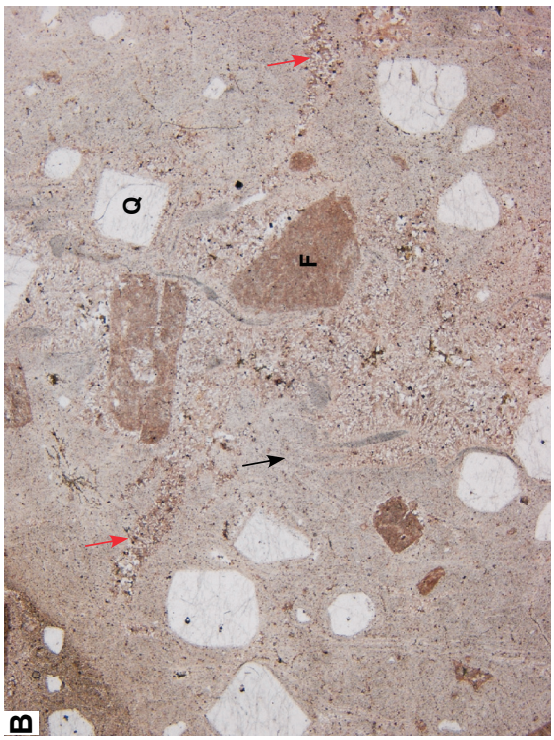

Figure 38. (A) Cut slab from the interior of the Fort Sill rhyolite on Jones Ridge showing discontinuous pink flow bands with flame-like terminations (black arrows) alternating with gray bands. Red arrows point to discordant pink domains cutting across the main banding and connecting adjacent pink bands. Dark-gray quartz and pink alkali feldspar phenocrysts are visible in the rhyolite. (B) Photomicrograph (plane light) of pink flow band in the center with coarse devitrification texture and gray bands showing delicate flow lamination to each side. Main banding is vertical in this view. Note the flame-like terminations of the pink band (black arrow) and discordant devitrification domains (red arrows) that cut across the flow lamination in the gray bands at a high angle. Quartz phenocrysts (Q) are clear and alkali feldspar phenocrysts (F) are cloudy. Width of view is ~2 cm.

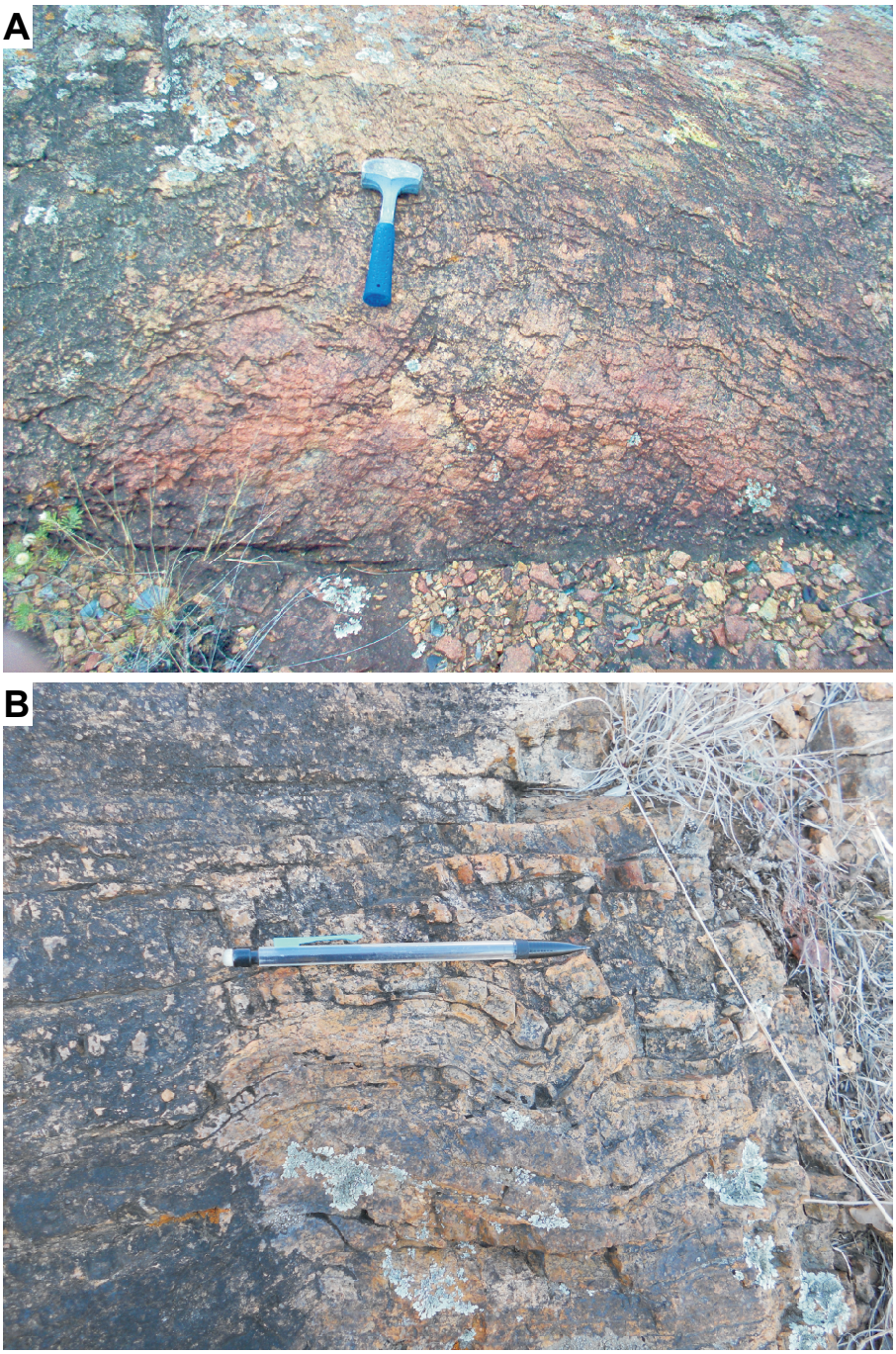

Figure 40. (A) Steeply plunging, open flow fold in the upper part of the Fort Sill rhyolite exposed on Heyls Hill. (B) Upright, open flow folds in the upper part of the Fort Sill rhyolite exposed on Apache Ridge.

phenocrysts, imparting a pinkish hue. Many alkali feldspar phenocrysts have been wholly or partly replaced by chessboard albite, indicating Na-metasomatism has affected those crystals (e.g., Smith, 1974). Rare plagioclase phenocrysts with albite twinning occur in places and are generally found as single isolated phenocrysts ≤1 mm in size and less commonly as a component in glomerocrysts.

Quartz phenocrysts make up 2.6 to 9.4 % of the rhyolite, with crystals as much as 3 mm in diameter. Some phenocrysts retain the dipyramidal outline of β-quartz, but many are rounded and extensively embayed. The quartz crystals typically show diffuse margins that poikilitically enclose microlites within the adjacent groundmass, which is inferred to result from small-scale silica mobility during devitrification. The Fort Sill rhyolite contains many examples of quartz phenocrysts with elongated, tube-like embayments with bulbous tips (Fig. 42A) that are thought to result from "bubble drilling," as produced experimentally by Donaldson and Henderson (1988). These workers theorize that small-scale convection of melt induced by non-equilibrium conditions near a bubble-crystal boundary can increase rates of locally enhanced dissolution of the solid. Granophyre inclusions as much as 2.75 mm across were found in several samples in different parts of the Fort Sill rhyolite (Fig. 42B) and are inferred to have been derived from zones of sidewall crystallization that developed in the magma chamber prior to eruption.

Mafic silicate phenocrysts as much as ~2 mm long have been completely replaced by green or brown clay and/or magnetite, hematite, goethite, limonite, leucoxene, chlorite, and more rarely, calcite (Fig. 43A). Based on their outlines, the primary mafic phase was probably pyroxene, although fayalite may also have been present. The mafic silicate phenocrysts are only found in some samples and generally occur in amounts of <1%. They are typically not visible on rock slabs and were not point counted.

Fe-Ti oxides, which range in abundance from 0.6 to 2.8 %, are disseminated throughout most samples and are variably altered to hematite and leucoxene. They are mostly anhedral and vary considerably in size but are generally <1 mm. Larger titanomagnetite crystals have octahedral outlines in some cases. Glomerocrysts are uncommon and generally con-

sist of two or three alkali feldspar and quartz phenocrysts as much as 5 mm in length (Fig. 43B). However, Fe-Ti oxides along with associated zircon are components of some glomerocrysts, as are quartz, rare plagioclase, and mafic silicate pseudomorphs (Fig. 43A). Subhedral to anhedral zircon is a common accessory phase in the Fort Sill rhyolite, where it has a particular affinity for Fe-Ti oxides. Isolated zircon crystals occur in the groundmass but they are most commonly found adhering to the margins of Fe-Ti oxide crystals.

It is not unusual to find secondary fluorite as much as 0.5 mm in size that has grown on quartz and alkali feldspar phenocrysts, partially fills rare amygdules (Fig. 44), or is present in quartz-rich veinlets in samples collected near contacts with intrusive granite. Fluorite is probably more common than was observed because it is easily overlooked during routine petrography. Its abundance is consistent with the A-type geochemical compositions of the rocks (see section on geochemistry below).

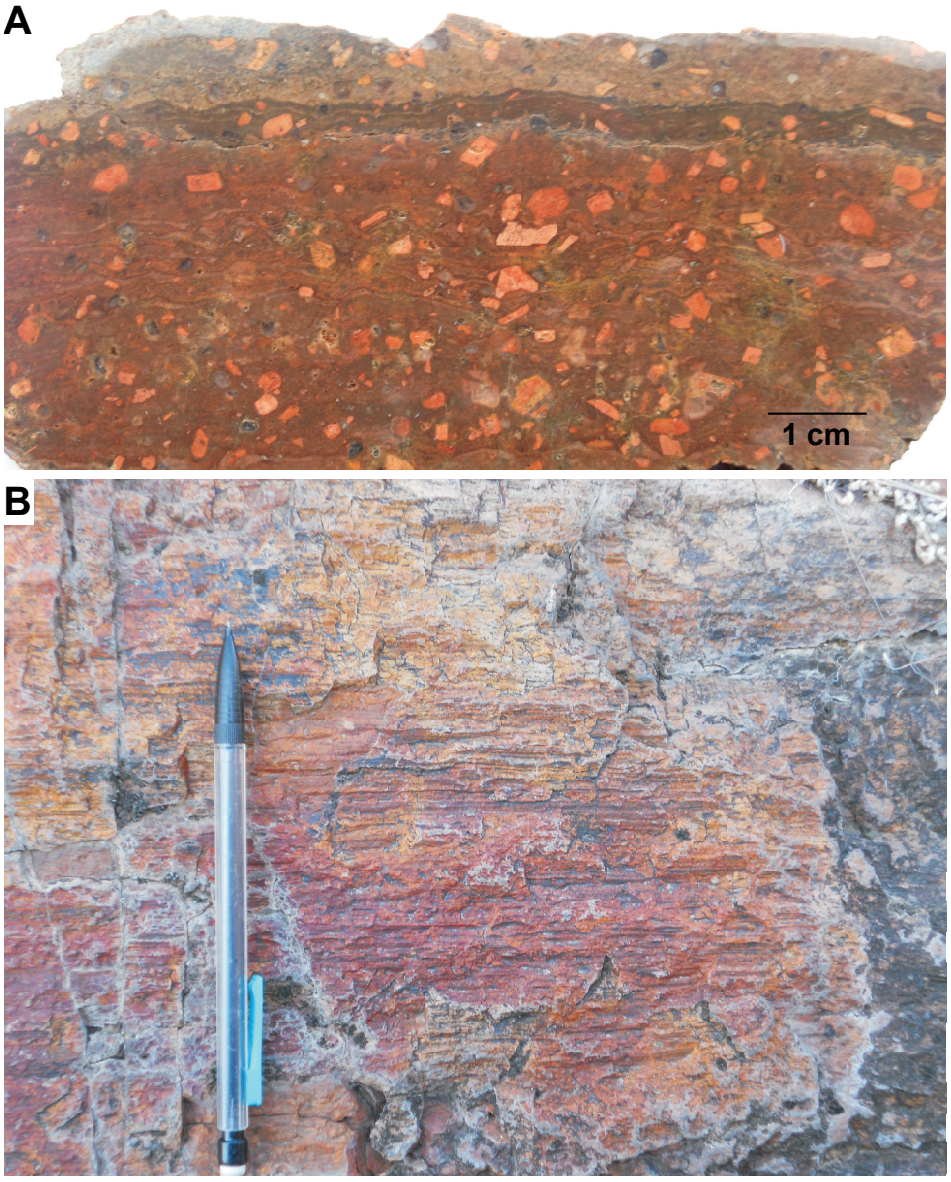

Figure 41. (A) Cut slab from the upper part of the Fort Sill rhyolite at Heyls Hill showing green, originally glassy band at top in contact with orange-gray band below that shows a delicate internal flow lamination. Dark-gray quartz and pink alkali feldspar phenocrysts are visible. (B) Flow lineation developed on a flow-band surface in the upper part of the Fort Sill rhyolite exposed on Apache Ridge.

Hydrothermal Alteration

Zones of intense hydrothermal alteration are locally present in some exposures of Fort Sill rhyolite. Highly altered rhyolite in a zone ~100 m wide is exposed along the north bank of Medicine Creek, directly across from Medicine Man's Walk, the saddle between two parts of Medicine Bluffs. There, domains of white to light-gray or green rhyolite ~2 cm to ~1 m wide trend N20°W to N45°W and are in contact with less-altered brick-red rhyolite (Fig. 45A). The altered zone is less resistant to erosion than the surrounding unaltered rhyolite, creating a slight depression. Alkali feldspar phenocrysts and feldspar in the groundmass have been completely replaced by very fine grained green clay and white mica. The altered feldspar phenocrysts have been partly dissolved away, leaving small rectangular pits (Fig. 45B). Quartz phenocrysts have not been altered and stand out in relief on weathered surfaces. A similar zone of highly altered gray to green rhyolite at least ~3 m long and ~0.5 m wide was found on the saddle between Heyls Hill and Rumbough Hill but is poorly exposed. Schoonover (1948) reported similar alteration on Mount Hinds but did not give any descriptive details. The alteration only occurs locally and its origin is unknown. Schoonover (1948) and

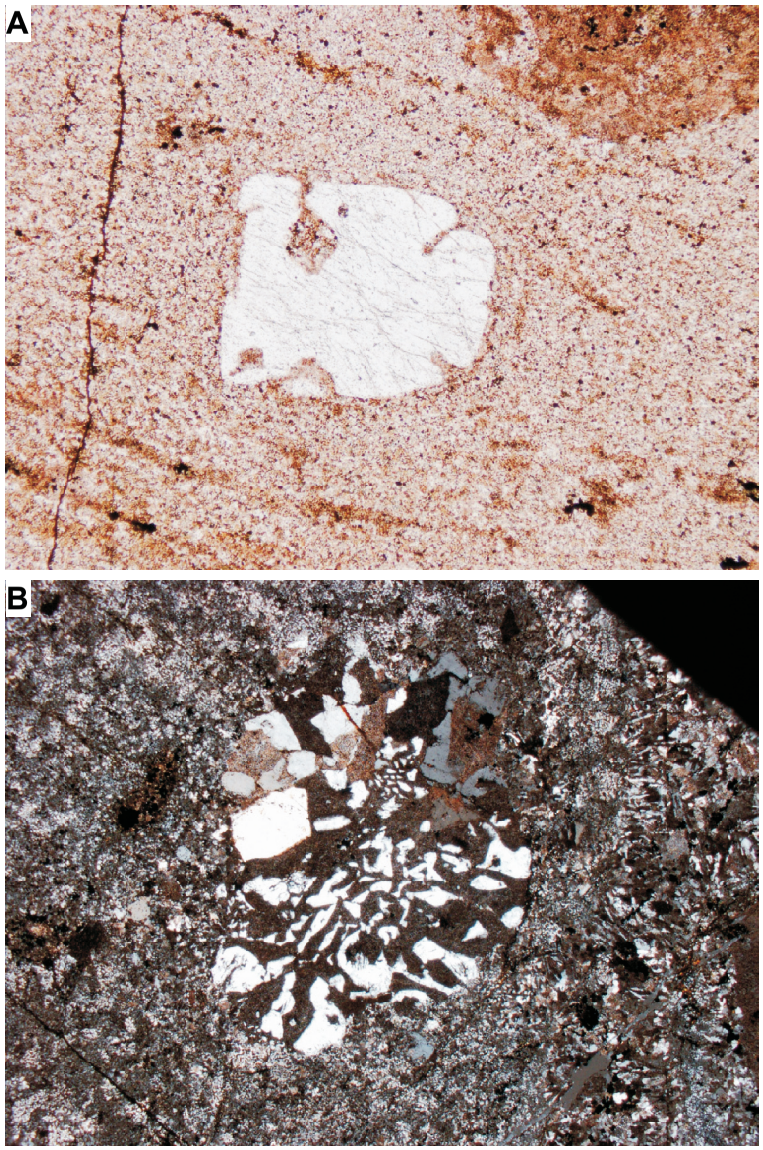

Figure 42. (A) Photomicrograph (plane light) of embayed quartz phenocryst. Note the bulbous tips of the embayments. Width of view is ~2.5 mm. Flow lamination is visible in the adjacent groundmass and an alkali feldspar phenocryst is present in the upper right. (B) Photomicrograph (crossed polars) of granophyre inclusion contained in groundmass showing snowflake texture. Note coarser flow band with randomly oriented tridymite to the right. Width of view is ~5 mm.

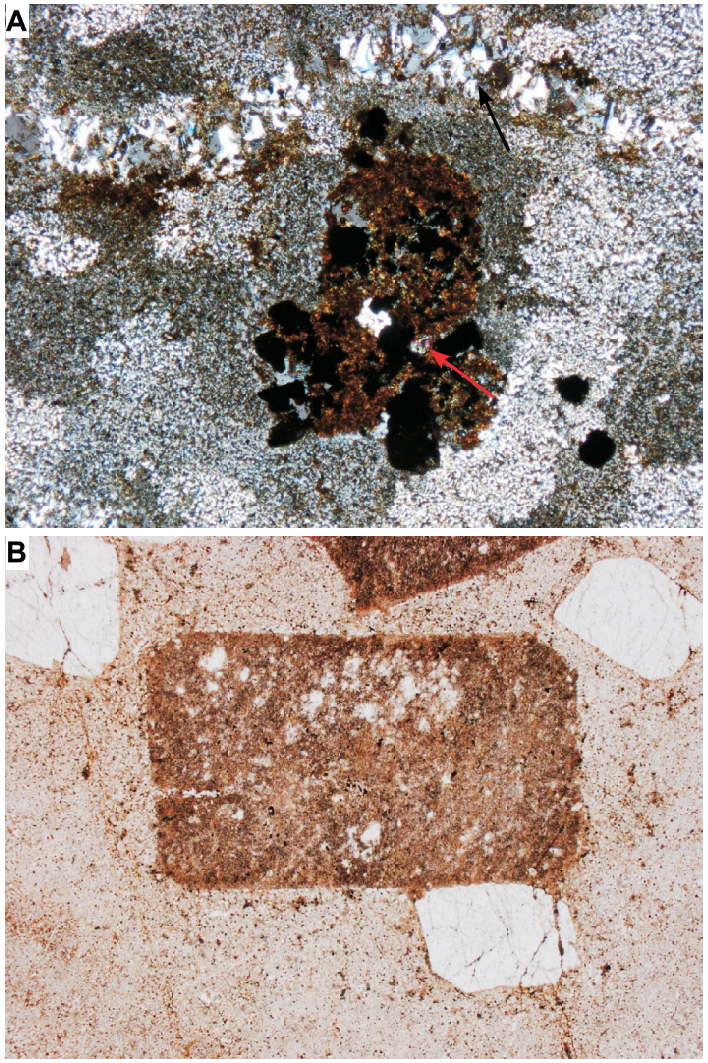

Figure 43. (A) Photomicrograph (crossed polars) of a glomerocryst composed of a mafic silicate pseudomorph and primary magnetite (partially replaced by hematite) and zircon (red arrow). The mafic silicate has been completely replaced by very fine grained green-brown clay intergrown with hematite and leucoxene. Note the flow lamination (black arrow) wrapping the glomerocryst and the well-developed snowflake texture in the rest of the groundmass. Width of view is ~2.5 mm. (B) Photomicrograph (plane light) of glomerocryst composed of alkali feldspar (cloudy) and quartz (clear). Width of view is ~5 mm.

Gilbert (1986) report the presence of a diabase dike and quartz veins within Medicine Man's Walk, and Schoonover (1948) inferred that the alteration of rhyolite across the creek from that feature was related to intrusion of the diabase dike. However, this type of alteration is not present elsewhere in the field area where diabase dikes can be directly observed cutting Fort Sill rhyolite, nor is it generally present where diabase intrudes other felsic units in the Wichita Province. An alternative and more likely possibility is that the hydrothermal alteration was caused by fluids that were released during intrusion of Mount Scott Granite and migrated along zones of weakness in the rhyolite. The diabase dike in Medicine Man's Walk likely followed the same zone of weakness that focused the hydrothermal alteration in that area.

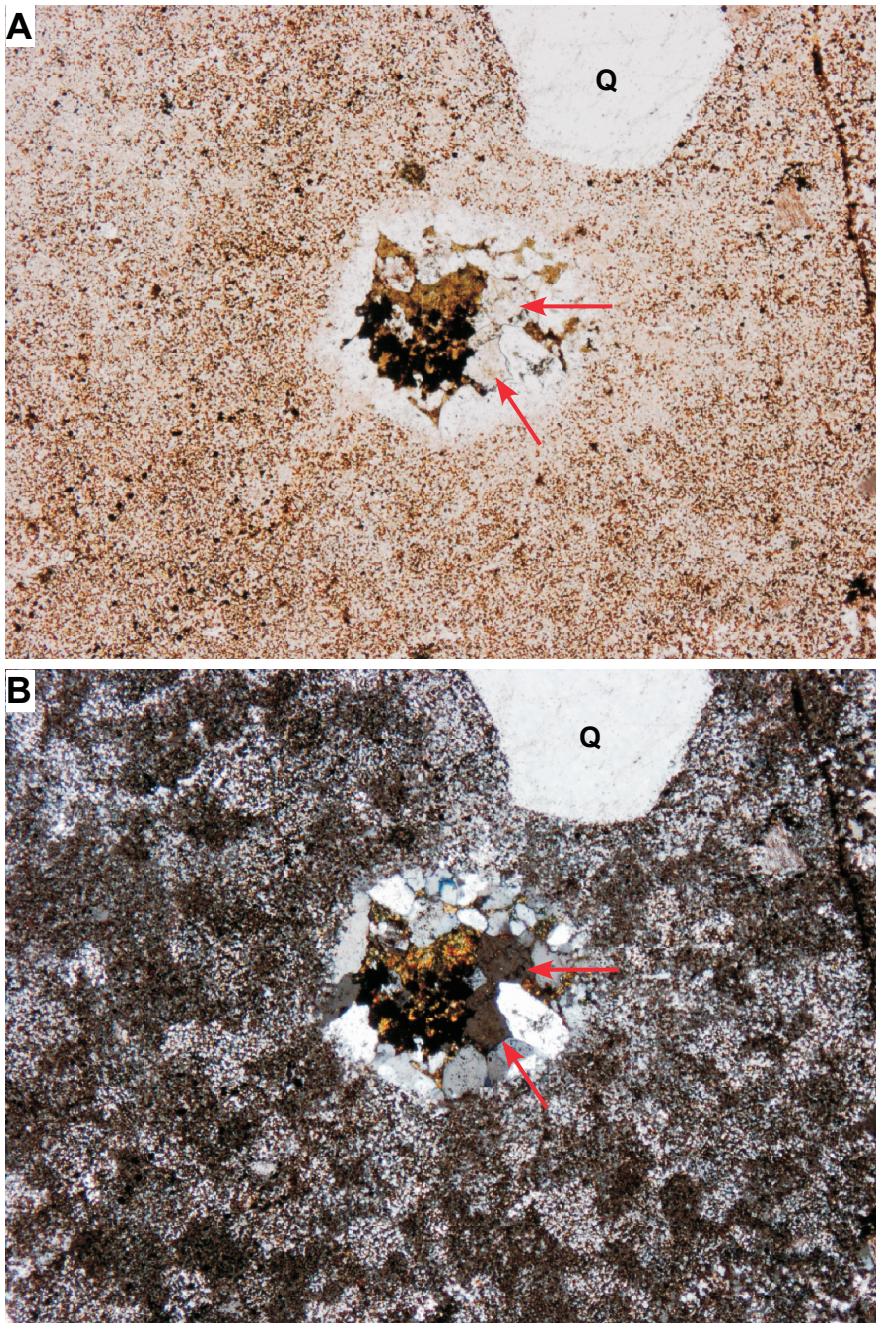

Figure 44. (A) Photomicrograph (plane light) of amygdule that is lined with drusy quartz and filled with fluorite (red arrows), titanomagnetite, and very fine grained green-yellow clay. Q = quartz phenocryst. Width of view is ~2.5 mm. (B) Photomicrograph (crossed polars) of same view as in A.

GEOCHEMISTRY

Introduction

Geochemical analyses were carried out on 15 representative samples from the Fort Sill rhyolite, three from the Davidson metarhyolite, and two from the rhyolite intrusions. Major and some trace elements were analyzed using x-ray fluorescence, and five samples from the Fort Sill rhyolite were analyzed for additional trace elements using ICP-MS. The data are shown in Table 2 and sample locations are shown in Figures 2 and 5.

Primary igneous chemical compositions and trends in ancient igneous rocks may be disturbed by secondary alteration. Samples from the Davidson metarhyolite show a strong metamorphic overprint and ubiquitous secondary silicification and sericitization. Geochemical data from this unit should therefore be treated with caution. Samples from the Fort Sill rhyolite are less altered, particularly away from intrusive granite contacts. However, many thin sections from the Fort Sill rhyolite contain chessboard albite that has replaced alkali feldspar phenocrysts, providing petrographic evidence for alkali metasomatism. Some samples also show varying degrees of sericitization. As such, care must be taken when interpreting the geochemical data from this unit as well, particularly with respect to Na_2O and K_2O contents and mobile trace elements such as Rb, Ba, and Sr.

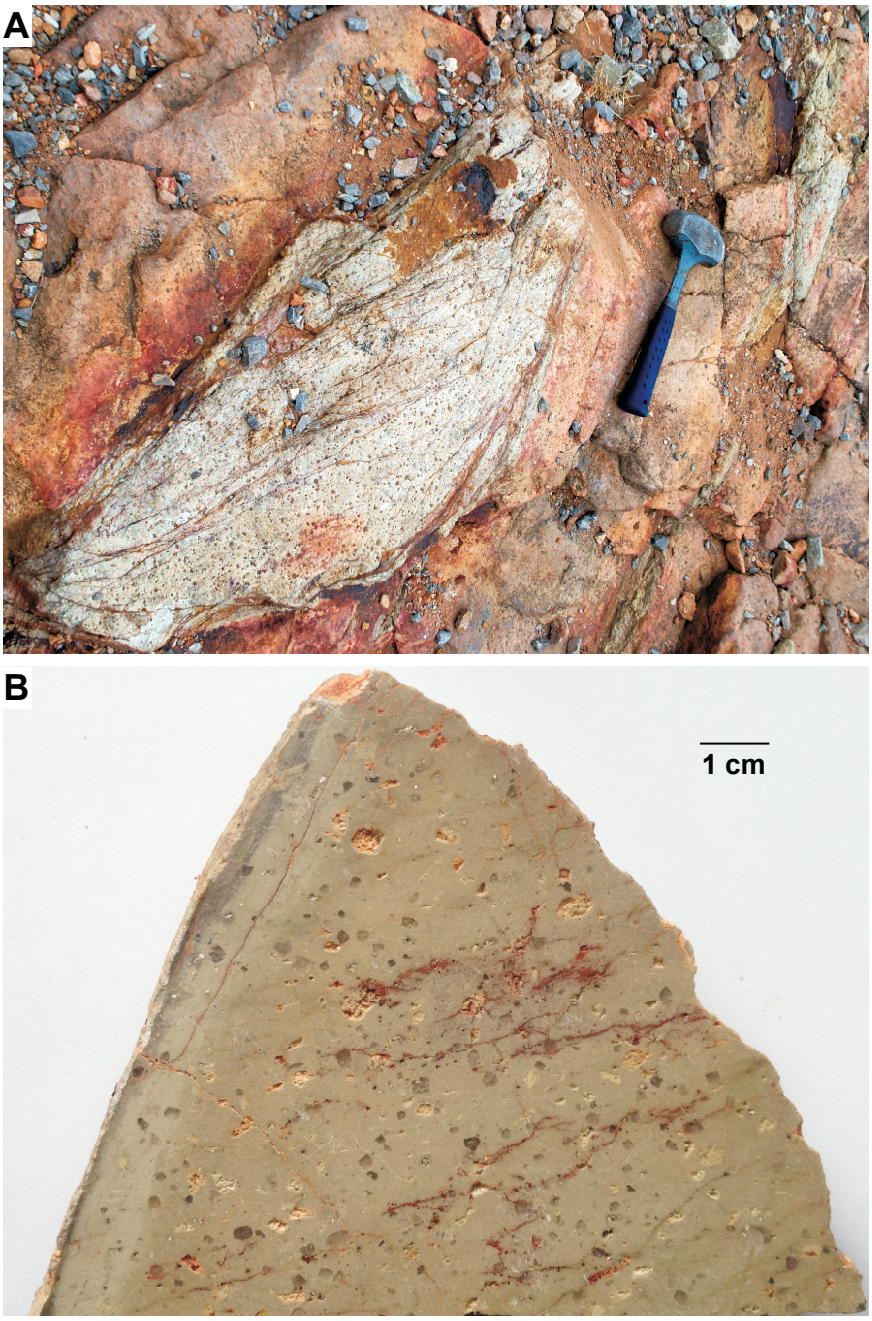

Figure 45. (A) Hydrothermally altered Fort Sill rhyolite bordered by less altered brick-red rhyolite. Dark-gray quartz phenocrysts are visible in the altered rhyolite. (B) Cut slab of hydrothermally altered Fort Sill rhyolite showing altered alkali feldspar phenocrysts and fresh quartz phenocrysts (dark gray).

Major Elements

Harker variation diagrams for the major elements in rhyolites from the Fort Sill area are shown in Figure 46, as are two samples of Davidson metarhyolite analyzed by Price (1998). The Davidson metarhyolite has silica contents ranging from 76.64 to 77.92 wt % (including data from Price, 1998), consistent with petrographic evidence for secondary silicification, and silica values for the Fort Sill rhyolite are 75.50 to 78.33 wt %. The two rhyolite intrusions have the lowest overall silica contents at 72.62 wt % and 73.38 wt %. The geochemical samples from the Fort Sill rhyolite and the rhyolite intrusions show little to no petrographic evidence for secondary addition of silica, and their silica values are inferred to be close to the primary igneous compositions.

CaO, MgO, FeO, Al_2O_3, TiO_2, and P_2O_5 show overall decreases with increasing silica, although in the Harker diagrams there is considerable scatter, which is likely at least partly the result of alteration. These trends, however, are broadly consistent with fractional crystallization or progressive partial melting of source rocks.

The range in data for the Fort Sill rhyolite suggests that this flow records eruption of compositionally heterogeneous magma. The Fort Sill rhyolite and Davidson metarhyolite show broadly similar compositions on the Harker diagrams. However, Al_2O_3 contents for the three samples of Davidson metarhyolite analyzed in this study are higher than those in the Fort Sill rhyolite, which is probably due to preferential loss of alkalis during alteration. The two rhyolite intrusions have significantly less evolved major element compositions than the Davidson metarhyolite and Fort Sill rhyolite, with consistently lower SiO_2 and higher TiO_2, FeO, MgO, and P_2O_5.

Na_2O and K_2O do not show well-defined trends on the Harker diagrams. Scatter in the data is interpreted to be due to alkali mobility during secondary alteration, as indicated by the presence of chessboard albite and sericite in thin section. Alkali mobility is also evident on the diagram of Hughes (1972), where three samples of the Davidson metarhyolite analyzed in this study plot outside the normal igneous spectrum (Fig. 47). Note that these three samples appear to have lost Na_2O relative to the other samples (Fig. 46).

TABLE 2. GEOCHEMICAL DATA FOR RHYOLITES IN THE FORT SILL AREA

	Davidson metarhyolite			Fort Sill rhyolite														Rhyolite intrusions	
Sample:	**FS-60**	**FS-159**	**FS-160**	**FS-126**	**FS-128**	**FS-131**	**FS-132**	**FS-136**	**FS-139**	**FS-140**	**FS-144**	**FS-18**	**FS-88**	**FS-124**	**FS-133**	**FS-137**	**FS-143**	**FS-146**	**FS-125**	**FS-130**
Normalized major elements (wt %)*																				
SiO_2	76.74	77.75	76.64	75.94	76.59	77.67	77.14	77.84	76.29	75.50	77.29	76.82	76.59	78.33	76.87	76.64	77.54	77.20	73.38	72.62
TiO_2	0.29	0.30	0.30	0.30	0.25	0.25	0.26	0.22	0.28	0.29	0.24	0.25	0.29	0.19	0.24	0.25	0.22	0.30	0.54	0.57
Al_2O_3	12.50	12.68	13.17	12.33	11.79	11.60	11.89	11.44	11.96	11.93	11.66	11.75	12.40	11.45	11.52	11.64	11.50	11.91	12.56	12.70
FeO	2.85	1.53	2.58	2.66	2.76	1.92	2.68	2.43	2.71	3.00	2.31	2.86	2.68	2.04	2.66	2.64	1.99	2.57	4.43	4.10
MnO	0.11	0.10	0.05	0.03	0.03	0.02	0.04	0.04	0.07	0.09	0.03	0.02	0.01	0.05	0.07	0.08	0.04	0.02	0.08	0.11
MgO	0.08	0.12	0.11	0.05	0.09	0.03	0.13	0.08	0.13	0.16	0.01	0.05	0.03	0.03	0.12	0.18	0.05	0.05	0.53	0.46
CaO	0.40	0.45	0.41	0.16	0.25	0.18	0.09	0.15	0.49	0.76	0.25	0.13	0.12	0.09	0.41	0.35	0.32	0.10	0.46	1.27
Na_2O	1.92	2.96	2.90	4.29	3.67	3.14	3.82	3.65	3.54	3.73	3.51	3.74	4.10	3.31	3.58	3.69	3.40	3.70	4.19	3.99
K_2O	5.08	4.11	3.82	4.19	4.55	5.18	3.92	4.14	4.49	4.50	4.68	4.34	3.75	4.48	4.51	4.51	4.91	4.11	3.73	4.09
P_2O_5	0.02	0.02	0.02	0.04	0.02	0.02	0.02	0.02	0.03	0.03	0.02	0.03	0.03	0.02	0.02	0.02	0.02	0.03	0.10	0.11
Total**	98.54	99.22	99.04	97.84	98.65	98.31	97.72	98.87	97.75	98.05	98.94	98.66	98.60	98.54	98.41	98.54	98.24	99.08	98.12	98.00
Trace elements (ppm)																				
Ni	3.70	3.00	1.00	1.90	2.50	1.00	2.30	1.90	2.70	2.80	1.90	2.40	1.10	2.00	1.80	2.30	2.10	2.30	3.20	4.00
Cr	1.70	1.50	2.90	0.40	0.30	2.40	1.20	2.00	2.10	0.50	0.30	1.20	1.50	1.20	1.00	0.30	1.50	1.00	2.00	3.00
V	1.10	2.90	0.10	1.20	1.70	3.50	2.20	0.40	2.20	4.00	1.30	3.10	3.10	1.00	2.00	2.50	0.40	3.10	22.00	27.10
Ga	29.70	29.80	30.60	21.20	24.50	21.20	24.50	22.10	23.50	24.50	22.50	23.80	22.30	22.20	24.50	23.60	22.20	24.50	24.30	26.60
Cu	6.30	2.60	1.90	3.90	3.10	5.80	10.10	3.00	3.20	1.20	3.10	0.60	1.50	1.90	1.80	2.00	2.40	4.60	3.40	8.70
Zn	238.10	170.30	175.00	29.70	80.80	41.90	382.40	108.80	165.80	154.80	51.30	88.30	71.80	29.30	143.30	213.30	111.10	73.90	125.10	165.60
La	100.80	110.20	90.70	75.40	96.30	48.00	123.60	69.60	86.10	84.40	72.00	38.70	81.10	90.64+	84.71+	85.49+	91.74+	56.31+	81.10	66.00
Ce	191.90	197.70	137.90	152.70	145.30	75.90	221.40	127.60	166.40	172.60	114.80	119.60	107.60	154.40+	167.37+	174.03+	178.26+	119.71+	150.00	147.20
Ba	1504.30	2202.60	1371.60	1853.40	1782.20	1622.80	1641.00	1404.80	1962.30	1820.20	1704.80	1646.80	1779.60	1582.00+	1667.00+	1676.00+	1434.00+	1773.00+	1765.80	1781.20
Th	13.90	13.10	13.40	11.90	12.00	12.10	12.20	12.30	11.30	12.00	13.60	11.00	11.30	12.49+	11.94+	12.22+	12.98+	11.15+	9.80	9.70
Nb	85.30	83.00	87.60	53.60	57.00	56.00	56.60	58.00	54.90	56.80	57.20	56.20	51.70	51.23+	57.30+	58.79+	62.83+	56.97+	55.20	55.70
Pb	36.40	18.50	15.80	13.30	13.90	20.20	10.10	8.00	13.50	13.20	15.60	10.90	5.90	9.63+	13.43+	9.26+	14.89+	6.32+	9.80	22.90
Rb	158.40	135.80	139.60	102.20	122.10	133.70	91.40	106.80	110.80	108.20	114.80	108.00	95.40	110.20+	109.00+	114.20+	127.90+	104.70+	94.90	113.70
Sr	103.30	262.00	177.60	51.60	37.30	29.50	27.20	21.20	47.10	47.10	29.50	31.00	35.80	25.00+	25.00+	32.00+	30.00+	39.00+	78.40	98.90
Sc	2.50	2.70	3.20	5.10	4.90	2.10	5.30	2.70	5.60	5.10	3.70	4.70	4.70	3.60+	4.30+	4.70+	3.90+	5.90+	8.80	8.70
Zr	726.50	758.40	763.80	694.10	617.10	607.10	638.10	559.70	662.50	673.60	604.70	620.80	702.30	536.00+	518.00+	577.00+	474.00+	617.00+	655.90	667.30
Y	110.30	118.10	99.00	73.10	86.90	63.60	87.90	72.80	76.40	81.00	64.80	57.20	71.40	89.39+	85.02+	87.30+	98.36+	94.61+	78.60	73.50
Nd	114.40	119.50	101.50	82.80	100.80	41.80	119.10	70.90	87.90	90.30	75.20	46.60	88.20	90.08+	89.86+	89.60+	94.73+	62.88+	88.50	75.80
Pr^+	-	-	-	-	-	-	-	-	-	-	-	-	-	22.26	22.46	22.45	23.93	15.67	-	-
Sm^+	-	-	-	-	-	-	-	-	-	-	-	-	-	18.68	19.09	18.88	20.46	13.90	-	-
Eu^+	-	-	-	-	-	-	-	-	-	-	-	-	-	3.26	3.58	3.78	3.28	3.14	-	-
Gd^+	-	-	-	-	-	-	-	-	-	-	-	-	-	17.90	17.79	17.39	19.25	13.10	-	-
Tb^+	-	-	-	-	-	-	-	-	-	-	-	-	-	2.93	2.93	2.84	3.25	2.45	-	-
Dy^+	-	-	-	-	-	-	-	-	-	-	-	-	-	17.56	17.59	17.10	19.79	16.87	-	-
Ho^+	-	-	-	-	-	-	-	-	-	-	-	-	-	3.50	3.47	3.39	3.90	3.64	-	-
Er^+	-	-	-	-	-	-	-	-	-	-	-	-	-	9.17	9.13	9.02	10.34	9.99	-	-
Tm^+	-	-	-	-	-	-	-	-	-	-	-	-	-	1.32	1.32	1.30	1.46	1.45	-	-
Yb^+	-	-	-	-	-	-	-	-	-	-	-	-	-	8.22	8.12	8.01	8.62	8.63	-	-
Lu^+	-	-	-	-	-	-	-	-	-	-	-	-	-	1.26	1.24	1.24	1.32	1.33	-	-
Hf^+	-	-	-	-	-	-	-	-	-	-	-	-	-	15.16	14.47	15.67	13.81	16.15	-	-
Ta^+	-	-	-	-	-	-	-	-	-	-	-	-	-	3.59	3.87	3.94	4.22	3.79	-	-
U^+	-	-	-	-	-	-	-	-	-	-	-	-	-	2.81	3.19	3.20	3.10	2.89	-	-
Cs^+	-	-	-	-	-	-	-	-	-	-	-	-	-	1.79	1.25	1.53	1.03	1.63	-	-

* Major elements are normalized to 100% on a volatile-free basis

**Total before normalization $^+$Values determined by ICP-MS

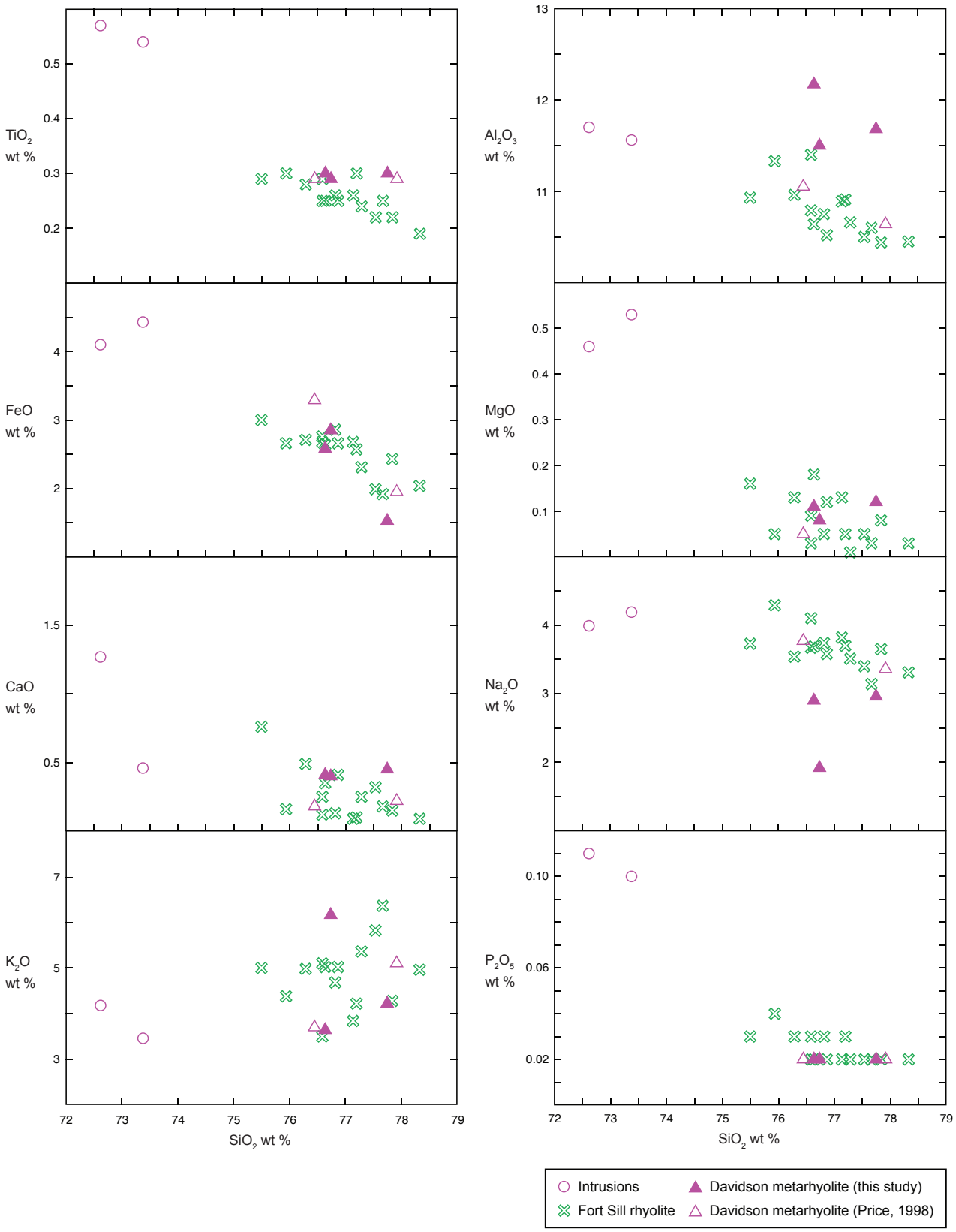

Figure 46. Harker variation diagrams for rhyolites in the Fort Sill area.

Rock Classification

Due to the evidence for extensive alteration, classification of rock types based on major-element contents is problematic. The samples are therefore plotted on the discrimination diagram of Winchester and Floyd (1977) in Figure 48A. This diagram utilizes ratios of immobile trace elements that are unlikely to be modified by secondary alteration and thus provides the best indication of original rock compositions. Data for the Fort Sill rhyolite straddle the boundary between fields for normal and peralkaline rhyolites in this diagram, with most samples falling within the peralkaline field. The Davidson metarhyolite samples cluster with the Fort Sill rhyolite data and fall entirely in the peralkaline field. The rhyolite intrusions plot farther into the normal rhyolite field, close to the boundary with the trachyandesite field, consistent with the less-evolved major-element compositions of the intrusions.

Trace Elements

In representative bivariate plots of immobile trace elements, rhyolite samples from the Fort Sill area consistently occupy two distinct groups (Figs. 48B, 48C, and 48D). Samples of the Fort Sill rhyolite define one group and data for the Davidson metarhyolite cluster in a separate group. This result indicates that the two flows exposed in the Fort Sill area tapped different magma reservoirs or sources, implying a complex magma plumbing system at deeper levels (see Hanson et al., this guidebook). The range in data for the Fort Sill rhyolite in these diagrams provides further evidence that this flow is characterized by significant primary compositional heterogeneities. Note that the two rhyolite intrusions plot with or near the Fort Sill rhyolite in Figures 48B, 48C, and 48D. This raises the possibility that the intrusions may be petrogenetically linked to the Fort Sill rhyolite in spite of their less-evolved major-element compositions. In these figures, as well as in Figure 48A, the two intrusions plot very close to each other, indicating that they were derived from a single magma batch.

In the multi-element diagram normalized to primitive mantle (Fig. 49A), rhyolite samples from the Fort Sill area all show obvious depletions in Ti, P, and Sr. Depletions in Ti and P indicate fractionation of titanomagnetite and apatite, respectively, and depletion in Sr records fractionation of plagioclase. Additionally, most of the samples show slight Ba enrichment, which suggests some alkali feldspar accumulation in these magmas. Most of the rhyolite samples show slight negative Nb-Ta anomalies, suggesting some involvement of older, subduction-modified lithosphere in the petrogenesis of the magmas.

Complete REE data are available for five samples of the Fort Sill rhyolite, which show LREE enrichment and negative Eu anomalies (Fig. 49B), consistent with fractionation of plagioclase. Four of the samples have very similar overall REE patterns, but the other sample shows lower LREE contents, consistent with other evidence for compositional heterogeneities in the Fort Sill rhyolite. A single sample of Davidson metarhyolite from Price (1998) shows

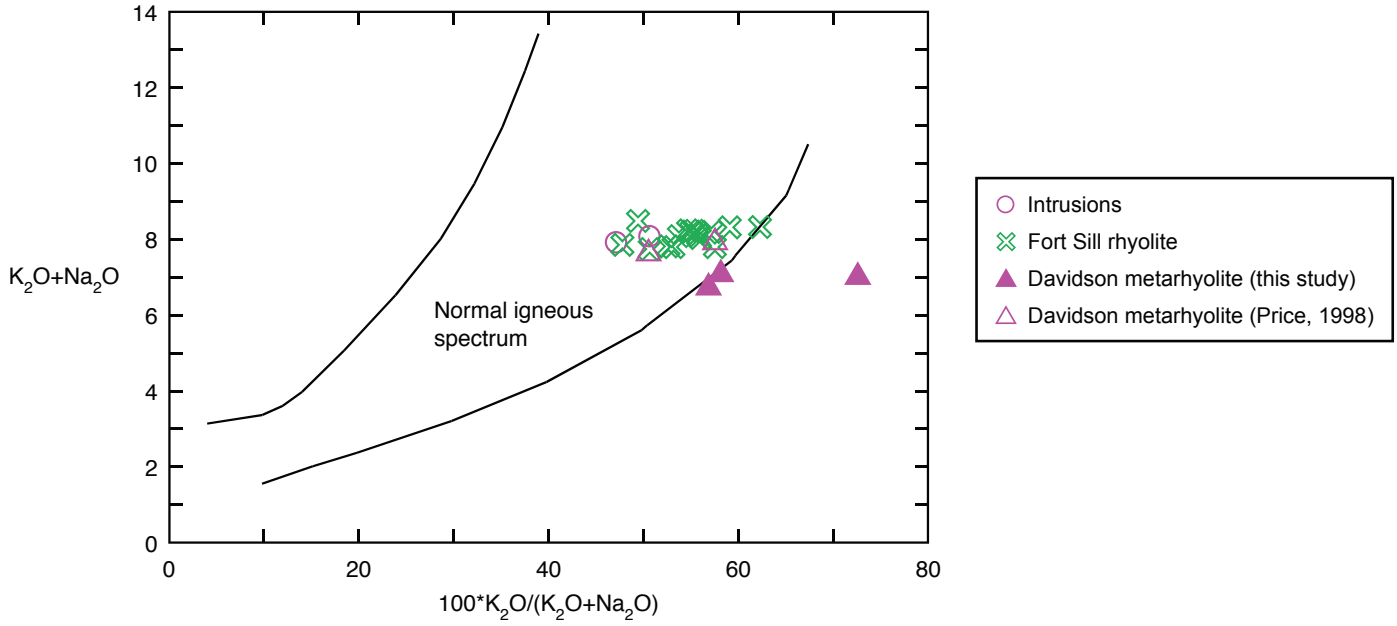

Figure 47. Igneous spectrum diagram of Hughes (1972) for rhyolites in the Fort Sill area.

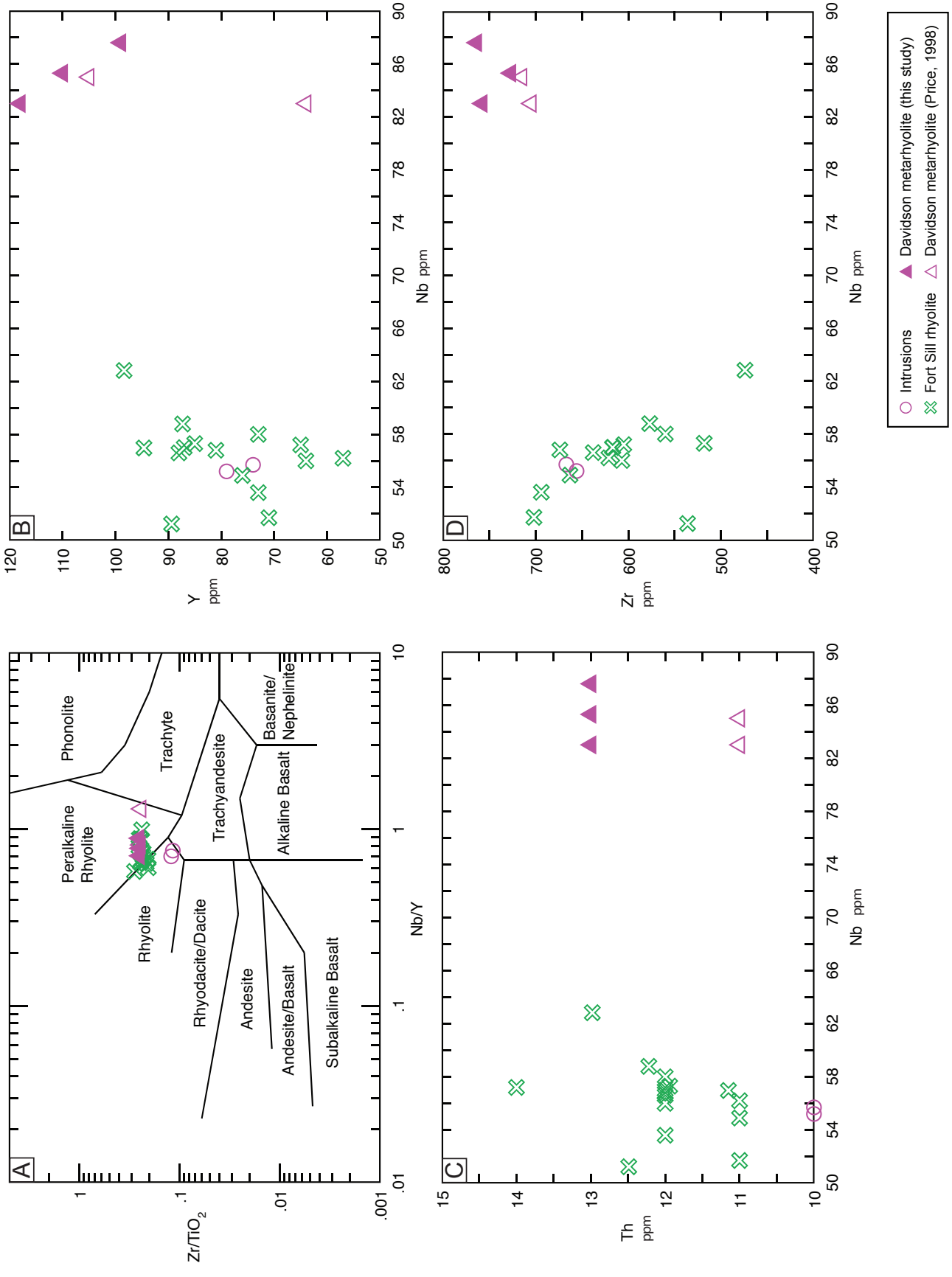

Figure 48. (A) Data for rhyolites in the Fort Sill area plotted on discrimination diagram of Winchester and Floyd (1977). (B) Plot of Nb versus Y. (C) Plot of Th versus Nb. (D) Plot of Zr versus Nb.

a somewhat comparable pattern to the Fort Sill rhyolite sample with the lower LREE contents, with some irregularities that could in part reflect mobilization of some of the REE in the Davidson metarhyolite.

In standard discrimination diagrams utilizing immobile trace elements, data for all the rhyolites in the Fort Sill area cluster fairly tightly in fields for within-plate, A-type felsic rocks (Figs. 50A and 50B), although the Davidson metarhyolite is clearly separated from the Fort Sill rhyolite and associated hypabyssal intrusions in these diagrams. In Figures 50C and 50D the rhyolite data plot close to the boundary between the A_1 and A_2 fields recognized by Eby (1992) for different categories of A-type felsic rocks. Note that a majority of the samples plot in the A_2 field, indicating that lithosphere modified by arc magmatism played a role in the petrogenesis of the magmas. This result is consistent with the negative Nb-Ta anomalies in Figure 49A, and is emphasized in Figure 50E, where the samples partly plot in the field for ocean-island basalt but spread toward average crust.

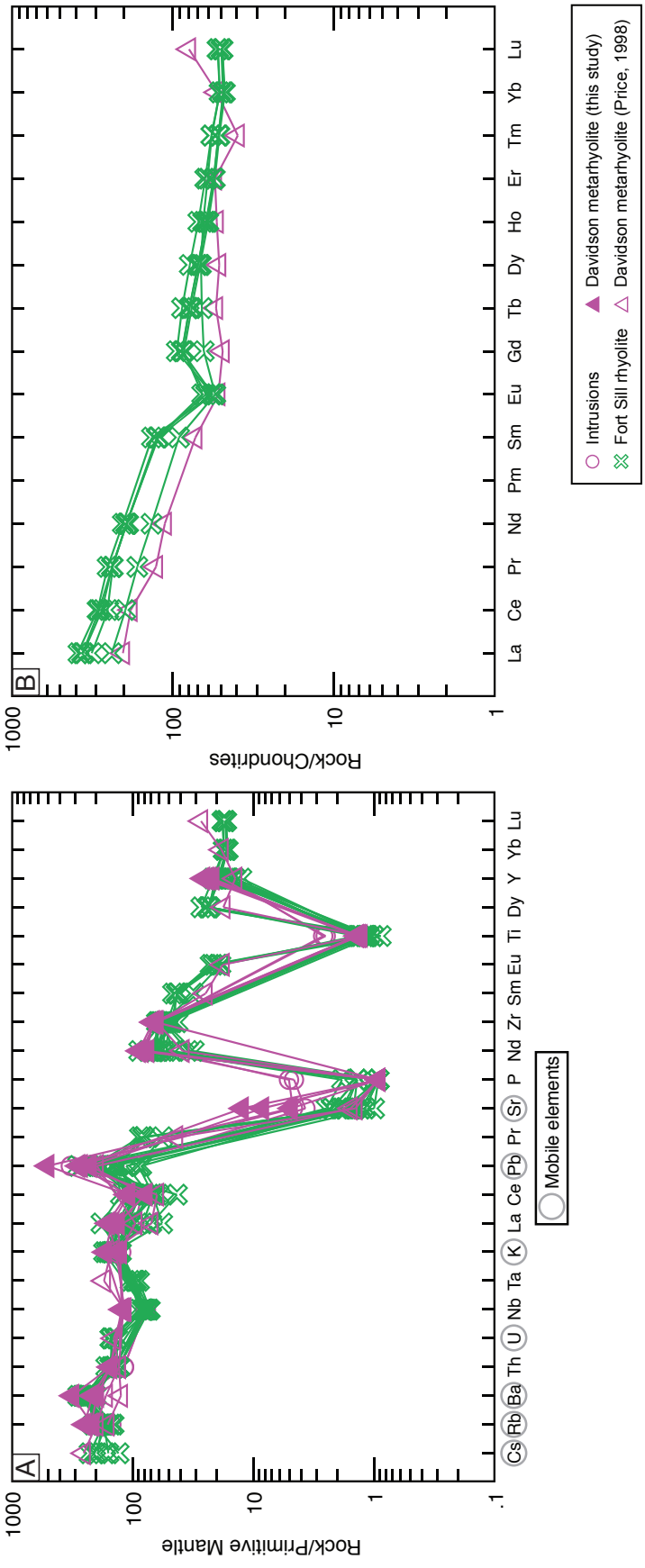

Figure 49. (A) Multi-element diagram for rhyolites in the Fort Sill area. (B) REE diagram for rhyolites in the Fort Sill area. Normalization values in both diagrams are from Sun and McDonough (1989).

REFERENCES CITED

Anderson, J.E., Jr., 1969, Development of snowflake texture in a welded tuff, Davis Mountains, Texas: Geological Society of America Bulletin, v. 80, p. 2075-2080.

Anderson, J.E., Jr., 1970, Recognition and time distribution of texturally altered welded tuff: Geological Society of America Bulletin, v. 81, p. 287-292.

Bigger, S.E., and Hanson, R.E., 1992, Devitrification textures and related features in the Carlton Rhyolite in the Blue Creek Canyon area, Wichita Mountains, southwestern Oklahoma: Oklahoma Geology Notes, v. 52, p. 124-142.

Bonnichsen, B., and Kauffman, D.F., 1987, Physical features of rhyolite lava flows in the Snake River Plain volcanic province, southwestern Idaho, *in* Fink, J.H., ed., The Emplacement of Silicic Domes and Lava Flows: Geological Society of America Special Paper 212, p. 119-145.

Bull, F.B., and McPhie, J., 2007, Fiamme textures in volcanic successions: Flaming issues of definition and interpretation: Journal of Volcanology and Geothermal Research, v. 164, p. 205-216.

Burkholder, B., 2005, Paleovolcanology of the Carlton Rhyolite, Zodletone Mountain, southern Oklahoma [B.S. thesis]: Fort Worth, Texas, Texas Christian University, 69 p.

Chase, G.W., Frederickson, E.A., and Ham, W.E., 1956, Resume of the geology of the Wichita Mountains,

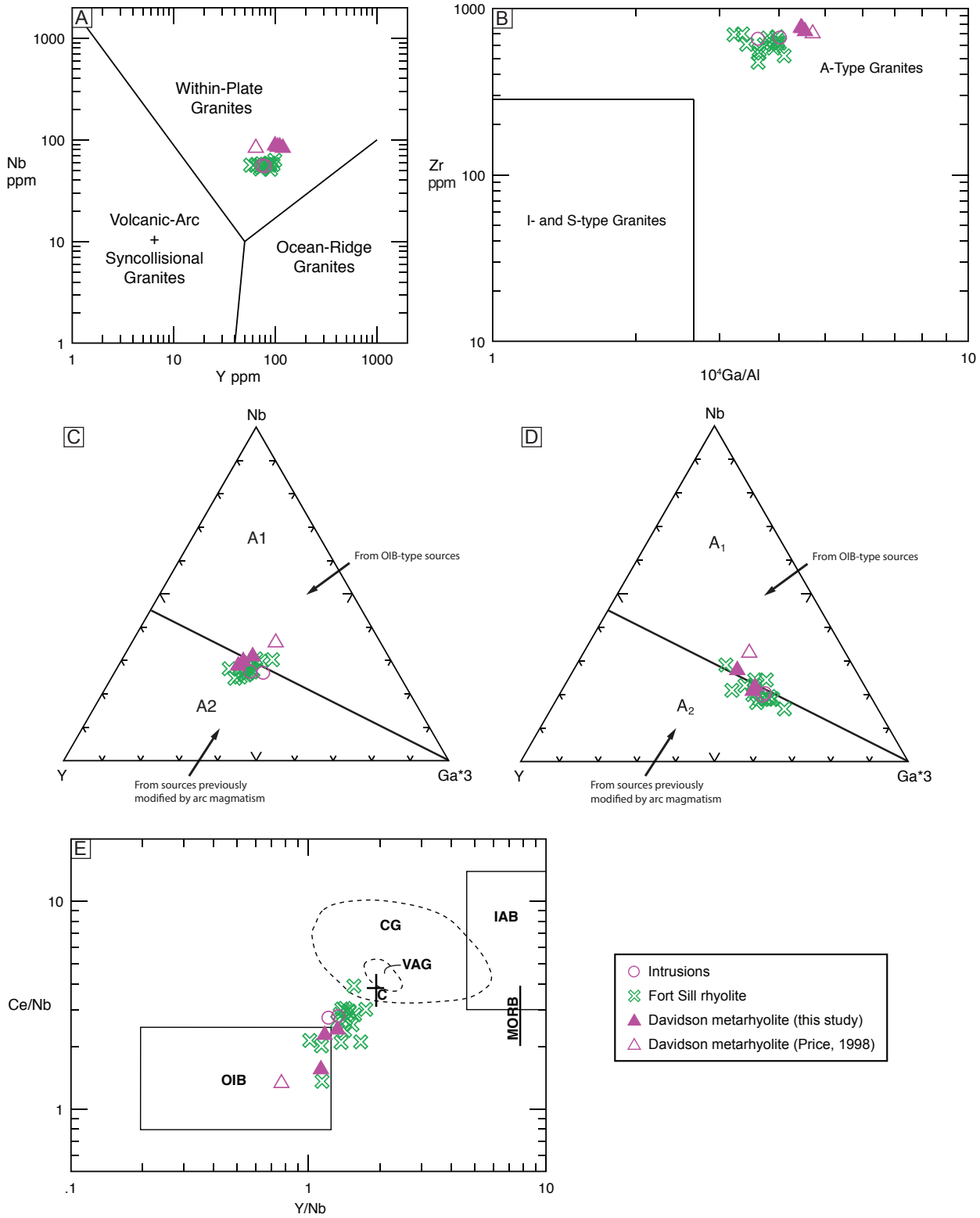

Figure 50. (A) Nb versus Y discrimination diagram of Pearce et al. (1984). (B) Zr versus 10^4Ga/Al discrimination diagram of Whalen et al. (1987). (C) Y-Nb-Ga discrimination diagram of Eby (1992). (D) Y-Nb-Ce discrimination diagram of Eby (1992). (E) Ce/Nb versus Y/Nb diagram of Eby (1990) for A-type felsic rocks. *MORB*: range for mid-ocean ridge basalts; *IAB*: field for island-arc basalts; cross labeled *C*: average crustal ratios; *CG*: field for syncollisional granite; *VAG*: field for volcanic-arc granite; *OIB*: field for ocean-island basalts.

Oklahoma, *in* Petroleum Geology of Southern Oklahoma: American Association of Petroleum Geologists, v.1, p. 35-55.

Dadd, K., 1992, Structures within large volume rhyolite lava flows of the Comerong Volcanics, southeastern Australia, and the Pleistocene Ngongotaha lava dome, New Zealand: Journal of Volcanology and Geothermal Research, v. 54, p. 33-51.

Donaldson, C.H., and Henderson, C.M.B., 1988, A new interpretation of round embayments in quartz crystals: Mineralogical Magazine, v. 52, p. 27-33.

Eby, G.N., 1990, The A-type granitoids: A review of their occurrence and chemical characteristics and speculations on their petrogenesis: Lithos, v. 26, p. 115-134.

Eby, G.N., 1992, Chemical subdivision of the A-type granitoids: Petrogenetic and tectonic implications: Geology, v. 20, p. 641-644.

Gilbert, M.C., 1982a, Geologic setting of the eastern Wichita Mountains, with a brief discussion of unresolved problems, *in* Gilbert, M.C., and Donovan, R.N., eds., Geology of the Eastern Wichita Mountains, Southwestern Oklahoma: Oklahoma Geological Survey Guidebook 21, p. 1-30.

Gilbert, M.C., 1982b, Stop 4 -- Mount Scott Campground, *in* Gilbert, M.C., and Donovan, R.N., eds., Geology of the Eastern Wichita Mountains, Southwestern Oklahoma: Oklahoma Geological Survey Guidebook 21, p. 118-123.

Gilbert, M.C., 1984, Comments on structure within the igneous core, Wichita Mountains crustal block: Oklahoma Geological Society, Technical Proceedings 1981 American Association of Petroleum Geologists Mid-Continent Regional Meeting, p. 177-190.

Gilbert, M.C., 1986, Stop 8 -- Medicine Bluffs, *in* Gilbert, M.C., ed., Petrology of the Cambrian Wichita Mountains Igneous Suite: Oklahoma Geological Survey Guidebook 23, p. 179-182.

Gilbert, M.C., and Hogan, J.P., 2010, Our favorite outcrop: The striking but enigmatic granite-gabbro contact of the Wichita Mountains Igneous Province: Shale Shaker, v. 61, p. 130-134.

Gilbert, M.C., and Powell, B.N., 1988, Igneous geology of the Wichita Mountains, southwestern Oklahoma, *in* Hayward, O.T., ed., South-Central Section of the Geological Society of America Centennial Field Guide, v. 4, p. 109-126.

Green, J.C., 1970, Snowflake texture not diagnostic of devitrified ash-flow tuffs: Discussion: Geological Society of America Bulletin, v. 81, p. 2527-2528.

Ham, W.E., Denison, R.E., and Merritt, C.A., 1964, Basement Rocks and Structural Evolution of Southern Oklahoma: Oklahoma Geological Survey Bulletin 95, 302 p.

Hanson, R.E., 1977, Petrology and geochemistry of the Carlton Rhyolite, southern Oklahoma [M.S. thesis]: Stillwater, Oklahoma, Oklahoma State University, 161 p.

Havens, J.S., 1977, Reconnaissance of the Water Resources of the Lawton Quadrangle, Southwestern Oklahoma: Oklahoma Geological Survey Hydrologic Atlas 6 (HA6), Sheet 1 of 4, Figure 2, Geologic Map, scale 1:250,000.

Hoffman, M.G., 1930, Geology and Petrology of the Wichita Mountains: Oklahoma Geological Survey Bulletin 52, 83 p.

Hogan, J.P., and Gilbert, M.C., 1995, The A-type Mount Scott Granite sheet: Importance of crustal magma traps: Journal of Geophysical Research, v. 100, p. 15779-15792.

Hogan, J.P., Price, J.D., and Gilbert, M.C., 1998, Magma traps and driving pressure: Consequences for pluton shape and emplacement in an extensional regime: Journal of Structural Geology, v. 20, p. 1155-1168.

Hogan, J.P., Gilbert, M.C., and Price, J.D., 2000, Crystallization of fine- and coarse-grained A-type granite sheets of the Southern Oklahoma Aulacogen, U.S.A.: Transactions of the Royal Society of Edinburgh: Earth Sciences, v. 91, p. 139-150.

Hughes, C.J., 1972, Spilites, keratophyres and the igneous spectrum: Geological Magazine, v. 109, p. 513-527.

Kokelaar, B.P., 1982, Fluidization of wet sediments during the emplacement and cooling of various igneous bodies: Journal of the Geological Society of London, v. 139, p. 21-33.

Lofgren, G.E., 1971, Experimentally produced devitrification textures in natural rhyolitic glass: Geological Society of America Bulletin, v. 82, p. 111-124.

Miller, J.R., Gilbert, M.C., and Sides, J.R., 1982, Stop 8 -- Hide-A-Way area, *in* Gilbert, M.C., and Donovan, R.N., eds., Geology of the Eastern Wichita Mountains, Southwestern Oklahoma: Oklahoma Geological Survey Guidebook 21, p. 140-143.

Miser, H.D., 1954, Geologic Map of Oklahoma: U.S. Geological Survey and Oklahoma Geological Survey, scale 1:500,000.

O'Donnell, S.P., 2008, Textural analysis of a rhyolite dike of the Southern Oklahoma Aulacogen at Medicine Park, Oklahoma [M.S. thesis]: Rolla, Missouri, Missouri University of Science and Technology, 114 p.

Pearce, J.A., Harris, N.B.W., and Tindle, A.G., 1984, Trace element discrimination diagrams for the tectonic interpretation of granitic rocks: Journal of Petrology, v. 25, p. 956-983.

Philips, C.M., 2002, Paleovolcanology of the A-type Carlton Rhyolite, Blue Creek Canyon area, Wichita Mountains, southern Oklahoma [M.S. thesis]: Fort Worth, Texas, Texas Christian University, 86 p.

Powell, B.N., Gilbert, M.C., and Fischer, J.F., 1980, Lithostratigraphic classification of basement rocks of the Wichita Province, Oklahoma: Geological Society of America Bulletin, v. 91, Part I, Summary, p. 509-514; Part II, p. 1875-1994.

Price, J.D., 1998, Petrology of the Mount Scott Granite [Ph.D. thesis]: Norman, Oklahoma, University of Oklahoma, 224 p.

Price, J.D., Hogan, J.P., Gilbert, M.C., and Denison, R.E., 1998, Field guide to the basement rocks of the Southern Oklahoma Aulacogen: Guidebook, South-Central Meeting of the Geological Society of America, March 20-24, University of Oklahoma, Norman, Oklahoma, 89 p.

Schoonover, F.E., 1948, The igneous rocks of the Fort Sill Reservation [M.S. thesis]: Norman, Oklahoma, University of Oklahoma, 123 p.

Sides, J.R., and Miller, J.R., 1982, Reinterpretation of metamorphic rocks along Carlton Rhyolite-Mount Scott Granite contact, Wichita Mountains, *in* Gilbert, M.C., and Donovan, R.N., eds., Geology of the Eastern Wichita Mountains, Southwestern Oklahoma: Oklahoma Geological Survey Guidebook 21, p. 40-46.

Smith, J.V., 1974, Feldspar Minerals: Volume 2, Chemical and Textural Properties: New York, Springer-Verlag, 690 p.

Sun, S.S., and McDonough, W.F., 1989, Chemical and isotopic systematics of oceanic basalts: Implications for mantle composition and processes, *in* Saunders, A.D., and Norry, M.J., eds., Magmatism in the Ocean Basins: Geological Society Special Publication No. 42, p. 313-345.

Taff, J.A., 1904, Preliminary Report on the Geology of the Arbuckle and Wichita Mountains in Indian Territory and Oklahoma: U.S. Geological Survey Professional Paper 31, 97 p.

Taylor, C.H., 1915, Granites of Oklahoma: Oklahoma Geological Survey Bulletin 20, 108 p.

Whalen, J.B., Currie, K.L., and Chappell, B.W., 1987, A-type granites: Geochemical characteristics, discrimination and petrogenesis: Contributions to Mineralogy and Petrology, v. 95, p. 407-419.

Winchester, J.A., and Floyd, P.A., 1977, Geochemical discrimination of different magma series and their differentiation products using immobile elements: Chemical Geology, v. 20, p. 325-343.